VARIABLE SLIM TDMA OPERATIONS PARAMETERS

FINAL REPORT

MILLER COMMUNICATIONS SYSTEMS LTD.

DOC-CR-SP-82-052

VARIABLE SLIM TDMA OPERATIONS PARAMETERS

FINAL REPORT

Date: August 12, 1982
MCS File No: 8260
DSS File No: 13ST.36100-1-0477

Prepared by: S. S. Kamal

Approved by: R. K. Tiedemann

SUBMITTED BY:

MCS MILLER COMMUNICATIONS SYSTEMS LTD.
300 Legget Drive,
Kanata, Ontario,
Canada K2K 1Y5

ABSTRACT

This report is intended to investigate the sensitivity of the slim TDMA terminal's performance to variations in the terminal's operational parameters. These parameters include the unique word's length and format, the detection apertures' widths, the sync-verification count before acquisition of downlink sync, the sync-loss count before relinquishing uplink sync and the detection thresholds. The indices defined to characterize the terminal performance are: (i) the mean time to acquire downlink sync, (ii) the probaiblity of false acquisition, (iii) the mean time interval between sync-loss events, and (iv) the probability of a false detection occurring within a detection aperture.

For a given unique word length correlation/detection properties are defined, and used as criteria for the selection of optimum word formats. Unlike most selection criteria, the approach presented here does not require the evaluation of all 2^n possible formats of an n-bit sequence. A smaller subset of candidate sequences is identified; a subset whose size increases with the word-length n at a rate slower than 2^n.

Finally, Markovian models are presented to evaluate the TDMA terminal's performance as a function of the operational parameters being used. The Slim TDMA terminal developed by MCS for CNCP is used as a representative configuration for this analysis. Results of a parametric analysis are presented to assess the sensitivity of the performance to these operational parameters. From such an analysis, it is possible to identify the necessary modifications to the current values used.

TABLE OF CONTENTS

GLOSSARY OF NOTATION*

UW	:	Unique Word
FRUW	:	Frame Reference Unique Word
DBUW	:	Data Burst Unique Word.
CR	:	Carrier Recovery sequence in the burst preamble.
BTR	:	Bit-Timing recovery sequence in the burst preamble.
T_b	:	Number of bits in a TDMA frame.
BER	:	Bit Error Rate.
p	:	Satellite Channel's BER.
η	:	TDMA frame's efficiency.
A_w	:	Wide aperture set after first detection of the FRUW in acquistion.
A_{VN}	:	Narrow aperture generated to gate the detection of the UW in steady-state operations.
I	:	UW detector's threshold (max. number of tolerable bits in error).
MTTA	:	Mean Time To Acquire downlink frame synchronism.
$MTTA_c$	:	Mean Time to Acquire downlink frame synchronism by locking onto the correct FRUW.
P_{FDO}	:	Probability of false detection of UW while aperture is open to the frame width, assuming random data being examined.
P_{FDB}	:	Probability of false detection of UW with aperture at A_{VN} bits and assuming random data being examined.
P_{NDW}	:	Probability that no detection is made within wide aperture A_w.
P_{NDO}	:	Probability that no detection is made in an entire frame scan.
P_{FDW}	:	Probability of false detection of the UW within the wide aperture A_w.
P_{caq}	:	Probability of correctly acquiring frame synchronism.
P_{FA}	:	Probability of falsely acquiring frame synchronism.
P_{NDB}	:	Probability that no detection is made within an aperture of A_{VN} bits.

*In the infrequent cases where a symbol has more than one meaning, the context (or a specific clarification) resolves the ambiguity.

P_{MD} : Probability of a misdetection of the UW during initial acquisition of frame synchronism.

P_{BSL} : Probability of losing burst synchronism.

$P_D(\ell)$: Probability of a detection occuring within the aperture at a distance of ℓ bits from the true UW.

MTBSL: Mean Time Before Loss of burst synchronism.

$t_E(i)$: The net accumulated timing error between two terminals over an interval of one frame, given that the flywheel count is i.

L : Acquisition threshold. Also called "Verification Count". The number of consecutive frames in which the FRUW is detected before the terminal considers itself to have acquired frame sync.

M : Loss Threshold. Also called "Flywheel Count". The number of consecutive frames in which the FRUW is not detected before the terminal ceases operations and relinquishes frame sync.

MTTO : Meantime to operate. The expected time required by a terminal to acquire frame sync once sync-loss has been detected. In a fully-automated recovery system MTTO≈MTTA.

UTR : Up-Time Ratio. Used to describe the burst synchronizer's availability, as the ratio MTBSL/(MTBSL+MTTO).

1.0 TDMA SYNCHRONIZATION

1.1 Introduction

In a time division multiple access (TDMA) network transmissions from active terminals arrive at the satellite transponder in non-overlapping time slots. Figure 1.1 illustrates TDMA scheduling of access to a satellite transponder. Each terminal assembles its inputs into a burst consisting of a fixed number of bits, and transmits it at a fixed time with respect to a time reference at the satellite transponder. The time reference is provided by a designated reference terminal which periodically transmits a reference burst every T_F seconds. During this interval T_F, called a frame, each active terminal in the network has an opportunity to transmit its burst. Consequently, a single interval of duration T_F represents one cycle of the multiple access sequence.

Since the position of a burst is fixed (for a given frame format), a terminal receiving the reference burst can ideally synchronize its receiver to accept any burst in the frame. Similarly, the terminal can instruct its transmitter to correctly position its own burst(s) within a frame. The ability of a terminal to establish correct receive-timing for the reference burst is denoted as downlink frame synchronism. If overall network synchronization is not sufficiently stable, downlink burst synchronism may also be required. The ability of a terminal to correctly position (and control) its own burst in a frame is denoted as uplink synchronism. Both downlink and uplink synchronism will be addressed further in Section 1.2 and 1.3 respectively.

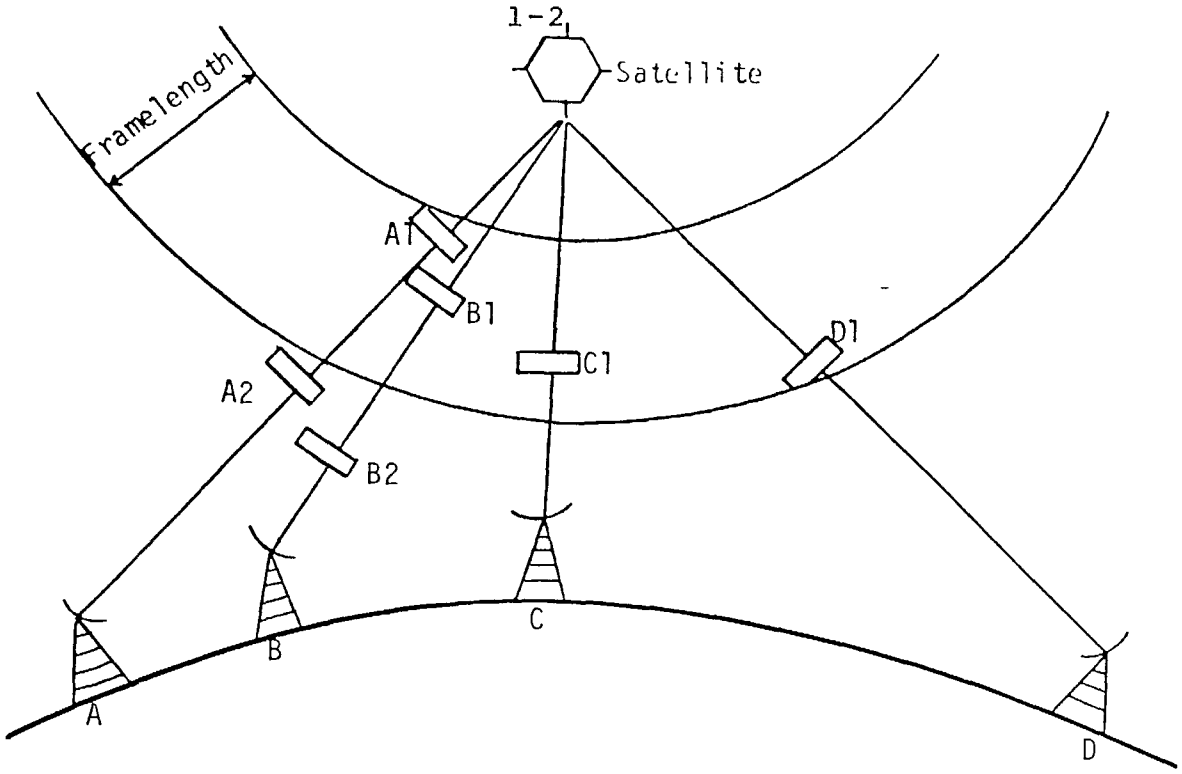

a) TDMA Network

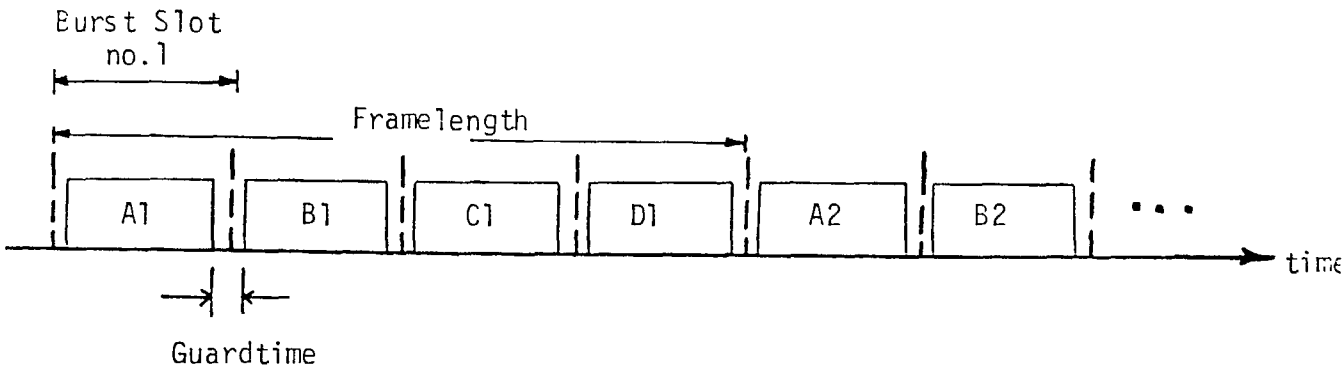

b) Transponder Input

Figure 1.1 TDMA Channel Allocation.

An aspect that is common to both uplink and downlink sync is the terminals' ability to operate synchronously in an imperfect environment, i.e. in the presence of channel noise and stochastic timing errors.

1.2 Downlink Synchronization

Determination of the beginning of a TDMA frame is the initial synchronization activity of any TDMA terminal. The time-keeper of the network is a reference station that sets frame timing by periodically transmitting a unique pattern of bits once per frame interval. The periodic detection of this frame reference unique word (FRUW) by a terminal constitutes its acquisition of downlink frame sync. However, in many cases this is not sufficient to imply the acquisition of downlink burst sync, since the position of a data burst in the frame cannot be accurately derived to within ±1/2 a symbol period. This is primarly due to timing-offsets between the reference terminal's clock and the user's clocks, and to satellite motion. Consequently, burst synchronism can be similarly acquired by detecting a data burst unique word (DBUW) appended to each data burst.

Unique word detection by the Slim TDMA terminal is performed by a digital correlator, shown in Figure 1.2. The detector operates on a stream of regenerated bits by digitally correlating n-bit segments of the received data $\{a_i: i=0, 1,...n-1\}$ with a stored version of the UW $\{U_i: i=0, 1,...n-1\}$. Channel errors may corrupt a valid UW beyond recognition, or cause an n-bit sequence to "appear" as a valid UW. Whether the channel errors are random, correlated or in burst is primarily dependent on the channel characteristics and demodulation method. The Slim TDMA terminal uses a QPSK modem which, over a satellite

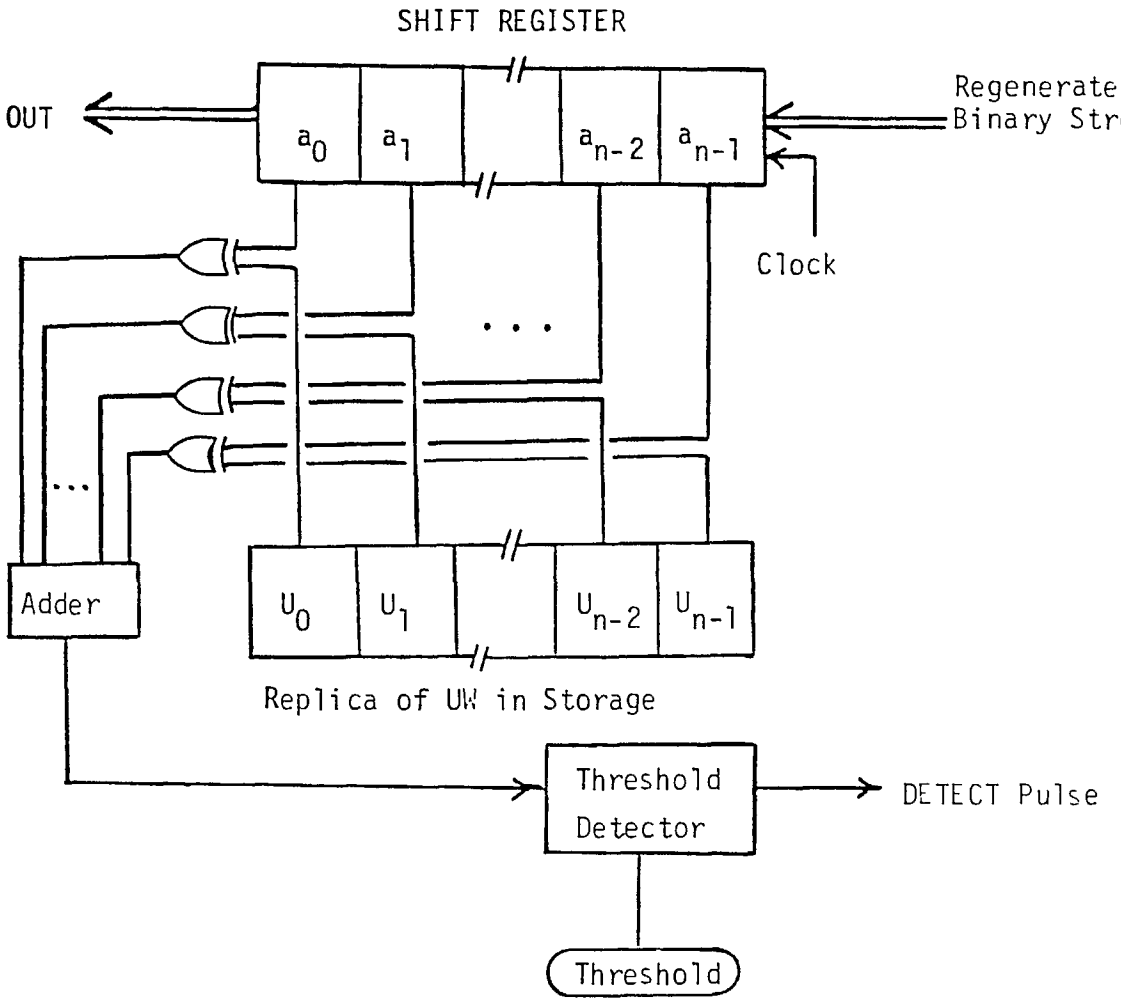

Figure 1.2 Block Diagram Of The UW Detector.

channel, results in near randomly distributed errors. However, bit-errors are paired when differential decoding is used*. In general, a detection threshold (I) for the UW detector is defined as the maximum number of bit-positions in which $\{a_i\}$ and $\{U_i\}$ differ if the detector is to accept the n-bit sequence as a valid pattern. Regulation of the detector's threshold controls its sensitivity to bit-errors.

From the above description of the detector's operation one of two failure-events can be envisaged during a frame duration:

(1) failure to detect the true UW due to excessive corruption - characterized by the probability of misdetection; or

(2) failure to reject an incorrect UW - characterized by the probability of false detection.

The minimization of the likelihood of both these events is essential to reliable acquisition and retention of downlink sync.

One method employed in the Slim TDMA terminal to reduce the probability of these failure-events takes advantage of the periodicity of the UW and the randomness of false patterns. By gating the output of the UW detector an aperture is defined as the length of time during which the terminal expects the UW (FRUW or DBUW) to arrive. In effect, the aperture acts as a narrowband filter since only those detections that coincide with the aperture will be passed onto the terminal. Figure 1.3 shows a timing diagram for the relative positions of the frame-sync and burst-sync apertures.

*The Slim TDMA terminal uses differential decoding to resolve carrier phase ambiguity during initial acquisition (see Section 2.0).

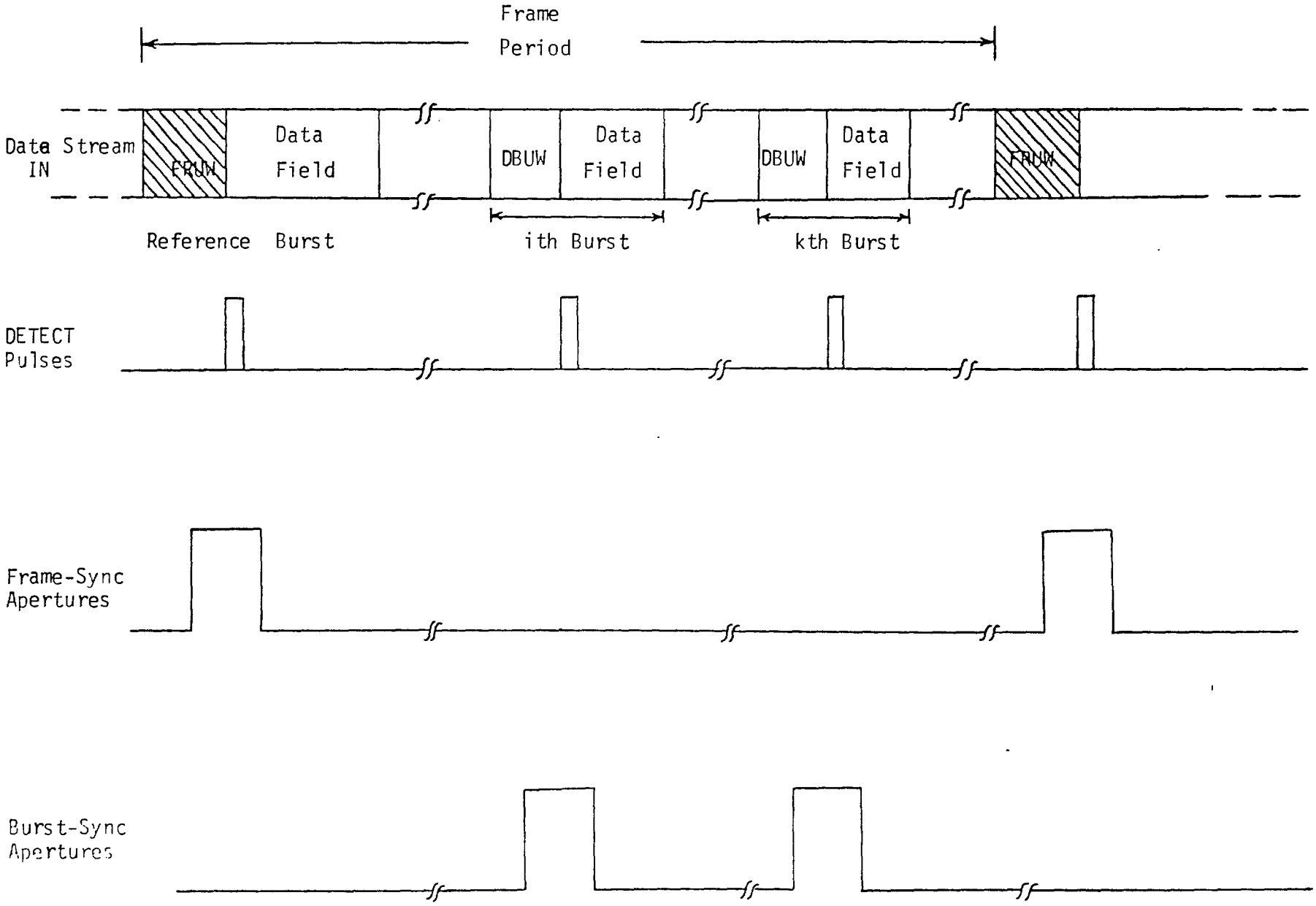
Frame
Period
Data Stream
IN
FRUW
Data
Field
DBUW
Data
Field
DBUW
Data
Field
FRUW
Reference Burst
ith Burst
kth Burst
DETECT
Pulses
Frame-Sync
Apertures
Burst-Sync
Apertures

1.3 Uplink Synchronization

Ideally, the effective position of a data burst is measured as a fixed offset t_o from the received reference burst, as shown in Figure 1.4. However, the true offset from the reference burst needed to position a data burst is the sum of two components:

(i) the nominal time offset of t_o from the start of the frame, plus

(ii) an additional time shift of t_m determined by the propagation distance to the satellite, denoted D, and the frame duration T_F seconds.

The time-space graph in Figure 1.5a details this composite offset. Because the terminal is at a distance D from the the satellite, a time-shift exists between the TDMA frame established at the satellite by the reference burst, and The frame returned to the satellite via the terminal. This time-shift t_m must be zero and hence the frame at the terminal is retarded by an equivalent shift. In effect, this only adds to the transmit-time offset from the received reference burst (as shown in Figure 1.5b for an example in which C denotes the propagation speed of light, D/C = 6 time slots, and frame duration T_F = 20 time slots). In general, the shift t_m is given by

$$t_m = MT_F - (2D/C) \text{ slots} \qquad (1.1)$$

where M is some integer such that t_m is a minimum positive value. In this expression both T_F and D are ideally time-invariant. However, misdetections, false detections and clock timing-errors inject a shochastic component in T_F. Similarly, fluctuations in the satellite's position (geostationary drift) cause variations in the range D.

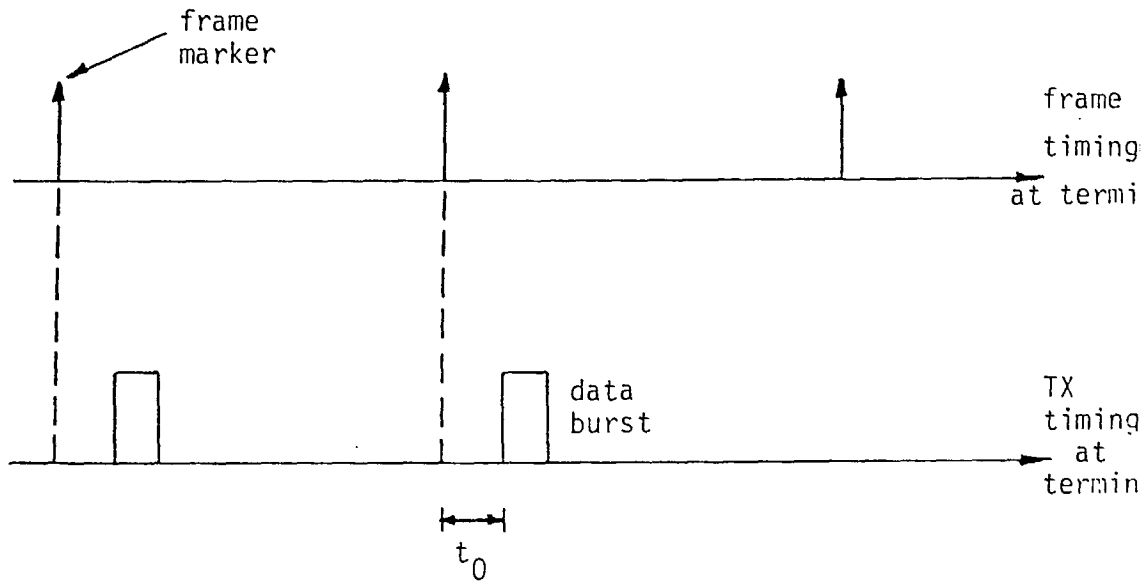

Figure 1.4 Ideal Transmit Offset At Satellite.

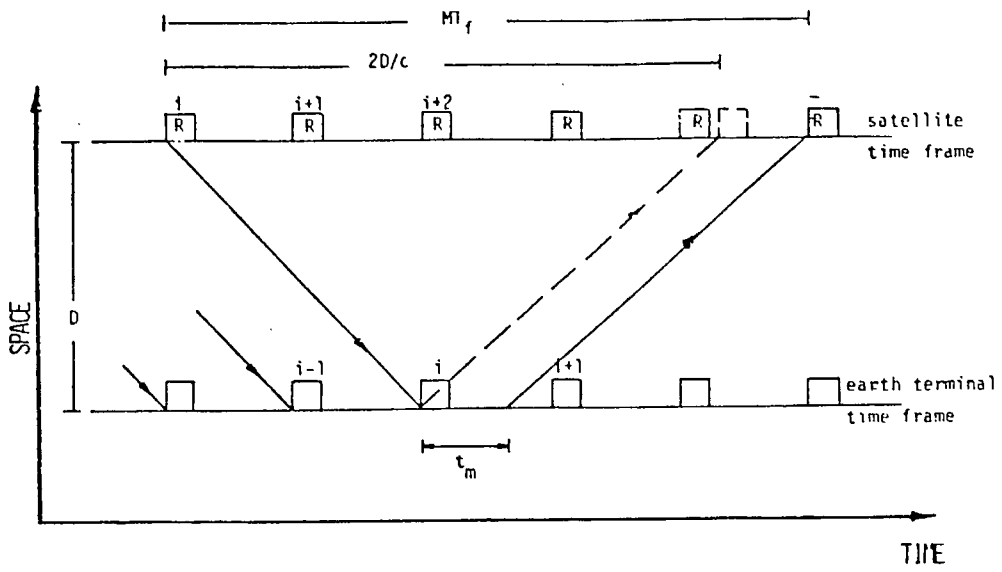

a) Time/space Graph For Transmit Time Offset

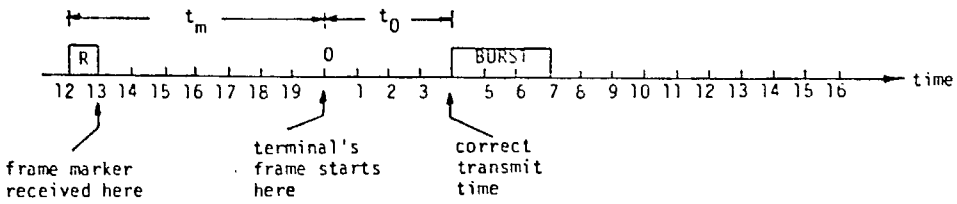

b) Time-Shift Between Satellite & Terminal Frames

Figure 1.5 Ideal Transmit Timing Relative To Received Frame Reference At Terminal

These variations in T_F and D result in uncertainties in uplink synchronization. Since accurate determination of the start-of-frame is a downlink sync problem, and the tracking of range variations is an uplink sync issue it is evident that both uplink and downlink synchronization of a TDMA terminal are inter-dependent issues.

To prevent burst overlap at the satellite, guard times are inserted between adjacent bursts. Their width represents the extent of uncertainty in a terminal's uplink synchronism, but contribute to frame overhead and therefore must be minimized. A design tradeoff exists between the width of the guard times and the complexity of the burst-positioning procedure (equipment). As in downlink sync, uplink sync must be initially acquired then retained. Initial acquisiiton refers to the procedure required to position a data burst into its allocated time slot without interfering with other burst in the frame. The execution of this procedure is required when a dormant terminal wishes to initiate transmission, or after lengthy outages. Retention refers to the procedure required to maintain (at the satellite) an accurate burst-phase control relative to the reference burst.

It is evident from equation 1.1 and Figure 1.5 that the terminal's transmit offset is dependent on: (i) the correct detection of the FRUW, and (ii) the accuracy with which it estimates its own uplink delay. These two inputs are the nucleus of any uplink synchronization schemes and are termed here the Transmission Inputs (see Figure 1.6a). Synchronization schemes that are termed "open-loop" use ranging and/or prediction algorithms to estimate the uplink delay (see Figure 1.6b). Schemes termed "closed-loop"

procedures are those that require the terminal to estimate its uplink delay from knowledge of the relative positions of the reference burst and its own data burst (see Figure 1.6c). If the terminal can receive its own data burst (e.g. global and regional antenna coverage) closed-loop sync is maintained by a simple feedback loop. Otherwise (e.g. in spot-beam environmnets) information concerning the postion of its transmitted data burst must be relayed back by the remote destination terminal. From Figure 1.6 it is clear that in both closed-loop and open-loop systems uplink sync is dependent on maintaining downlink sync. What distinguishes these two uplink synchronization methods is that in open-loop systems, uplink delay estimate (t_m) are predicted or measured; in closed-loop systems a terminal derives this delay from observing the position of its own burst relative of the FRUW.

Having identified the establishment (and retention) of downlink frame sync as a prerequisite to subsequent receive and transmit TDMA operations, the following section details the specific acquisition and retention algorithms used by the Slim TDMA terminals. Indices will be defined to evaluate the terminal's performance, as will the terminal's operational variables which influence this performance.

2.0 PERFORMANCE INDICES FOR SYNCHRONIZATION

2.1 Acquisition And Retention Algorithms

At start-up, and after lengthy outages, a TDMA terminal initially seeks the periodic reference burst. In attempting to determine the start of the frame the terminal must minimize the acquisition time yet maximize the probability that it has identified the true occurrence of the FRUW. Although the minimum time required to acquire frame sync is a unit frame interval, it is clear that a single false detection would result in a false acquisition. Figure 1.4 and 1.5 have shown that false acquisition distorts the terminal's receive and transmit capability. Consequently, high confidence limits must be set for rapid acquisition of frame sync. Similarly, a terminal must continue to transmit and receive data bursts only as long as it retains frame sync and no longer. This section briefly examines how the Slim TDMA terminal acquires and relinquishes frame and burst sync.

2.1.1 Acquisition and Retention of Frame Sync

To establish downlink sync, the Slim TDMA terminal completes a three-mode acquisition algorithm: (i) SCAN mode: in which the apertures are suppressed and the UW detector scans the received data on a bit-by-bit basis, (ii) VERIFY mode: after the first detection of the FRUW, a WIDE aperture A_W is set in which the FRUW must appear for an integer number of consecutive frames; and (iii) LOCK-UP mode: in which the Lth consecutive detection of the FRUW constitutes a final verification of frame sync acquisition.

*The latter may also cause the renegade terminal to disrupt the transmissions of other terminals in the network.

This algorithm is depicted in Figure 2.1. Both the aperture width A_W and the verification count L impact on the acquisition time and the likelihood of false acquisition.

A unique aspect of the Slim TDMA terminal's operation is the use of differential decoding during the SCAN mode of the initial acquisition algorithm. This requirement arises from the terminal's means of resolving phase ambiguity. Typically, the four-fold phase ambiguity resulting from the coherent demodulation of a QPSK signal is resolved by one of two methods:

(1) by differntial encoding and decoding of the data burst, which can result in correlated bit-errors and imposes operational constraints on the FEC codec; or

(2) by using a bank of four UW detectors to detect the FRUW in any of its phase positions, which renders a four-fold increase in the word's false detection probability.

To avoid the performance degradation of both conventional procedures, the Slim TDMA terminal's network operations require a transmitting terminal to transmit an unmodulated carrier-recovery sequence. This approach is applicable to terminals that have acquired frame sync and thus can determine the location of the carrier-recovery sequence in the preamble. However, during the SCAN mode of the initial acquisition algorithm neither the start-of-frame nor the location of the preamble is known. Differential decoding

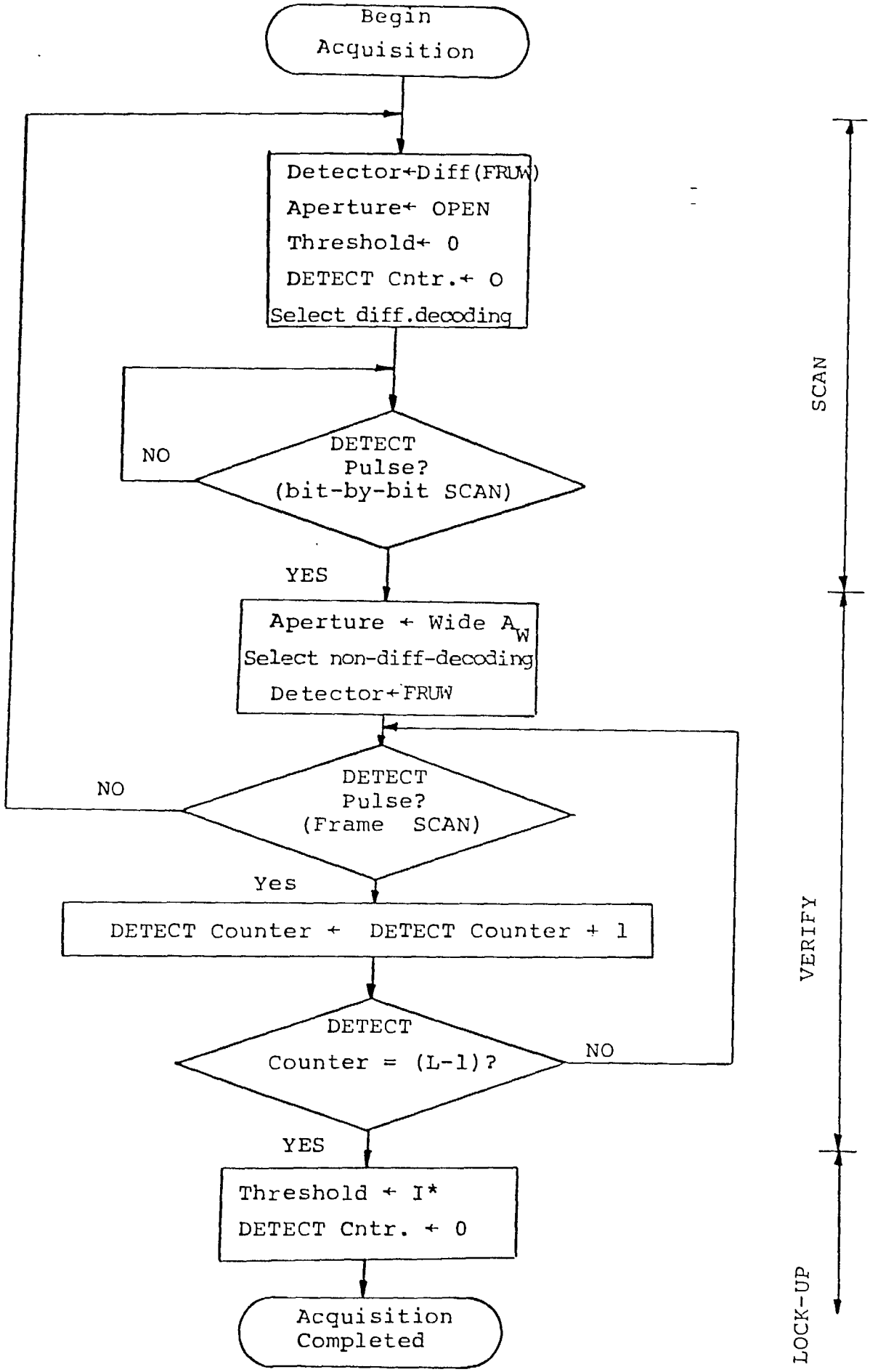

Figure 2.1 Initial Acquisition Procedure
*threshold subject to specific scheme

is used to map all four possible variations of the FRUW into a single UW to which the detector is sensitized. The increased likelihood of false detections or mis-detections as a result of differential decoding is reduced by setting the detector's threshold to zero (i.e. in the SCAN mode the detector seeks a "perfect match").

During steady state operations the terminal periodically sets an aperture of A_{VN} bits in which the FRUW is expected to appear. This aperture is narrower than the WIDE aperture set during the VERIFY mode of acquisition. Furthermore, the detector's threshold is no longer set to zero to allow for limited bit-errors in the UW. At the occurrence of the first non-appearnce of the FRUW in its aperture the terminal executes a two-mode retention algorithm before it relinquishes frame sync: (i) FLYWHEEL: in which the terminal injects locally generated DETECT Pulses (see Figure 1.2) for (M-1) consecutive frames or until FRUW re-appears; and (ii) SYNC-LOSS: at the Mth flywheel count the terminal suspends its transmit/receive operations and begins re-acquisition procedures. Figure 2.2 illustrates this algorithm.

If the components of equation 1.1 were deterministic then the flywheel count M could continue indefinitely. However relative timing errors between the local and reference terminals' clocks, and path-delay variation due to satellite motion set an upperbound to the flywheel interval. Figure 2.3 illustrates how a terminal A, after flywheeling for several frames, can accumulate sufficient timing error (ε_i) for its transmitted burst to encroach on terminal B's burst.

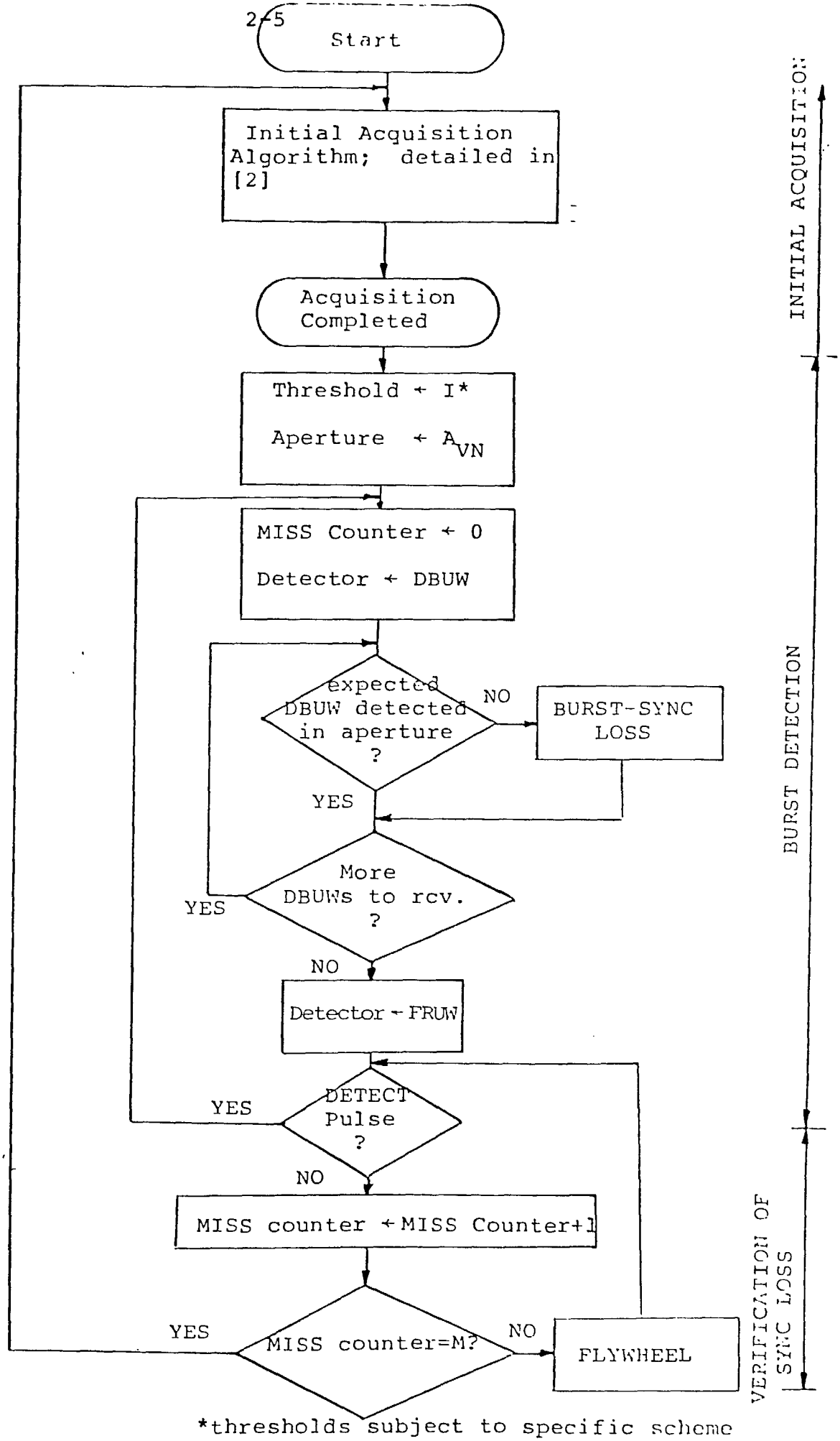

*thresholds subject to specific scheme

Figure 2.2 Retention Procedure

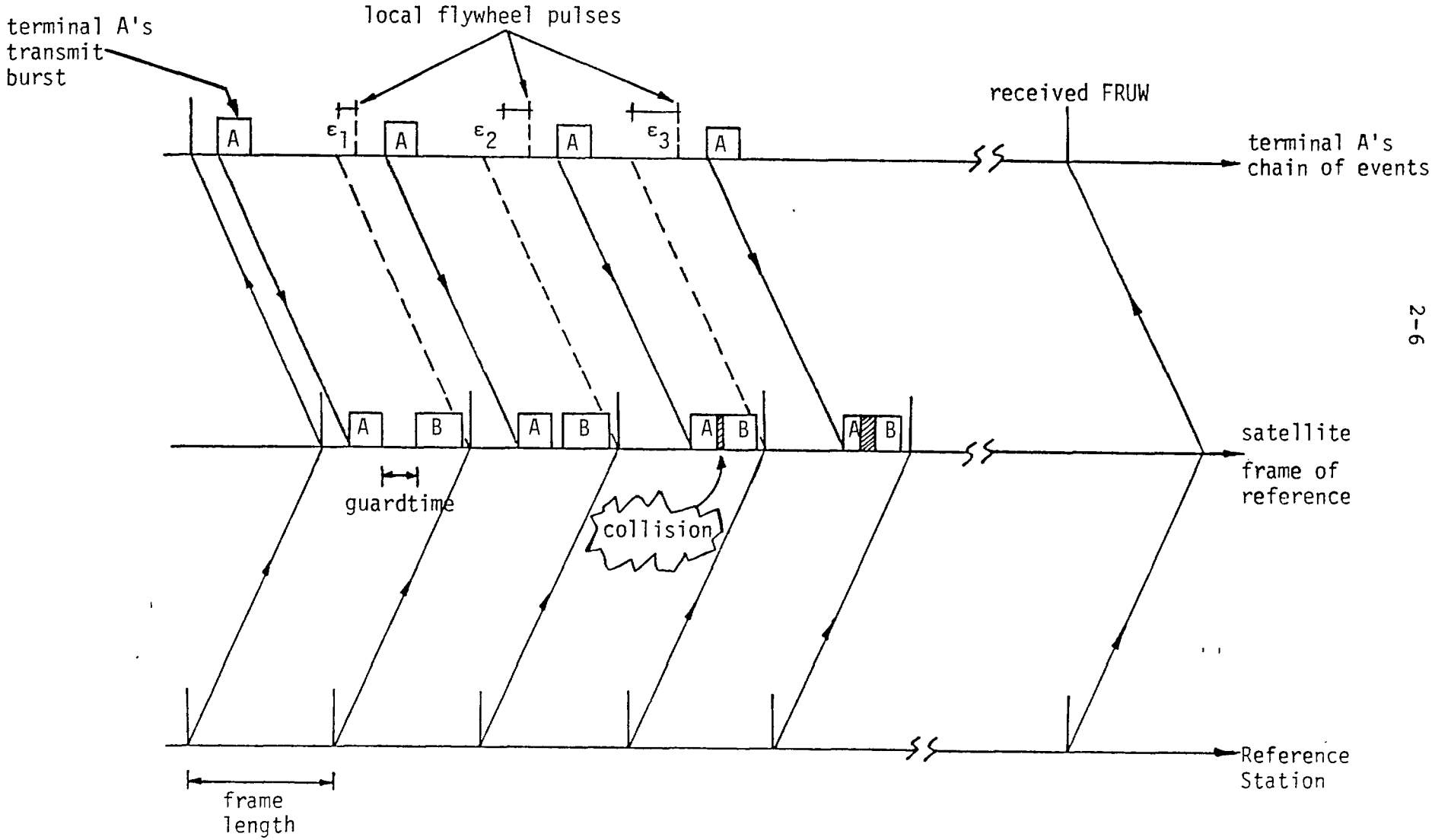

Figure 2.3 Burst Interference Due To Lengthy Flywheeling of FRUW

Timing errors accumulated during flywheeling are the primary cause of frame sync loss. However, due to the method by which detection apertures are generated, successive false detections within the aperture can also result in sync loss. Figure 2.4 presents a schematic of how the FRUW apertures are generated by the terminal. The aperture generated to detect the j-th FRUW is controlled by a time-into-frame (TIF) counter that counts clock pulses into the frame, and is reset by the detection of the (j-1) FRUW. The TIF counter is modulo- T_b, where T_b is the number of clock pulses within a nominal frame interval. Overflow of the TIF counter activates the flywheel unit to inject a pseudo-DETECT pulse to replace the missing FRUW. Since the aperture generated for the jth FRUW is derived from the reset of the TIF by the (j-1) FRUW, it is clear that a false detection will result in a relative shift between the next FRUW and its aperture. Figure 2.5 dipicts how two consecutive false detections may result in sync loss.

Subject to the above effects of timing errors and false detections, the selection of aperture width, detection threshold and flywheel count must reconcile the need to: (a) maximize the interval in which the terminal retains frame sync, and (b) minimize the possibility of adjacent burst interference by terminals that have lost frame sync. Parameter selections that unilaterally maximize sync retention time will not likely protect the network from transmissions by terminals that have lost sync and continue to flywheel.

Continued identification of the start-of-frame is a prerequisite to any TDMA function. As a result emphasis is typically directed to optimization of the terminal's ability to seek and periodically detect the FRUW.

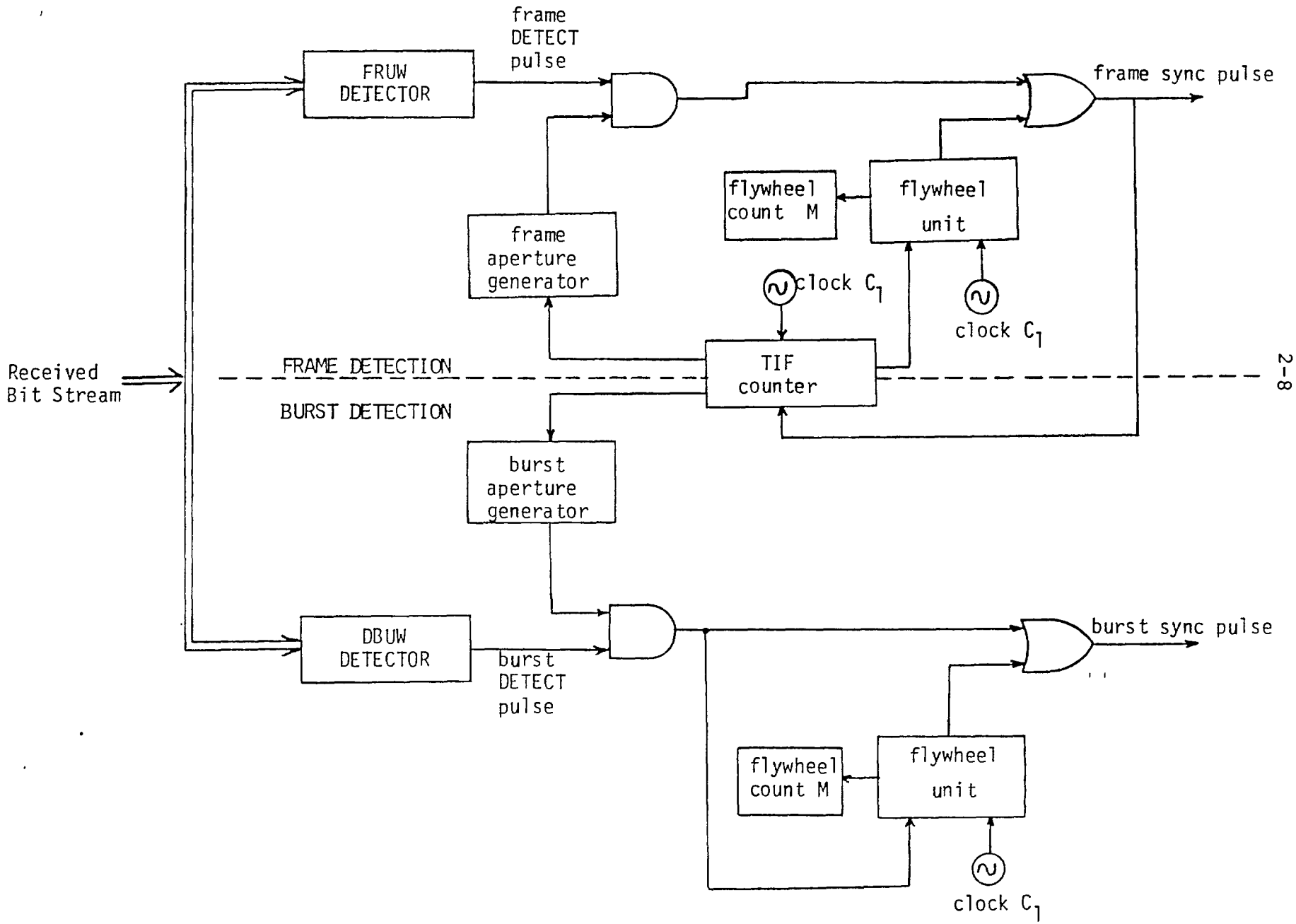
frame
DETECT
pulse
FRUW
DETECTOR
frame sync pulse
flywheel
count M
flywheel
unit
frame
aperture
generator
clock C_1
clock C_1
Received
Bit Stream
FRAME DETECTION
TIF
counter
BURST DETECTION
burst
aperture
generator
DBUW
DETECTOR
burst sync pulse
burst
DETECT
pulse
flywheel
count M
flywheel
unit
clock C_1

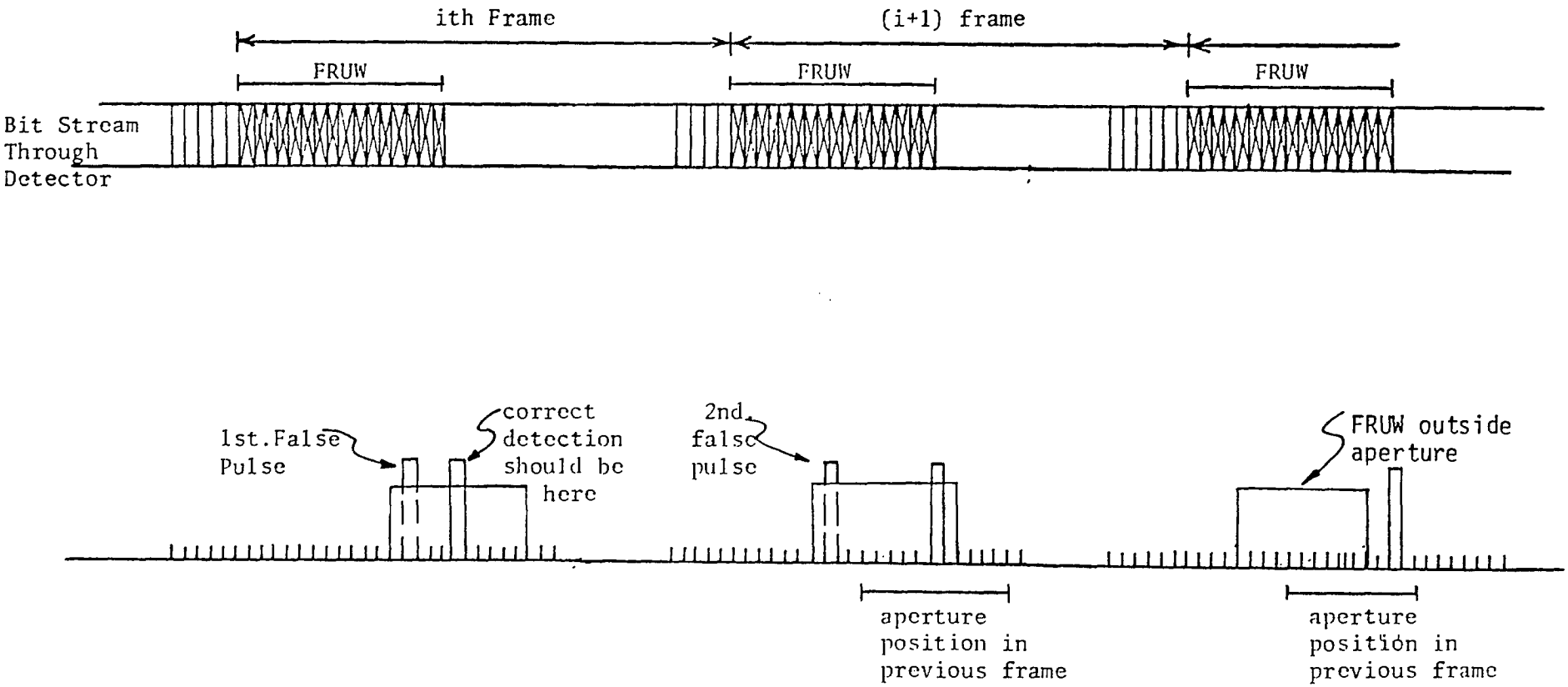

Figure 2.5 FRUW Aperture Drift Due To False Detections.

Maintaining downlink burst sync only affects the terminal's receive capability and yet defines some unique operational constraints of its own. Some of these constraints are addressed in the following section.

2.1.2 Acquisition And Retention of Burst Sync

After acquiring frame sync the terminal is able to generate apertures to receive any data burst in the frame. The burst's DBUW is also detected by digital correlation. No bit-by-bit scan or multi-mode acquisition algorithm is executed in establishing burst sync. The TIF counter used to generate apertures for the FRUW is also used to generate the required burst aperatures in the frame. Currently, no provision is made for the Slim TDMA terminal to "seek" a given data burst.

In steady-state operations the non-appearance of a DBUW within its aperture also results in the activation of a burst flywheel unit. Here two distinctions must be made:

(a) If a closed-loop terminal is unable to detect its own data burst then a flywheel count M must be imposed (as in frame sync) beyond which transmission is inhibited. This is due to closed-loop terminals deriving their transmit-timing from the offsets between the FRUW and their own burst.

(b) If the closed-loop terminal is flywheeling a remote DBUW (not its own) then loss of burst sync need not inhibit the terminal's operations. Continued non-detection of this data burst does, however, cause the receiving terminal to issue a "carrier-fail" alarm that is relayed to the terminal's baseband interface [1].

Another unique aspect of a terminal's burst-detection operations concerns the tracking of timing-errors in the burst's position. If the terminal is receiving the data burst from a terminal operating in closed-loop uplink sync then the burst apertures are generated at a fixed interval equal to the nominal frame length. Path delay variations and clock timing errors are tracked by the transmitting terminal which periodically adjusts its transmit-timing. However, if the received data burst originates from a terminal in open-loop sync then the above timing errors are tracked by the receiving terminal. This is done by aperture-tracking. Two such tracking algorithms are detailed below, namely: (i) free aperture tracking (FAT), and (ii) constrained aperture tracking (CAT).

In the FAT algorithm the only constraint on the aperture's movement is that its displacement should not exceed one half of the inter-burst guard time. However, this freedom of aperture movement to track the DBUW introduces the possibility of false detections luring the aperture away from the actual current position of the DBUW. Figure 2.6 illustrates how this unconstrained aperture adjustment can cause the UW detector to miss the DBUW.

In the CAT algorithm the aperture adjustment is limited to a correction of X bits per frame. Although various heuristic values of X can be used, no analytical justification of any presently exists. Figure 2.7 presents one such scheme in which movement is restricted to one-bit position per frame (X=1) in response to a perceived shift in the DBUW's position. Note that the loss of the DBUW within the aperture depicted in Figure 2.6 cannot occur here as a result of only two false detections in the CAT

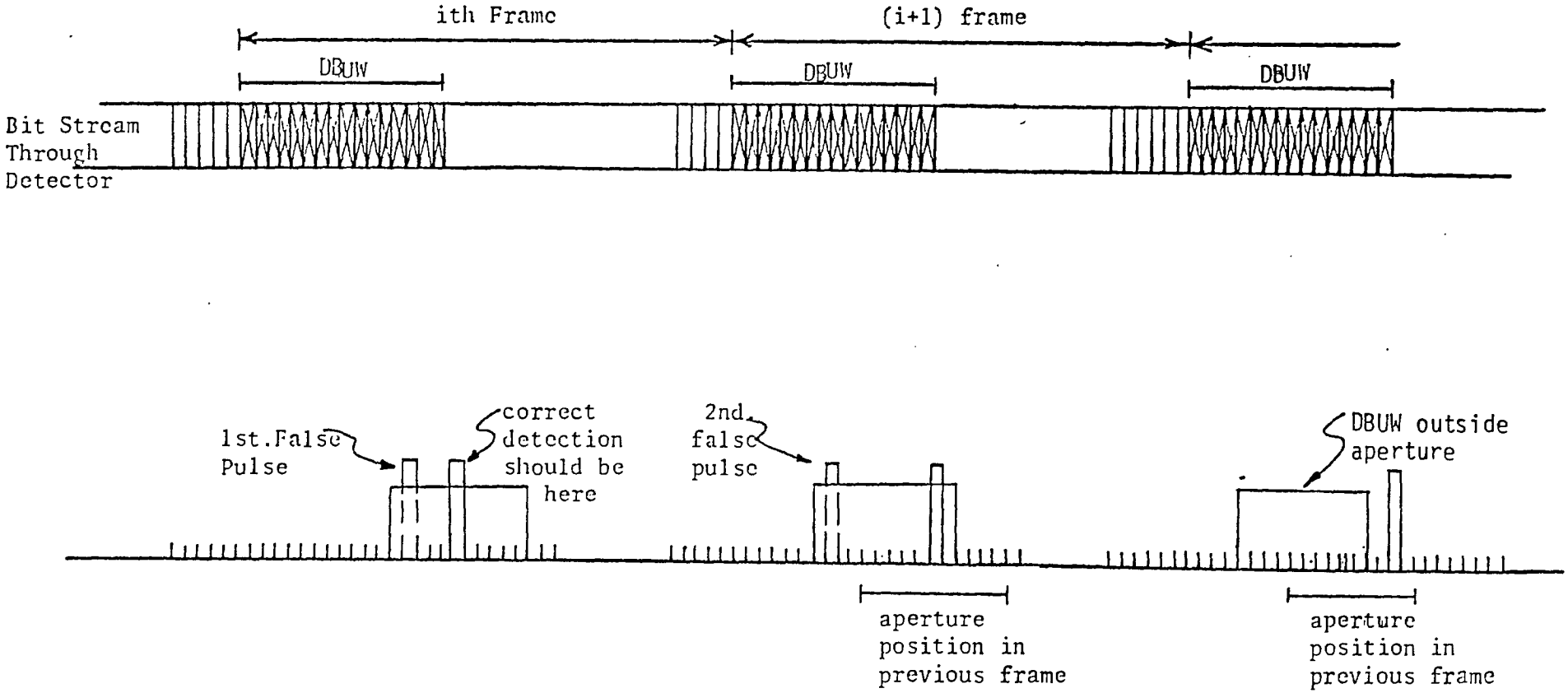

Figure 2.6 DBUW Aperture Drift Due To False Detections; Open-loop Using FAT Algorithm.

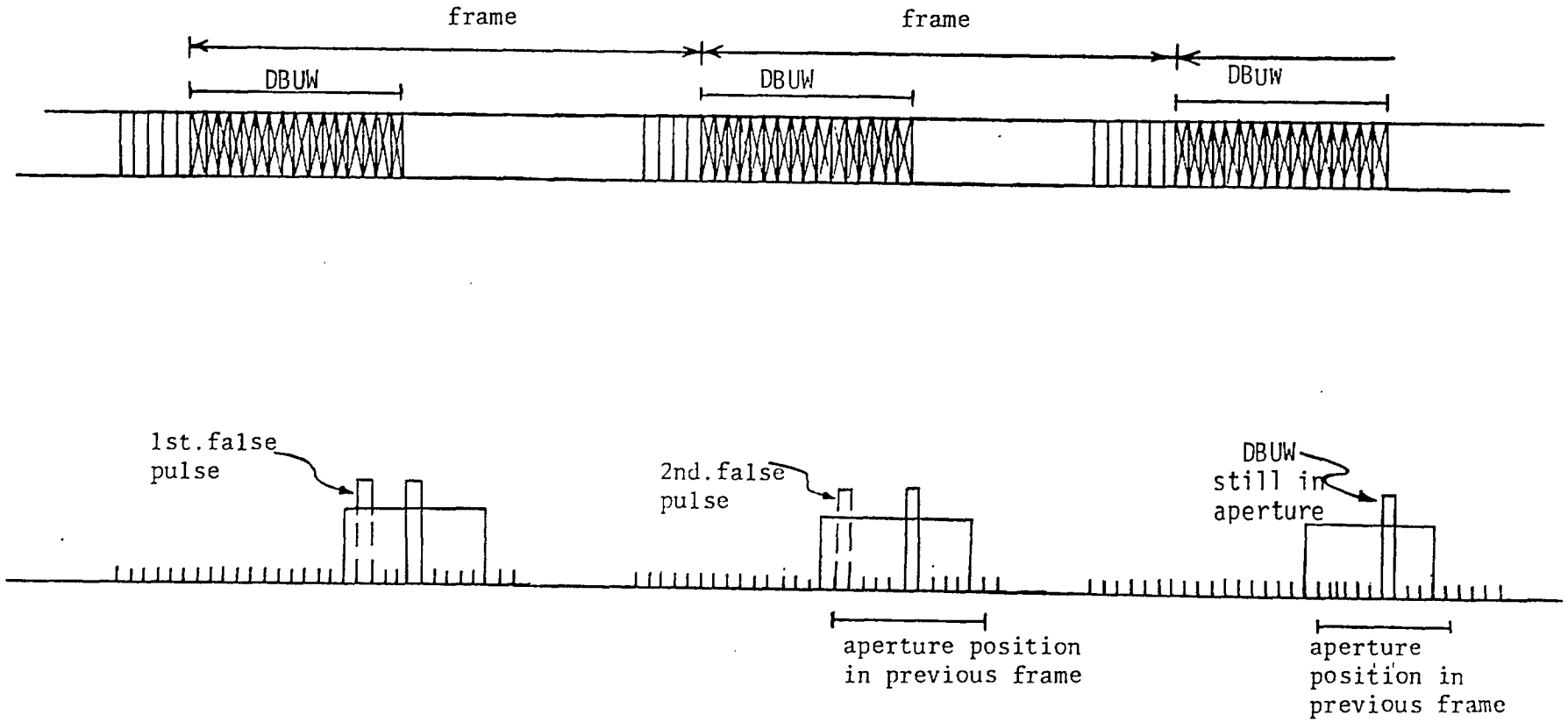

Figure 2.7 DBUW Aperture Drift Due To False Detections; Open-loop Using CAT Algorithm (one bit/frame).

algorithm. However, too constrained an algorithm (small x) may be of little use for bursts experiencing significant drifts in their receive positions. Furthermore, data burst aperture tracking must be inhibited during flywheeling the DBUW unless the flywheel unit has access to ranging information to update the position of the DBUW aperture.

The tracking algorithms executed by the Slim TDMA terminal for the FRUW and DBUW can be summarized as follows:

(1) The FRUW's aperture automatically tracks the FRUW as a result of how the aperture's timing is derived from the frame sync pulse (Figure 2.4). Drifts of the FRUW relative to its aperture are primarily due to timing errors caused by doppler frequency variations and oscillator instabilities.

(2) DBUWs originating from terminals in closed-loop sync are not tracked by their apertures as their transmit-times are adjusted at their respective origins. Shifts in their relative positions are similarly due to doppler variations and oscillator instabilities; but also to errors in the originating terminal's adjustment of transmit timing.

(3) DBUWs originating from terminals in open-loop sync are tracked by their apertures using the FAT/CAT algorithm. Shifts in the relative positions of a DBUW and its aperture are also due to doppler variations and oscillator instabilities. However, errors in open-loop range measurements (or predictions) also contribute to this displacement.

In cases 1 and 3 above, false detections will also cause a shift in the UW's position within its aperture. With respect to the terminal's transmit/receive operations, a flywheel count M (inhibiting transmission) need only be applied to the retention of the FRUW and the terminal's own data burst.

The following section briefly identifies the indices by which a terminal's acquisition and retention performances will be evaluated.

2.2 Operational Performance Indices

2.2.1 Acquisition Performance

The performance indices for the terminal's acquisition capability are:

(i) The mean time to acquisition of frame sync (MTTA); and is measured from the instant the detector begins a bit-by-bit scan of the received bit stream.

(ii) The probability of false acquisition (P_{FA}); and represents the probability that the terminal completes its acquisition algorithm by locking onto an incorrect n-bit pattern.

These indices are a function of the length and format of the FRUW, the wide aperture A_W and the verification count L. The indices will be evaluated as a function of the channel's BER.

2.2.2 Retention Performance

Similarily, the performance indices used to evaluate the terminal's ability to retain frame sync are:

(i) The mean time between consecutive losses of frame sync (MTBSL); and represents the average duration spent by a terminal in frame sync (and capable of executing its TDMA functions).

(ii) The probability of false detection (P_{FDB}) occurring within the narrow aperture A_{VN} during the steady-state operations.

These indices are a function of the length and format of the UW, the narrow retention aperture A_{VN}, the detection threshold I, the relative timing error and the flywheel count M. As in acquisition, the retention performance indices are evaluated as a function of the channel's BER.

2.2.3 Link Availability

Individually, neither the performance indices for acquisition nor retention can adequately represent the expected fractional amount of time (in a continuum of operating time) that the terminal is in an "up" state. Consider for example the illustrative scenario where the termnal's MTBSL is 24 hours, but its MTTA is 1 hour. It will be shown that such performance corresponds to an "up-time ratio" UTR of 0.96, i.e. in continuum the terminal maintains frame sync (and hence its receive-capability at least) for 96% of the time. This is far below typical link availabilities guaranteed by common carriers. Renewal theory is a convenient vehicle with which to estimate this relevant percentage of time during which the Slim TDMA terminal can maintain uninterrupted traffic links [15]. It is one of several measures of a common carrier's grade of service over a satellite link.

In general, we denote MTTO to be the terminal's meantime to operate. This the expected time required for a terminal to

be capable of supporting active TDMA links (receive or transit) measured from start-up (or from its most recent sync-loss). The terminal's MTTO can be the sum of several epochs which include: i) the mean time lapsed before sync-loss is detected, ii) the interval required to complete the manual or automated procedures to initiate the reacquisition algorithm, and iii) the time to execute the algorithm itself* The terminal's UTR can thus be defined as

$$UTR = \frac{MTBSL}{MTTO+MTBSL} \qquad (2.1)$$

It is clear that attempts to maximize the UTR by increasing the MTBSL must be at the "cost" of reducing timing errors and the probabilities of false detection and no-detection. Similarly, attempts to reduce the MTTO are at the risk of increasing the probability of false acquisition. In short, designing the terminal's synchronization performance involves a tradeoff between the MTBSL and the MTTO. In [16] the nominal bound set for the UTR was specified by the inequality

$$UTR \geq 0.9999 \qquad (2.2)$$

Other design constraints can be envisaged. for example, it may be required to determine the pair {MTTO, MTBSL} for which the UTR is maximum subject to a cost constraint. Or the pair for which the cost is a minimum but the UTR exceeds a prescribed lower bound. A generalized investigation of these tradeoffs is presented below.

---

*In fully automated control/monitoring facilities MTTO ≈ MTTA.

If the UTR must be at least α, then from equation 2.1

$$\frac{MTBSL}{MTTO + MTBSL} \geq \alpha \qquad (2.3a)$$

or

$$MTBSL \geq \frac{\alpha}{1-\alpha} MTTO \qquad (2.3b)$$

The set of valid pairs {MTTO, MTBSL} which satisfy this latter inequality are depicted by the shaded region in Figure 2.8. Practical limitations on the MTTO are defined by the acquisition algorithm's verification count and the recovery procedures deployed. We denote this lower bound by X_1. Similarly, a lower bound X_2 can be envisaged for the MTBSL (defined by practical traffic requirements), and an upper bound X_3 (defined by state-of-the-art limitations). Figure 2.9a and 2.9b illustrate the resultant regions of feasibility for $X_2 \geq \alpha X_1/(1-\alpha)$ and $X_2 \leq \alpha X_1/(1-\alpha) \leq X_3$ respectively.

Practically, it is not unreasonable to assume a cost function, denoted by C(MTTO, MTBSL), such that

$$\frac{\partial c(MTTO, MTBSL)}{\partial MTBSL} \geq 0 \qquad (2.4)$$

i.e. the cost function is a non-decreasing function of the MTBSL. Consequently, if the design objective is to select the pair {MTTO, MTBSL} such that the UTR is maximized subject to a cost constraint C(MTTO, Mtbsl) $\leq$ C then the Lagrange multiplier approximation technique can be used to maximize the function [18,19]:

$$U(MTTO,MTBSL) = \frac{MTBSL}{MTTO+MTBSL} - \lambda c(MTTO,MTBSL) \qquad (2.5)$$

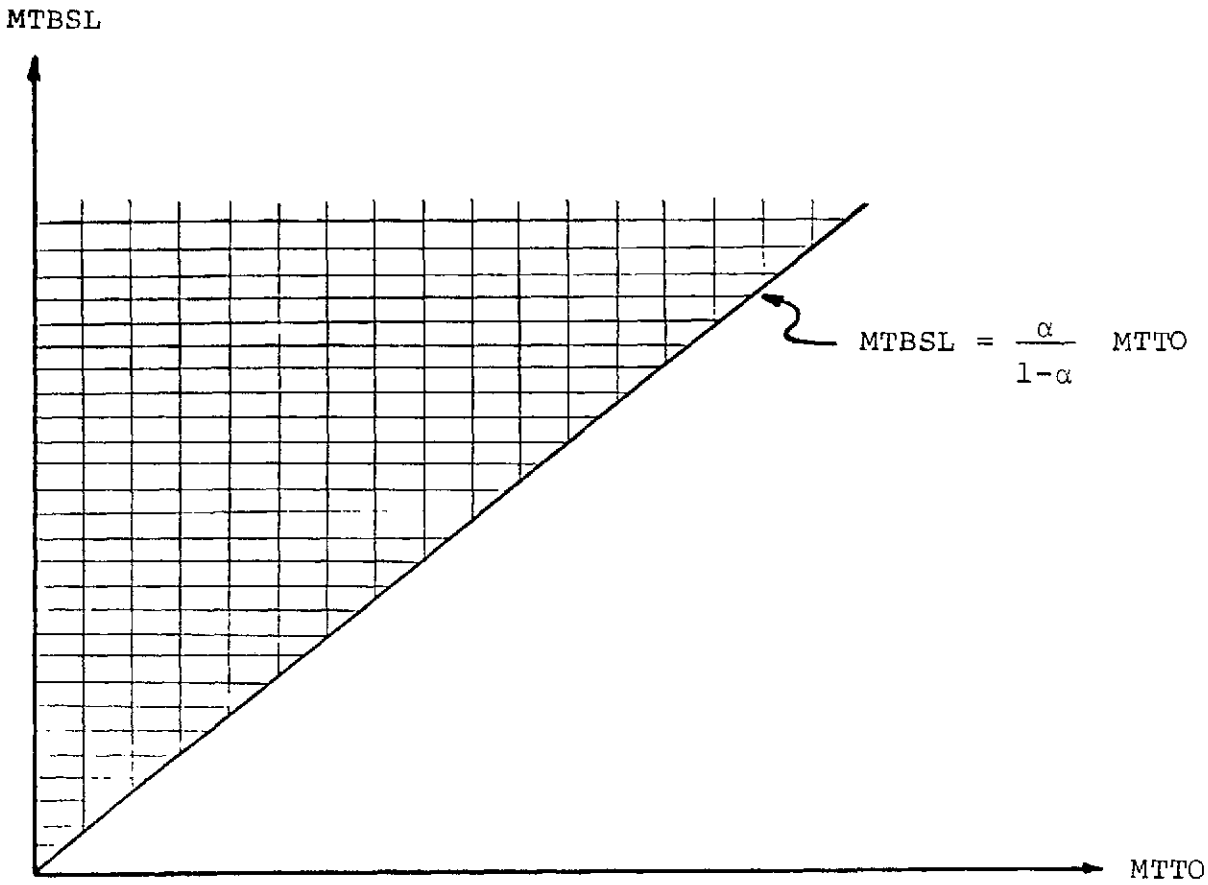

Figure 2.8 Design Feasibility Region (MTTO, MTBSL)

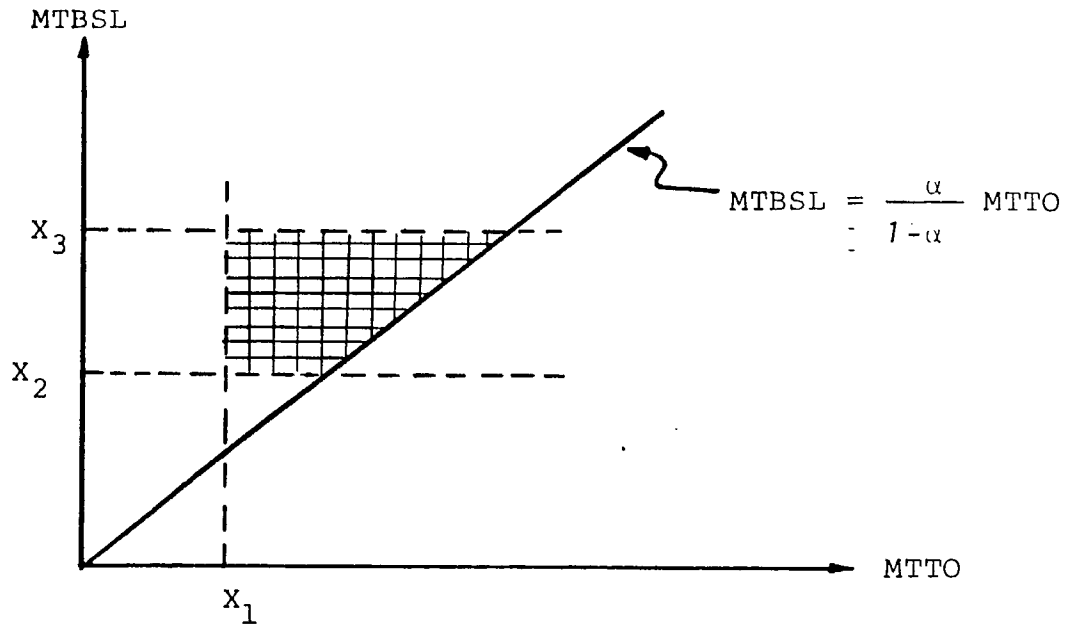

a) $X_2 \geq \frac{\alpha}{1-\alpha} X_1$

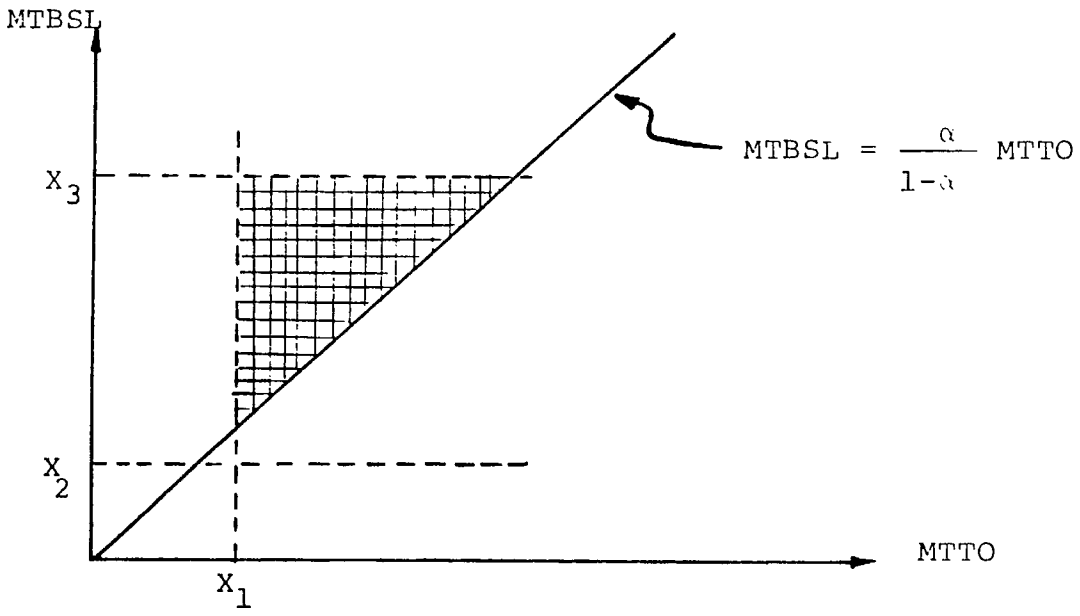

b) $X_2 < \frac{\alpha}{1-\alpha} X_1 \leq X_3$

Figure 2.9 Constrained Feasibility Region (MTTO, MTBSL)

subject to the constraints

$$MTBSL \geq 0$$
$$MTTO \geq 0$$
$$c(MTTO, MTBSL) = C \qquad (2.5)$$

However, in this report no cost function has been formulated and the parametric analysis of acquisition and retention will focus on satisfying the inequality given by equation 2.2. The development of a cost-constraint detailed in equations 2.3 to 2.6 is presented as a possible design approach if a cost function is formulated.

Qualitative tradeoffs in selecting the terminal's parameters can be made by identifying their impact on the above performance indices. Table 2.1 summarizes the predominant tradeoffs for each terminal parameter. The remainder of this report focuses on the analytical models used to quantify these tradeoffs.

Omitted from Table 2.1 are the affects of selecting the UW format. The following points are made regarding the format of the n-bit pattern:

(1) A UW consisting of all 0's or all 1's is not an acceptable format because any n-bit positional shift of the correlator may be registered as a detection. The probability of this event is highest during the wide-aperture SCAN mode in which bits preceding and succeeding the UW each have a 0.50 probability of being 0 or a 1 and thus false detections can occur $T_b - 1$ times during the frame scan of T_b bits;

SYNC MODE	PARAMETER	COMMENTS
INITIAL ACQUISITION	UW Length	(a) too short a UW results in rapid acquisition but high probability of false acquisition; (b) too long a UW results in low probability of false acquisition but lengthy acquisition times as the long word is vulnerable to bit-errors and the detector seeks a perfect match;
	Aperture A_W	(a) too wide an aperture renders the detector vulnerable to false detections (filter analogy); (b) too narrow an aperture may cause the UW to drift beyond the aperture as a result of satellite motion and/or local terminal's timing errors;
	Verification count L	(a) too low a count results in rapid acquisition but high probability of false acquisition (b) too high a count ensures correct acquisition but unnecessarily prolongs the MTTA;
RETENTION	UW length	(a) too short a UW results in reduced preamble length but frequent false detections within the aperture A_{VN}; (b) too long a UW reduces prob. of false detection but increases preamble length and probability of mis-detection;
	Aperture A_{VN}	see aperture A_W above
	Detection Threshold I	(a) too low a threshold causes frequency rejection of the true UW and activation of the flywheel unit; (b) too high a threshold renders the detector vulnerable to false detections that may disrupt the generation of apertures;
	Timing Errors	(a) very small timing errors over a frame interval are achieved at the cost of highly stable network synchronization and tight station-keeping; (b) high timing errors limit the flywheel count and reduce the MTBSL;
	Flywheel count M	(a) too high a flywheel count will result in renegade terminals that have lost frame sync but continue to transmit blindly; (b) too low a flywheel count will unnecessarily reduce the MTBSL and withdraw the terminal from operation

Table 2.1 Summary of Parameters Influencing Performance Indices

(2) A UW consisting of alternating 0's and 1's means that the average output of the correlator (number of agreements with current contents of shift register) is n/2. The correlator's output at the correct UW is n, but since surrounding data is assumed random then false detections can occur at multiples of 2-bit positions displaced from the true UW;

(3) Note that the use of differential decoding during initial acquisition prevents the FRUW and DBUW from being logical complements.

(4) The performance of Pseudo-Noise (PN) sequences (and their Barker Codes subset - see [3 - 4]) as a UW in TDMA experiments has been quite successful. A primary advantage of such sequences is that their auto-correlation function reaches a maximum at coincidence (zero delay) and is near zero at other delays, yielding a high tolerance to bit errors within an aperture narrower than twice the UW length and minimizing false detections in the SCAN mode (see [5], p.342).

In [6] a discriminating criterion, the Inherent Error Tolerance of a code, is proposed. This selection criterion is used to quantify the pattern's susceptibility to false detections as a function of its correlation properties and the channel's BER. Such a criterion presents a mathematical (and more rigorous) argument against the selection of the first two patterns discussed above. Most PN sequences and Barker codes of reasonable length satisfy this criterion. Section 3 presents an alternate selection method also based on correlation properties of the n-bit pattern.

3.0 CRITERIA FOR SELECTION OF UNIQUE WORD FORMAT

3.1 Introduction

The bibliography in [2] presents an extensive list of references in which varied mathematical structures are used to define an "optimum" PCM synchronization pattern subject to one or more constraints. However, the differences between the performances of several "good" UW formats should not be dwelled upon, as it is overshadowed by the practical problem of: (a) acquiring reliable synchronization quickly; and (b) maintaining it for a reasonable length of time. Both operational objectives must be satisfied in the presence of channel noise and network synchronization errors, both are reflected in the performance indices defined in Section 2.2, and both are practical objectives that view the problem in perspective by realizing the surprisingly acceptable performance attained from a UW pattern derived by flipping an unbiased coin n times.

3. Correlation Properties of Sync Words

Irrespective of the application, a practical means of providing frame synchronization over a digital link is to peridocially insert a fixed-length bit-pattern (or "sync word") into the data stream. Assuming that symbol synchronization has been acquired by the receiver, frame sync can be obtained by locating the position of the sync word. Typically, the search for the sync word is performed by a digital correlator as shown in Figure 1.2.

By far, the majority of work defining correlation criteria that can be used to select sync words is based on the assumptions that: (a) the word is embedded in random binary data, and (b) the digital link is an additive white gaussian noise (AWGN) channel. Both assumptions are valid for applications in space telemetry. In [7] optimal decision rules are derived for such an environment, and extended to cases where the data bits are gaussian random variables (instead of random binary) as in some pulse-amplitude modulated schemes (e.g. digitized voice).

Figure 3.1 points out that the assumption of random data is not valid in view of the deterministic preamble preceding the FRUW*. Deriving an optimum correlation rule for sync words appended to deterministic preambles is an exercise beyond the scope of this report. Furthermore, several existing code structures promise very acceptable performance. In [8] it is shown that when a bit correlation sync rule is used, the probability of a false detection is minimized by selecting the n-bit word for which $|C_m|$ is minimized over the range $1 \leq m \leq n-1$, where C_m is given by

$$C_m = n-m-2 \sum_{i=0}^{n-m-1} (S_i \oplus S_{i+m}) \quad 0 \leq m \leq n-1 \tag{3.1}$$

and plotted in Figure 3.2 for a sample 8-bit word. Ideally, this autocorrelation function should have the property

$$|C_m| \leq 1 \qquad 1 \leq m \leq n-1 \tag{3.2}$$

*The AWGN channel, however, is a typical model for a digital satellite link.

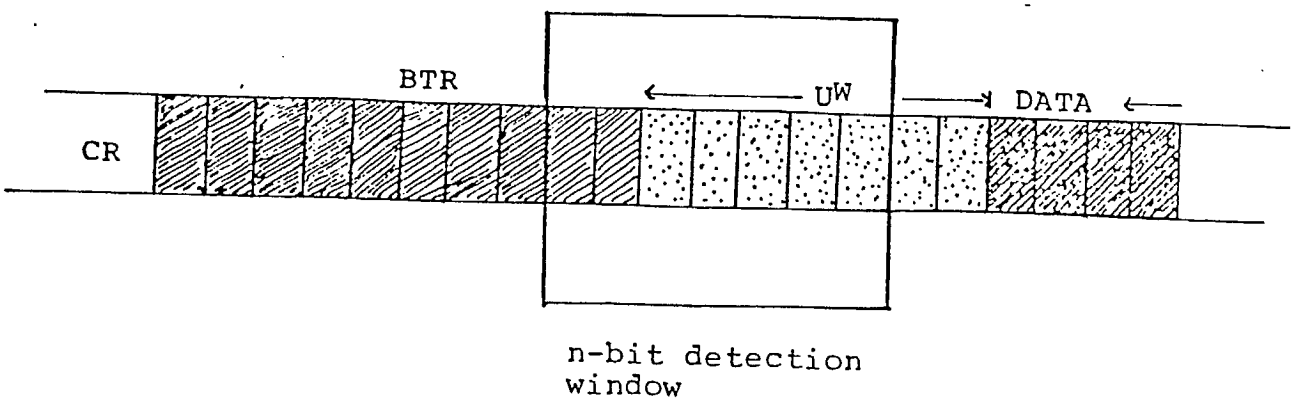

Figure 3.1 Detection Window Scanning Preamble

	S_0	S_1	S_2	S_3	S_4	S_5	S_6	S_7
Sync word:	0	1	0	0	1	0	1	1

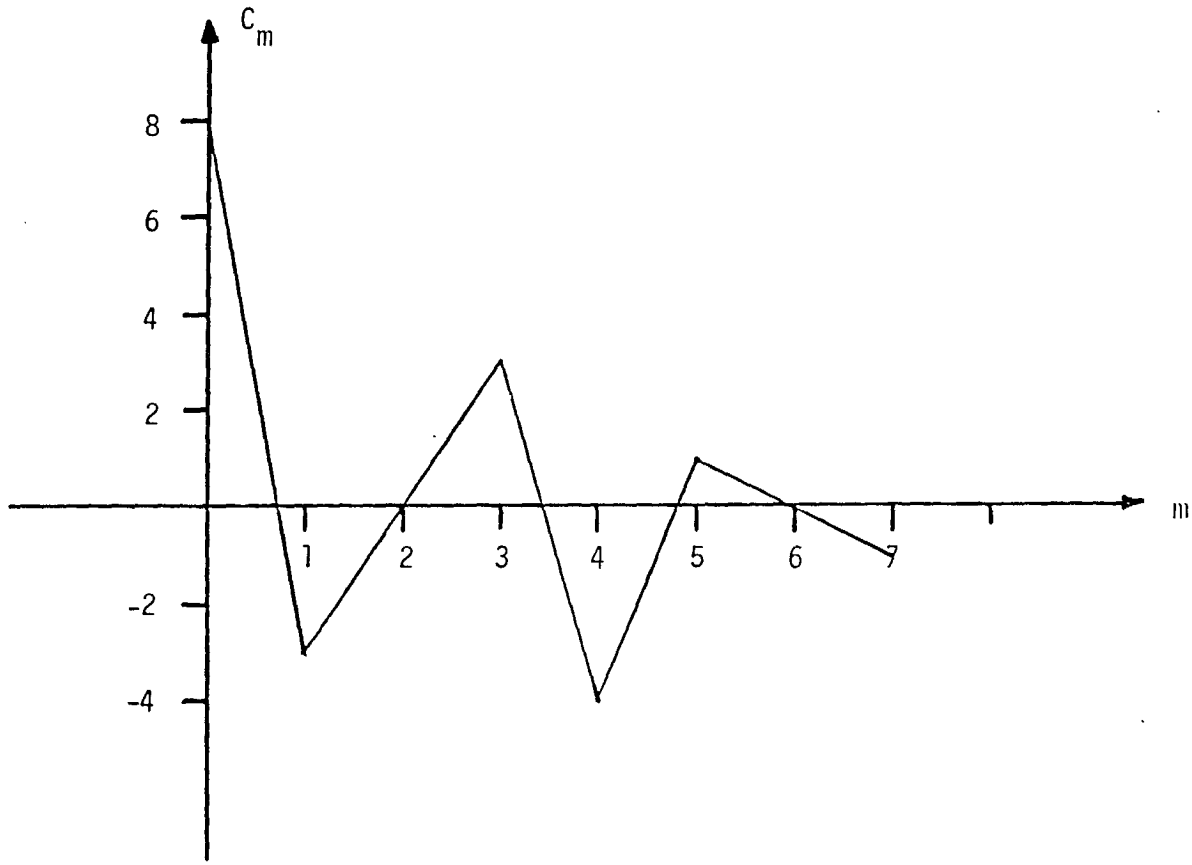

Figure 3.2 Sample Correlation Plot C_m

Sequences with sidelobe correlations satisfying this property are called Barker codes [5, 7], and are considered excellent sync words for the AWGN channel. However, no Barker sequence of length greater than n=13 bits has been generated as yet [5]. In [7] simulation results indicate that a class of codes termed Newman-Hofman codes match the performance of Barker codes for $n \leq 13$ in random and gaussian variable data environments. In [10] Newman and Hofman generate their codes for any length n by the following criteria:

(a) for channels with high BER, C_{max} is minimized over all 2^n candidate words;

(b) for channels with low BER, D_{min} is maximized over all 2^n candidate words;

where C_{max} defines the maximum sidelobe correlation given by

$$C_{max} = \max\{|C_m|;\ 1 \leq m \leq n-1\}; \tag{3.3}$$

and D_{min} is defined as the minimum distance

$$D_{min} = \min\{D_m;\ 1 \leq m \leq n-1\} \tag{3.4}$$

where D_m is given by

$$D_m = n - \sqrt{m} - |C_m| \tag{3.5}$$

Note that although it is still desirable that $|C_m|$ be near zero for $m \neq 0$, the constraint in equation 3.2 must be relaxed for non-Barker codes.

Stated simply, the reasoning presented in this section is developed along the following lines:

(i) most correlation criteria for selecting a sync word were developed with PCM telemetry in mind and are not directly applicable to TDMA's unique preamble constraints;

(ii) the objective of this report is not to digress into efforts to provide the "optimal unique word";

(iii) several simulation results in the recent literature indicate classes of codes that perform very well in comparison to the optimized correlation constraints.

A sample set of such code words is generated (for a pattern length n) by applying the Newman-Hofman criteria in equation 3.3 and 3.4 to all 2^n candidates. A computational obstacle to this approach is the search effort required for long sync words. In [10] it is shown that the search can be limited to 2^{n-2} binary tuples (instead of 2^n) by realizing that complementary and reversed sequences yield identical values of C_{max} and D_{min}. However, for long sync words the search remains prohibitive. In the following section, selection criteria from [8, 9] are proposed as a means of limiting the search to a subset I_n code words, where $\{I_m\} \ll 2^{n-2}$.

3.3 Proposed Selection Criteria

In [8] Levitt proposes to confine the search for a sync word of length n to a subset I_n of words which are prefixes of pn sequences of length 2^k-1 where k is defined by

$$2^{k-1} < n+1 < 2^k \qquad (3.6)$$

It must be clearly noted that the suitability of these prefixes as sync words in not directly derived from their association with pn sequences. Conditions and constraints satisfied by one group need not be satisfied by the other. However, the set I_n does present two practical advantages:

(1) the cardinality (size) of the set grows much more slowly than 2^n; and

(2) all n-bit pn sequences for $61 \leq n \leq 63$ can be generated by a finite set of linear recursion formulae [11].

These advantages present a storage gain and a search-time gain, particularly for long sync words. To the set I_n, Levitt [8] applied the following selection algorithm derived from the Newman-Hofman study [10]:

criterion I: For high BER applications, select the word(s) in I_n that achieve the minimum C_{max}; of these, select that word having the maximum D_{min}.

criterion II: For low BER applications, select the word(s) in I_n that achieve the maximum D_{min}; of these, select that word having the minimum C_{max}.

Note that for some values of n, the same n-tuple may satisfy both criteria. Figure 3.3 presents the flowchart for the above selection algorithm, and includes the testing of the selected n-tuple(s) using the acquisition and retention models presented in Section 4. Table 3.1 lists the set of recursion formulae required to generate pn

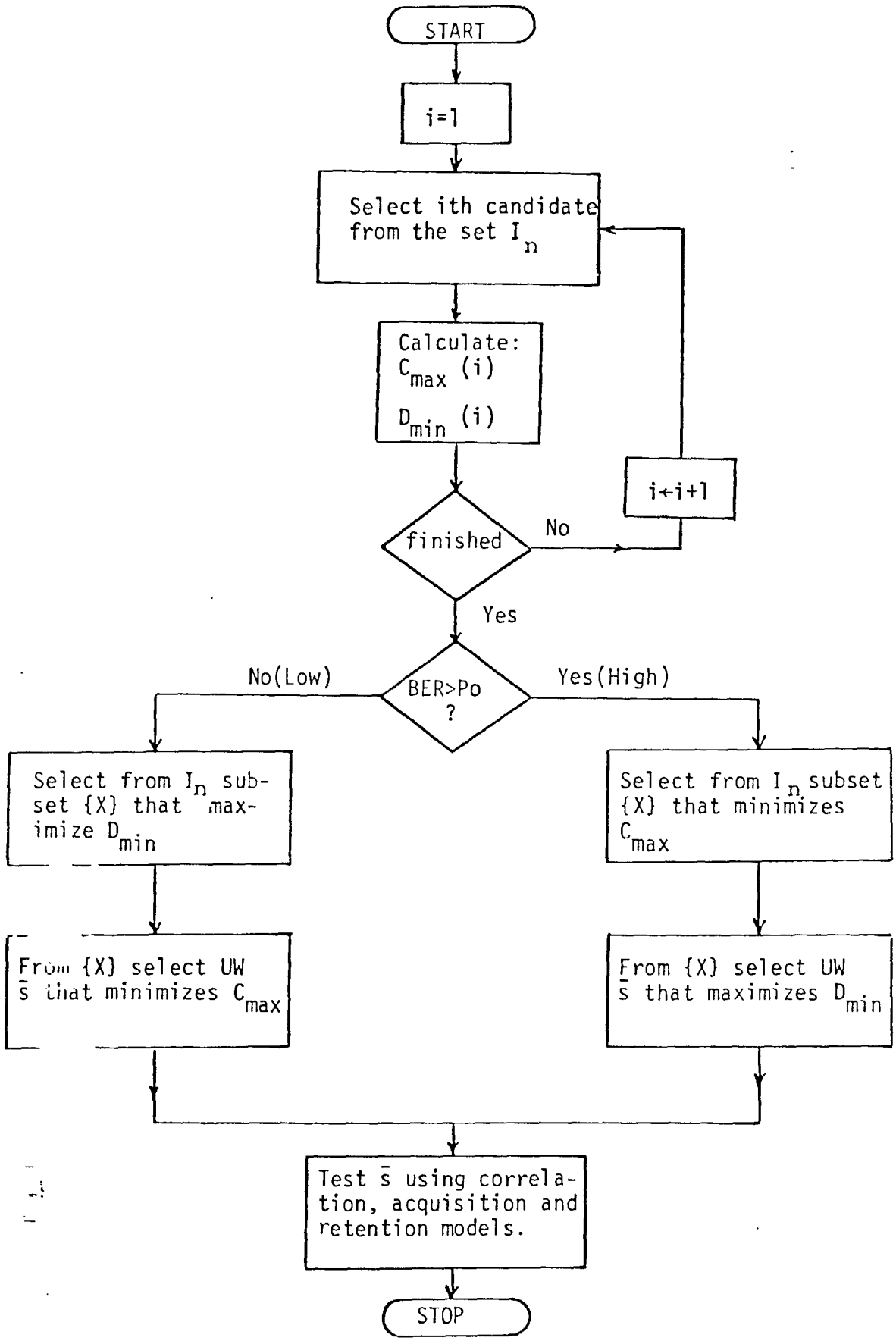

Figure 3.3 Performance Evaluation of Selected Sync Word

sequences of length n, for $16 \leq n \leq 63$ [9, appendix C]. Each configuration of length k can generate (2^k-1) different pn sequences depending upon which of the k-bit seeds $\{d_0, d_1, \ldots d_{k-1}\}$ is used (excluding the all-zero seed). Comparison to simulation results presented in [10] supports Levitt's contention that little is lost by confining the selection of a sync word to I_n.

Presented in this section is one of several algorithms for selecting suitable sync words. Two practical advantages distinguish it from the majority of existing search methods: (a) computational storage requirements, and (b) search time. These advantages are compatible with the realization that of the 2^n binary n-tuples, only a small subset are unsuitable as sync words. The algorithm proposed here ensures that the candidate n-tuple generated is <u>not</u> a member of this subset. Section 4 presents a brief description of the Markovian models used to estimate the TDMA terminal's acquisition and retention performance, using a FRUW generated by the selection algorithm in this section.

WORD LENGTH n BITS	RECURSION FORMULAE	SEEDS $\{d_0, \ldots d_{k-1}\}$
$16 \leq n \leq 31$	5A: $S_i = S_{i-3} \oplus S_{i-5}$ 5B: $S_i = S_{i-1} \oplus S_{i-2} \oplus S_{i-3} \oplus S_{i-5}$ 5C: $S_i = S_{i-1} \oplus S_{i-3} \oplus S_{i-4} \oplus S_{i-5}$	{00001 → 11111}
$32 \leq n \leq 63$	6A: $S_i = S_{i-5} \oplus S_{i-6}$ 6B: $S_i = S_{i-1} \oplus S_{i-4} \oplus S_{i-5} \oplus S_{i-6}$ 6C: $S_i = S_{i-1} \oplus S_{i-3} \oplus S_{i-4} \oplus S_{i-6}$	{000001 → 111111}

Table 3.1 Linear Recursion Formulae To Generate the Set I_n

4.0 PERFORMANCE MODELS: ACQUISITION AND RETENTION

4.1 Introduction

The Markovian models developed in this section are proposed as convenient analytical tools used to emulate the Slim TDMA terminal's burst synchronizer as it executes the prescribed acquisition and retention algorithms. The flexibility of the Markovian models is in contrast to earlier work that derived estimates for the performance indices $\{MTTA, P_{FA}, MTBSL, P_{FDBB}\}$ by expressing them as infinite sums of all possible combinations of events (see refs. 11, 27 - 30 in [2]). Not only did this require reformulation for distinct algorithms but for a given algorithm, exhausting all possible combinations of events becomes untenable. In Markovian analysis the "states" of the UW detector are defined and embedded in the states of a Markov chain. Conventional matrix operations are used to derive steady-state probabilities that the detector is in a given state, or the average time required before a given state is reach. In the following sections, the detector's states during initial acquisition and retention of frame sync are identified. Illustrative examples of the transitions between these states are also given. The generalized models used in the software programs are relegated to appendices for reference.

4.2 Markov Model For Acquisition

The unit of time is defined to be the unit frame duration. The model's states are only defined at the beginning of a unit of time. The probability of an event occurring that may cause the detector to alter its present state is termed a transition probability. The set of transition probabilities describing the detector's shifts from state (i) to state (j) is expressed as a transition matrix $P[p_{ij}]$ where p_{ij} is the transition probability between these states.

From Section 2 it is clear that the events which alter the detector's status during initial acquisition are all detection events (or non-detection events). The likelihood of these events will be defined as a function of the following probabilities.

(i) P_{FDO}: the probability of a false detection occurring in the random data while the aperture is suppressed and the detector is in the SCAN mode;

(ii) P_{ND}: the probability of no detection, false or otherwise, within a period of one frame length;

(iii) P_{FDW}: the probability of a false detection occurring within an aperture A_W imposed around the expected position of the UW;

(iv) P_{NDW}: the probability of no detection, false or otherwise, occurring within the aperture A_W.

The acquisition model's transitions are expressed as functions of the above probabilities. Two sample models are presented below to distinguish between CORRECT acquisition and acquisition which results from any L consecutive detections (false or not).

4.2.1 Correct Acquisition

Let state no.1 represent the detector at the start of its SCAN mode, state no.2 to represent the detector's interception of a false sync word, and state nos.3 to (L+1) represent the detector's interception of the true sync word. State no. (L+2) represents the LOCK-UP mode as a

result of the Lth true detection. Figure 4.1 depicts the resulting Markov chain for a verification count of L=2. An issue to note in this model is that although the verification counter records any detection, false detections are confined to a single state (no.2) and the detector is prevented from reaching the LOCK-UP state (no. 4) unless the detection is of the true sync word. Although this does not reflect the detector's actual behaviour, the correct-acquisition model is used to estimate the average time required for the detector to acquire correctly. This includes the time lost in tracking false detection and is used to select operational parameters that will ensure a high probability of correct acquisition. The following model allows any detection to advance the verification count toward lock-up.

4.2.' False/Correct Acquisition

Again state no. 1 represents the detector in the SCAN mode. States nos. 2 to L represent the detector's interception of the true sync word, and states nos. (L+2) to 2L represent the interception of a false word. State (L+1) represents the occurrence of the Lth consecutive detection (false or otherwise). Figure 4.2 illustrates this model's Markov chain for L=2. Note that the lock-up state (L+1) can now be reached by L consecutive true detections or L consecutive false detections.

To establish the validity of this analytical representation, results from Markovian models were compared to simulations and other analytical works [2, section 2.4]. These comparisons emphasized the facility with which the state diagrams can be reconfigured to yield results in close agreement with simulation and other complex analysis.

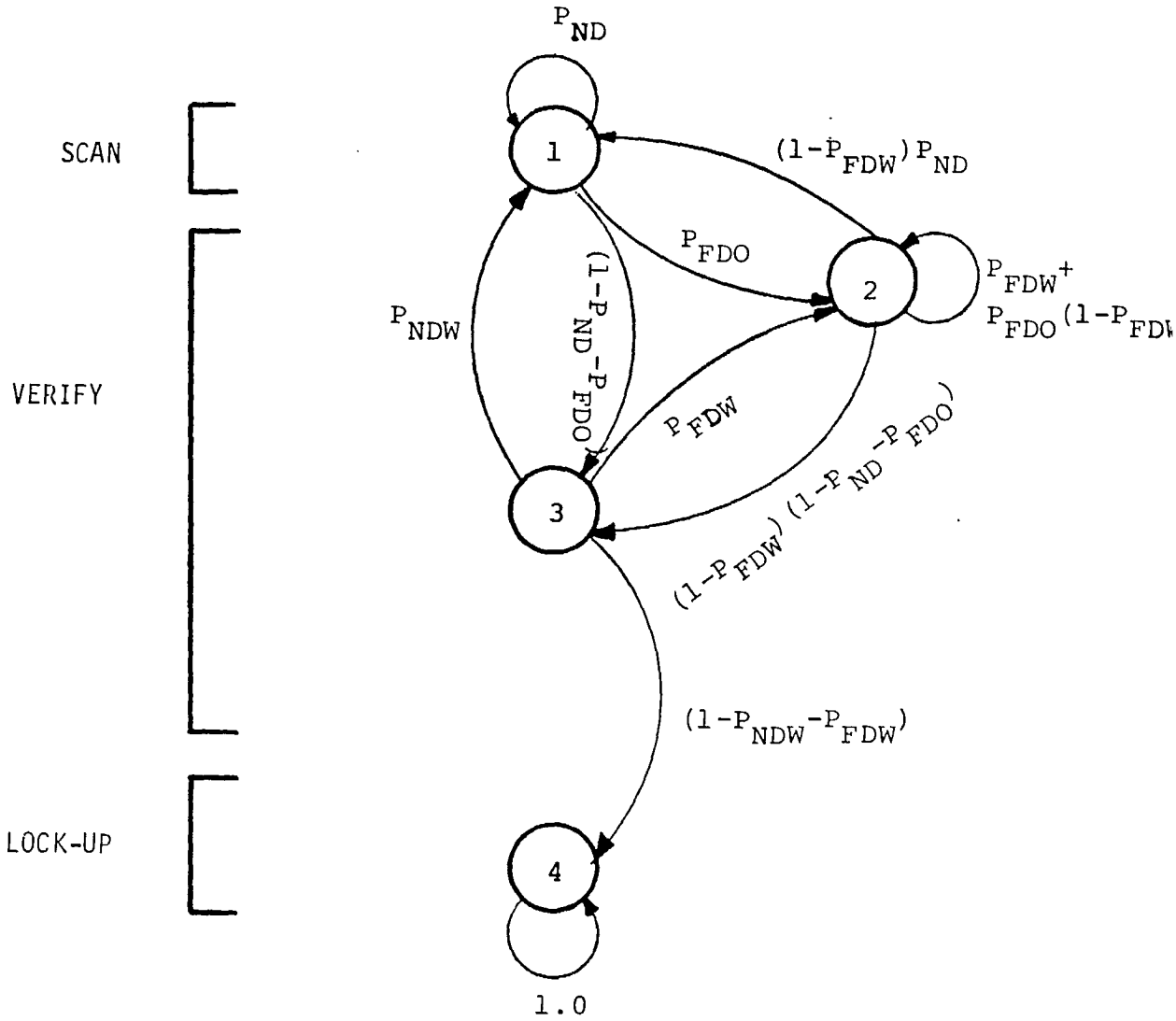

a) State Chain Diagram

$$\underline{P} = \begin{bmatrix} P_{ND} & P_{FDO} & (1-P_{ND}-P_{FDO}) & 0 \\ P_{ND}(1-P_{FDW}) & P_{FDW}+(1-P_{FDW})P_{FDO} & (1-P_{ND}-P_{FDO})(1-P_{FDW}) & 0 \\ P_{NDW} & P_{FDW} & 0 & (1-P_{NDW}-P_{FDW}) \\ 0 & 0 & 0 & 1 \end{bmatrix}$$

b) State Transition Matrix

Figure 4.1 Markow Model For Correct Acquisition (L=2)

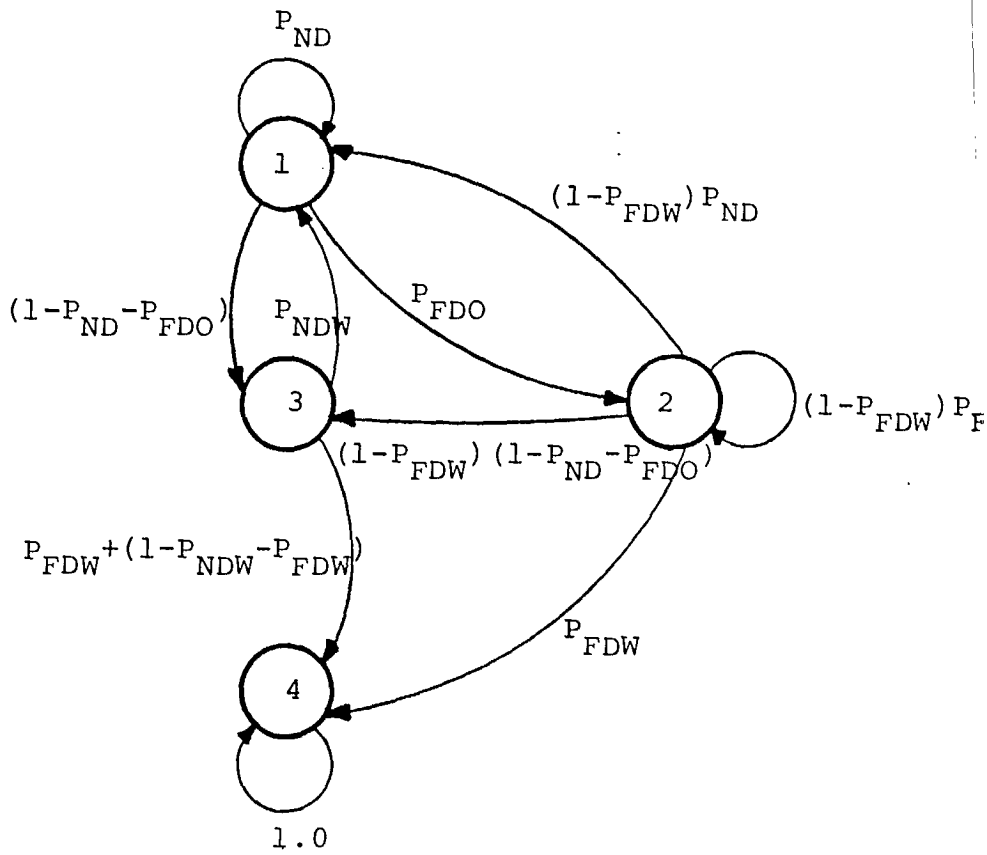

a) State Chain Diagram

$$\begin{bmatrix} P_{ND} & P_{FDO} & (1-P_{ND}-P_{FDO}) & 0 \\ P_{ND}(1-P_{FDW}) & P_{FDO}(1-P_{FDW}) & (1-P_{FDW})(1-P_{ND}-P_{FDO}) & P_{FDW} \\ P_{NDW} & 0 & 0 & P_{FDW}+(1-P_{NDW}-P_{FDW}) \\ 0 & 0 & 0 & 1 \end{bmatrix}$$

b) State Transition Matrix

Figure 4.2 Markov Model For Correct/False Acquisition (L=2)

4.2.3 Markovian Analysis For Acquisition

By defining $\underline{P}[p(k,j)]$ to be the transition matrix for the chain, $\vec{X}(0)$ to be the row vector of initial state assignment probabilities (notably [100.....0], and $\vec{X}(\alpha)$ to be the state assignment probabilities after α frame transitions, we have from [14]

$$\vec{X}(\alpha) = \vec{X}(0)\underline{P}^{\alpha} \qquad ;\alpha = 1, \ 2,... \tag{4.1}$$

We define a set S to be the set of non-recurrent states in the chain and Q to be the matrix

$$Q \triangleq [p(i,j): \ i, \ j \ \varepsilon \ S]. \tag{4.2}$$

In our model, S={1, 2,...L+1} for Figure 4.1, and S={1,2,...L, L+2, L+3,.....2L} for Figure 4.2. It is shown in [14] that the Mean Time To Acquire (MTTA) frame sync is given by the sum of the first-row entries in the matrix

$$N = [I-Q]^{-1} = [n_{ij}] \tag{4.3}$$

where [I] is the identity matrix.

Furthermore, a second moment can be derived for these important parameters by defining:

(a) N_S to be a column vector $[\sum_j n_{ij}]$, and

(b) N_{SQ} to be a column vector whose kth component is the square of the kth component in N_S

such that

$$N2 \triangleq (2N-I)N_S \tag{4.4}$$

is the second-moment matrix of the time to acquire, and

$$V \triangleq N2 - N_{SQ} \triangleq [v_{ij}] \tag{4.5}$$

is the variance vector. Consequently, the second moment $E\{t_A^2\}$ and variance σ_A^2 about the MTTA are given by

$$E\{t_A^2\} = \text{last element on first row of N2} \tag{4.6}$$

and

$$\sigma_A^2 = \text{last element on first row of V} \tag{4.7}$$

The detection and acquisition probabilities, and the first/second order statistics for the acquisition time are only a sub-set of the detection parameters that can be derived from the Markovian model. Although not all such parameters will be reduced to closed form expressions, the above technique does yield a closed form solution for the $MTTA_c$ given by:

$$MTTA_c = \begin{cases} \dfrac{P_{FDO}+(1-P_{FDW})(1-P_{FDO})}{(1-P_{FDW})(1-P_{ND}-P_{FDO})} & ; \text{ for } L=1 \\ \dfrac{P_{FDO}+(1-P_{FDW})(1-P_{FDO}) +(1-P_{FDW})(1-P_{ND}-P_{FDO})\dfrac{1-(1-P_{NDW})^{L-1}}{P_{NDW}}}{(1-P_{FDW})(1-P_{ND}-P_{FDO})(1-P_{NDW})^{L-1}} & \text{for } L>1 \end{cases} \tag{4.8}$$

Note that, as $P_{FDW} \rightarrow 1$ $MTTA_c \rightarrow \infty$ as expected. However, the corresponding MTTA converges to a finite value since the probability of false acquisition approaches one.

The detection probabilities $\{P_{FDO}, P_{ND}, P_{FDW}, P_{NDW}\}$ are derived in Appendix A as a function of: (i) the frame length T_b in bits, (ii) the UW length n, (iii) the aperture width A_W, (iv) the BER P and (v) the detector threshold I. In the Slim TDMA terminal's acquisition algorithm (see Section 2.1.1) the detection threshold is set to I=0.

In the general model's transition probabilities an approximation to the detector's performance is made to simplify the state representation. Figure 4.3 illustrates the aperture's recovery from a single (or double) false detection. After the first occurrence of the false sync word an aperture A_W is set in the next frame. The non-appearance of the false pattern causes the detector to immediately begin a new SCAN for the remainder of the frame. However, in the model, it is assumed that the detector will begin the SCAN mode from the start of a new frame. This approximation avoids the complexity of needing to define the location of the false sync occurrence in the frame and does not seem to distort the estimate of acquisition performance indices.

The following section develops a parallel presentation for the proposed retention model.

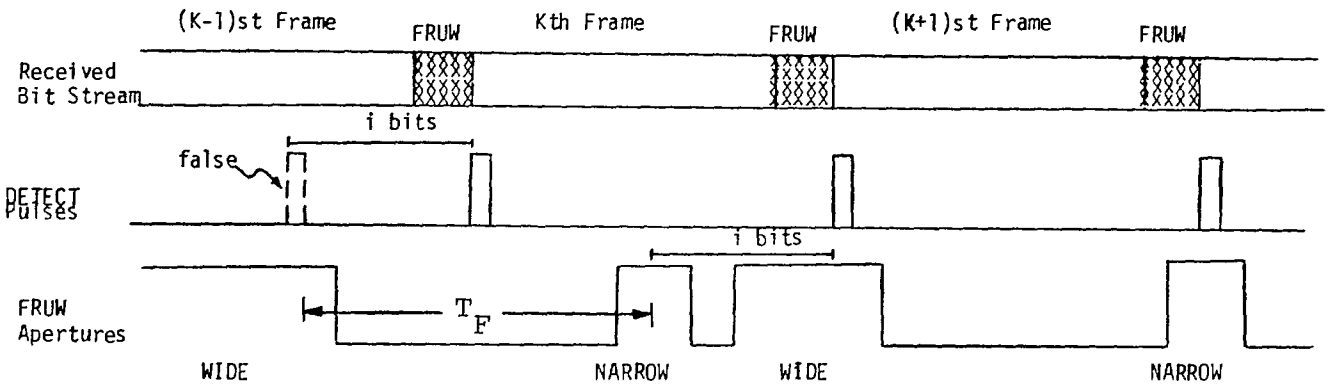

a) Aperture Behaviour : Single False Pulse.

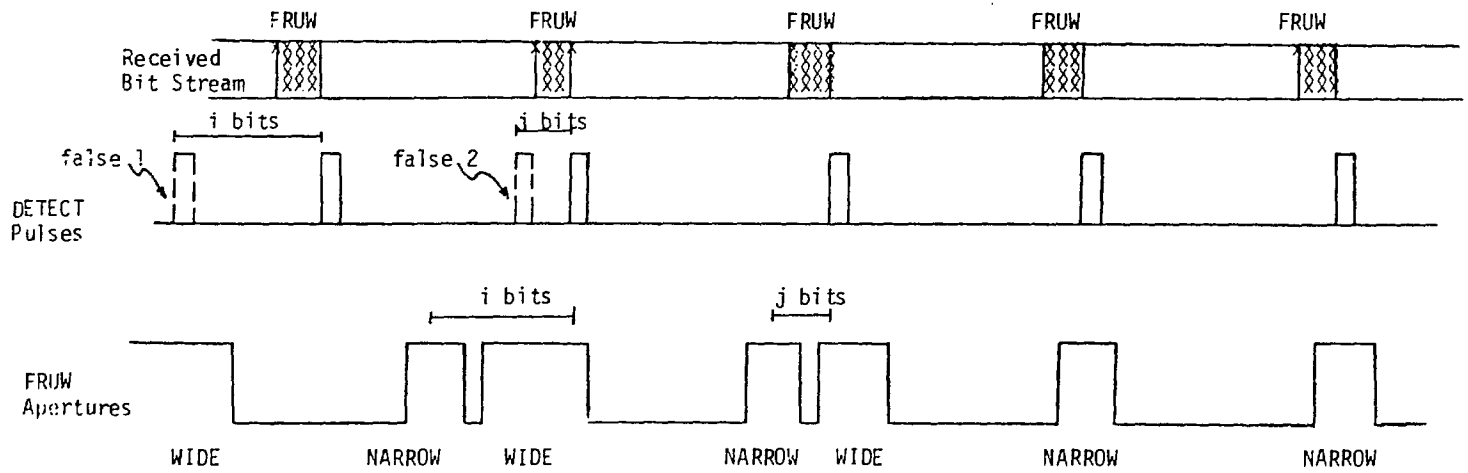

b) Aperture Behaviour : Double False Pulses.(j<i)

Figure 4.3 Aperture Recovery From False Detections.

4.3 Markov Model For Retention

Two inputs to the Markov model developed to represent retention of frame sync must first be addressed: (i) the occurrence of a false detection within the narrow aperture A_{VN}; and (ii) the accumulated time-shift between the received sync word and its locally generated aperture over a time interval of one frame.

4.3.1 False Detection In a Narrow Aperture

In the derivation of the detection probabilities for the acquisition model (in Appendix A) it was assumed that the aperture A_W is sufficiently wide that the detector continues to see the sync word embedded in random data. However, with a narrow aperture A_{VN} the possibility of a false detection becomes heavily dependent on the cross-correlation between the sync word and the preceding deterministic preamble. From Figure 3.1 it is clear that a portion of the bit-timing recovery (BTR) sequence is within the detector while the aperture is enabled. As a result, a better estimate for the probability of a false detection within an aperture must be derived.

We define the variable ℓ to be the distance (time shift) of the current contents of the detector from the true UW, and $P_D(\ell)$ as the probability of a detection at this time. Thus, $P_D(0)$ is the probability of detecting the UW when it occupies the detector and we can further define for a UW length n:

$Y(\ell)$: the output of the binary correlator when the UW is at position ℓ; [$Y(0) = n$ in the absence of bit errors]

$\varepsilon(\ell)$: $n-Y(\ell)$, the number of disagreements between the UW and the contents of the detector when the UW is at position ℓ;

$\phi(\ell)$: $\varepsilon(\ell) - I$, is the excess number of disagreements (above the detection threshold I) between the UW and the contents of the detector when the UW is at position ℓ*.

Figure 4.4a illustrates the position of the FRUW in relation to the detector. Note that values of $0 \leq \ell \leq A_{VN}/2$ fall within the aperture if it is centered. In Figure 4.4b the n-bit UW is conceptualized geometrically as a vector in an n-dimensional space. On the same space, we project the **expected** (i.e. error free) n-bit contents of the detector $T(\ell)$ for a given UW position ℓ. In this geometrical representation, we can depict the region of detection as a sphere of radius I centered about the true UW. The first n-bit sequence within the aperture that falls within the sphere will be accepted as the UW. Similarily, if the received UW is sufficiently corrupted by bit erros such that it falls outside the sphere, detection will not occur when $\ell=0$. If the output exceeds the threshold for any $\ell>0$ within the aperture, then a false detection results. Note that false detection can also occur <u>after</u> the UW but with much lower probability since it depends on missing the UW at $\ell=0$).

It is clear from Figure 4.4b that a false detection can occur, at distance $\ell>0$ from the UW, if $T(\ell)$ is sufficiently corrupted to fall within the sphere of radius I . This can be the outcome of only a finite number of events:

(1) the $T(\ell)$ bits are received correctly but all $\phi(\ell)$ of the $\varepsilon(\ell)$ bits are in error; or

---

*I must be sufficiently small that in the absence of bit errors $\phi(\ell)>0, \forall \ell \neq 0$. Otherwise, a false detection will occur even without channel errors.

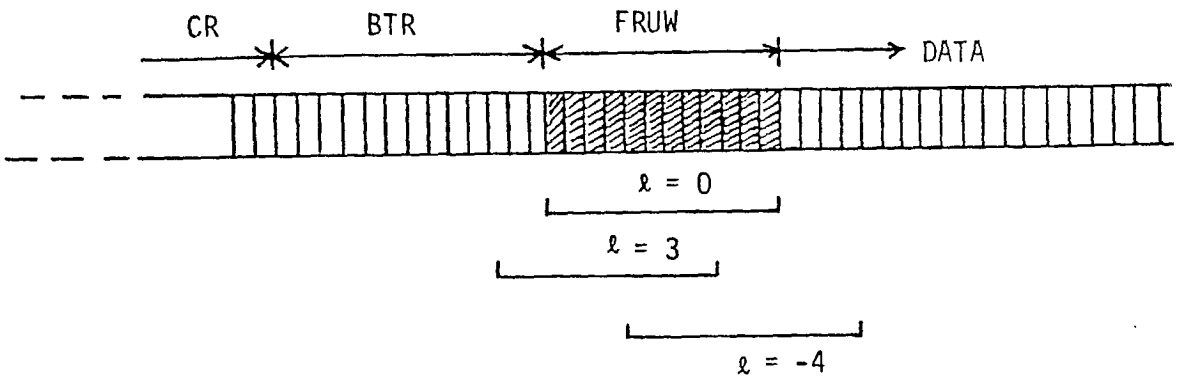

a) Sign convention for detector distance from the FRUW.

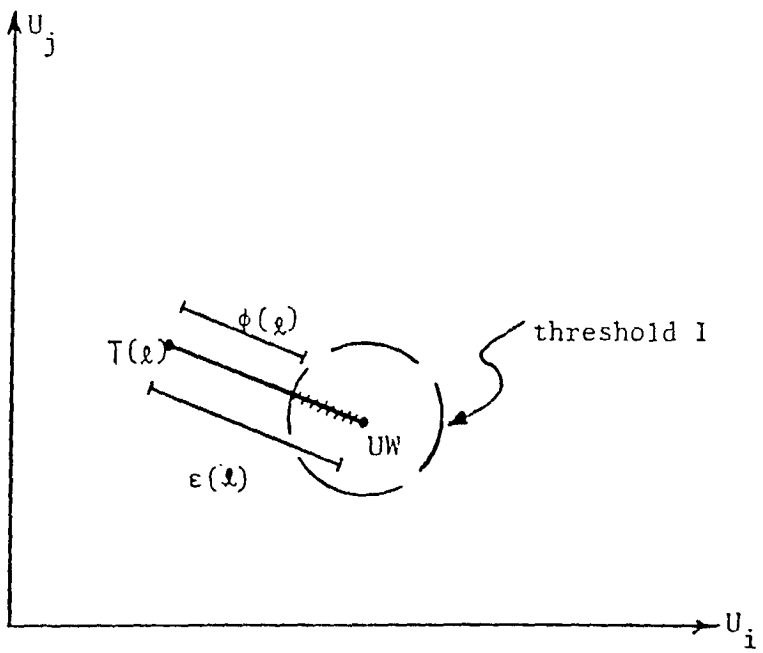

b) False detection as a function of displacement.

Figure 4.4 Conceptual Definition of False Detection

(2) the $T(\ell)$ bits have, at most, one bit in error and $[\phi(\ell) + 1]$ of the $\varepsilon(\ell)$ bits are in error; or

.
.
.

the $T(\ell)$ bits have, at most, I_2 bits in error and all $\varepsilon(\ell)$ bits are in error.

Since these events are mutually exclusive and each consists of two independent outcomes, then the sum of their probabilities defines the conditional detection probability

$$P_D(\ell) = \sum_{i=\phi(\ell)}^{\varepsilon(\ell)} \binom{\varepsilon(\ell)}{i} p^i (1-p)^{\varepsilon(\ell)-i} \sum_{j=0}^{i-\phi(\ell)} \binom{Y(\ell)}{j} p^j (1-p)^{Y(\ell)-j} \qquad (4.9)$$

This represents a conditional probability for the false detection at a distance ℓ from the true position of the FRUW, and is a function of the cross-correlation of the UW and the preceding preamble. It will be used to derive an approximation for the unconditional probability of a false detection within the aperture, P_{FDB}.

4.3 Time-Shift Between the UW And Its Aperture

In Section 2.1 relative displacements between the received UW and its locally generated aperture were attributed to a false detection preceding the occurrence of the true UW, or to relative instability of the reference terminal and local terminal clocks. Doppler frequency variations and satellite-drift also contribute to the timing errors.

Let d represent the net displacement of the received UW within its locally generated aperture in a given frame. Similarly the following displacements are defined:

t_d = displacement of a UW within its aperture due to a pre-emptive false detection;

t_e = displacement of a UW within its aperture due to clocks' misalignment;

t_p = displacement of a UW within its aperture due to doppler frequency variations

such that

$$d = t_d + t_e + t_p \tag{4.10}$$

where (t_d, t_e, t_p) are independent random variables. Figure 4.5 illustrates how the net effect of these displacements can result in the aperture being enabled beyond the location of the true UW.

The timing-error resulting from the misalignment of the reference and local clocks accumulates between detection of successive sync words. The reset of the TIF counter at the detection of each FRUW eliminates this accumulated error. As a consequence, while the terminal is flywheeling no reset of the error can take place. In Appendix C of [2] an argument is proposed to support the approximation that: (a) the accumulated timing-error over an interval T due to clock stabilities is linear in T (see equation C.7 and C.8 in [2]); and (b) the timing-error is a zero-mean gaussian variable whose probability density function is truncated outside the aperture. The timing-error $t_E(i)$ after a flywheel count of i frames is given by (see Figure 4.6)

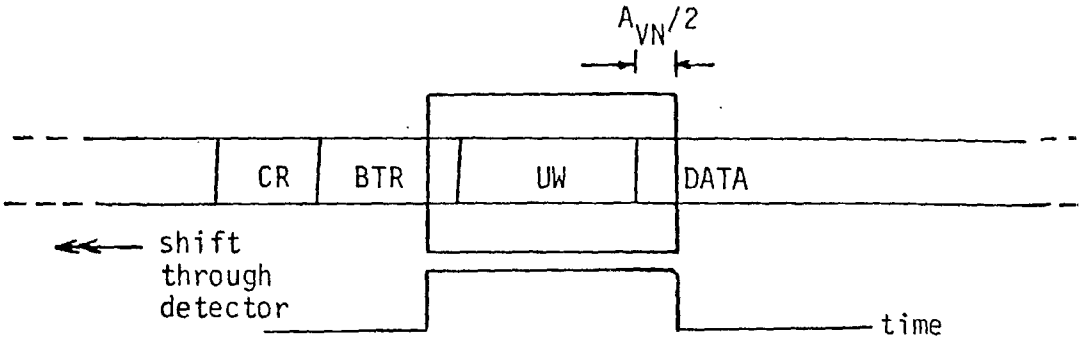

a) Nominal aperture position.

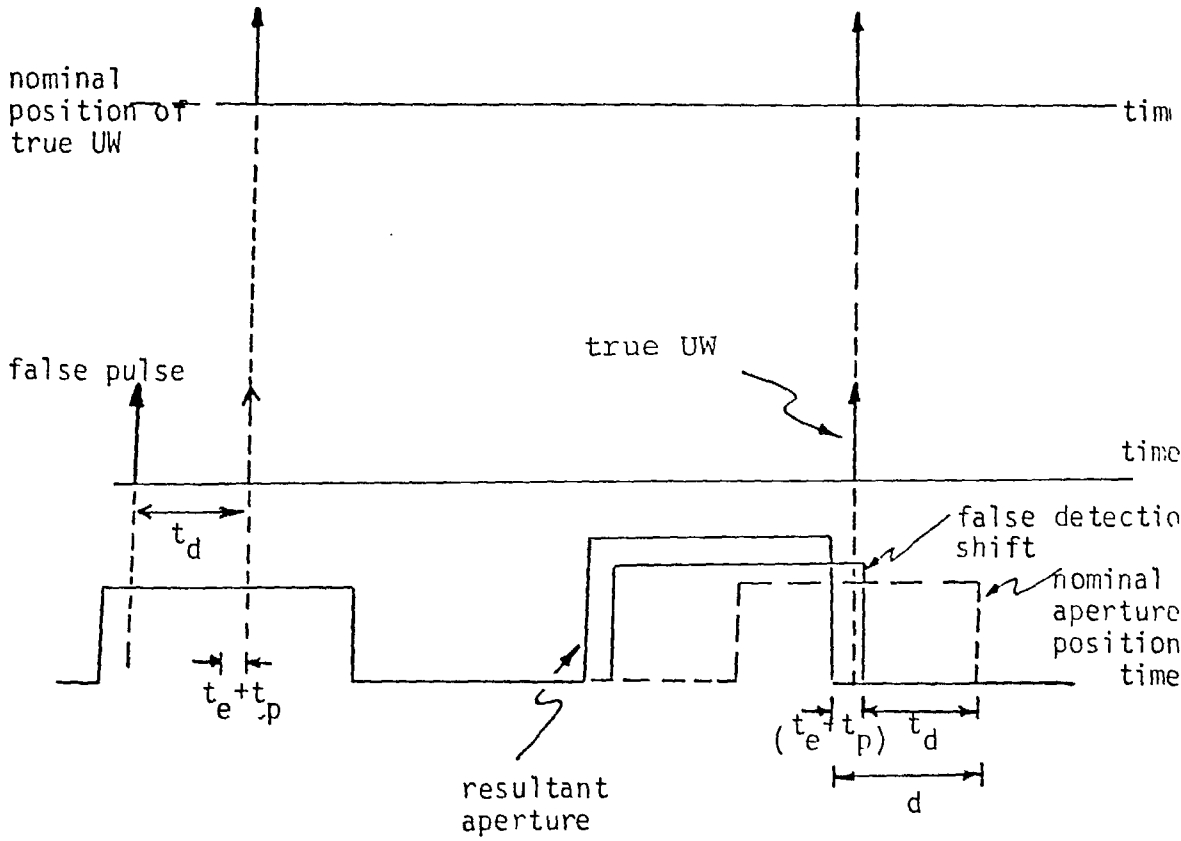

b) Effect of false detections and timing errors

Figure 4.5 Net Displacement d Due To Timing Errors And False Detections.

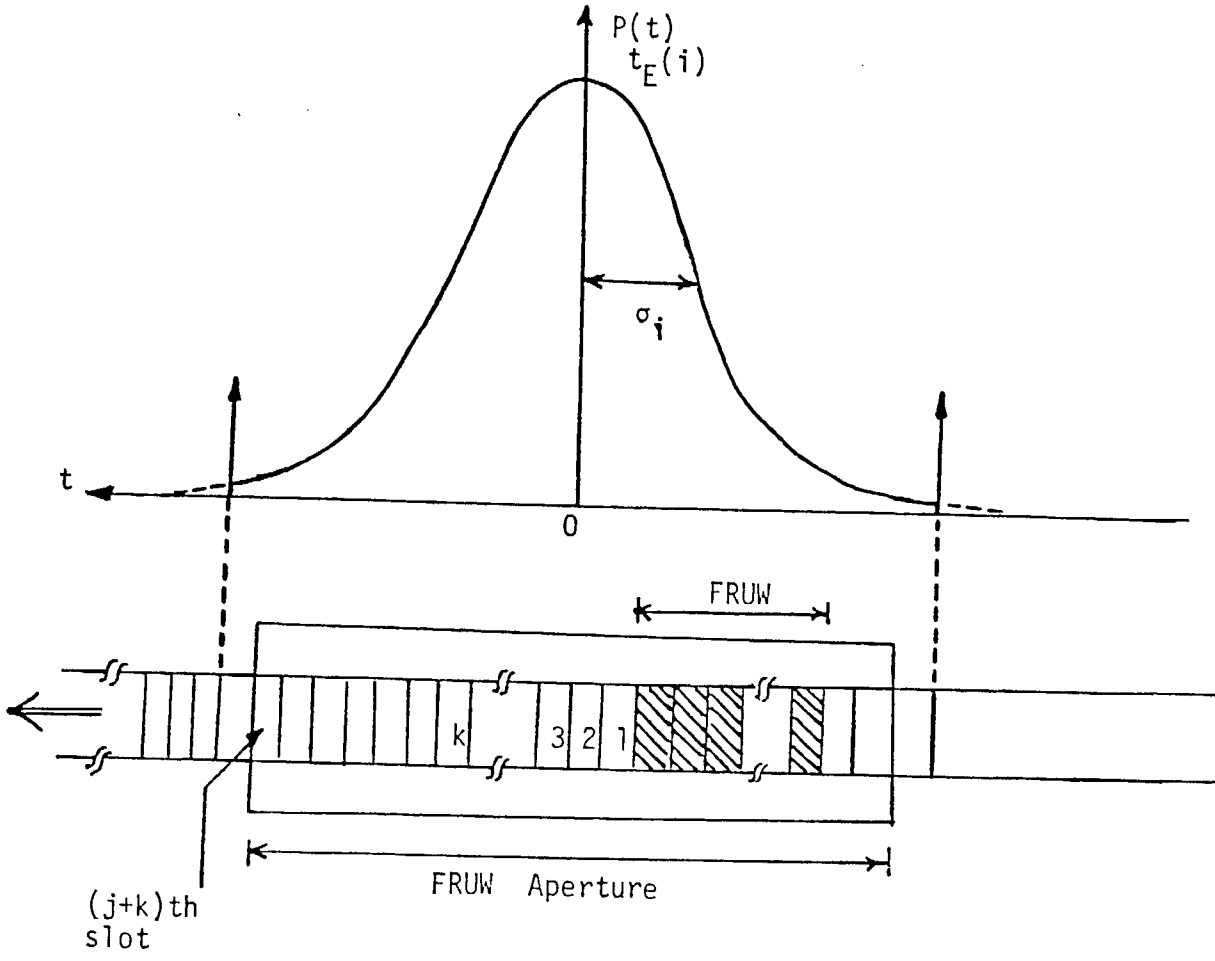

Figure 4.6 Density Function Of FRUW Drift In Aperture.

$$P_{t_{E(i)}}(X)=\frac{1}{\sqrt{2\pi}\sigma_i}\exp\left[\frac{-x^2}{2\sigma_i^2}\right] + K\delta\left(x-\left|\frac{A_{VN}}{2}+1\right|\right)$$

$$+K\delta\left(x+\left|\frac{A_{VN}}{2}+1\right|\right);\ \text{for}\ |x|<(A_{VN}+2)/2 \qquad (4.10)$$

$$= 0 \qquad ;\ \text{elsewhere} \qquad (4.11)$$

where

$$K = \frac{1}{2}\ \text{erfc}\ \left(\frac{A_{VN}}{2\sigma_i}\right)^{*}$$

and

$$\sigma_i = (i+1)\bullet(\text{rms oscillator stability + doppler shift})T_b \qquad (4.12)$$

Equations (4.9) to (4.12) are used in the following section to define the retention model's transition probabilities.

The Retention Markov Chain

The unit time interval is the unit frame interval. The state assignments for retention are as follows:

state(0): represents the nominal state of the detector with the aperture A_{VN} enabled, the detection threshold I set and the UW appearing at the centre of A_{VN};

---

* erfc(•) = complimentary error function.

state ($1 \leq i \leq A_{VN}/2$): represent the "displacement states" in which the UW is displaced by i bits to the <u>right</u> of its nominal position.

state ($A_{VN}/2 \leq i \leq \frac{A_{VN}}{2}+M-1$): represent the "flywheeling states" in which the UW is not detected for ($I - \frac{A_{VN}}{2}$) consecutive frames, and M is the upperbound on this flywheel count before relinquishing frame sync.

state ($\frac{A_{VN}}{2}+M$): represents the "sync-loss" state which can only occur after the Mth flywheel count and returns the detector to the initial acquisition mode as transmit/receive functions are suspended.

Figure 4.7 illustrates the chain for this general retention model ($K = A_{VN}/2$).

As in Section 4.2.3 transition probabilities p(i,j) are derived in Appendix B and used to construct a transition matrix P[p(i,j)]. Similarly, we define T to be the set of non-recurrent states, such that

$$Q \triangleq \{p(i,j);\ \ i,\ j\ \varepsilon\ T\} \tag{4.13}$$

is the matrix of transition probabilities from states in T into states in T. From Figure 4.7, T is the set of all states but the sync-loss state ($\frac{A_{VN}}{2} + M$). From [14] let

$$N = [I - Q]^{-1} = [n_{ij}] \tag{4.14}$$

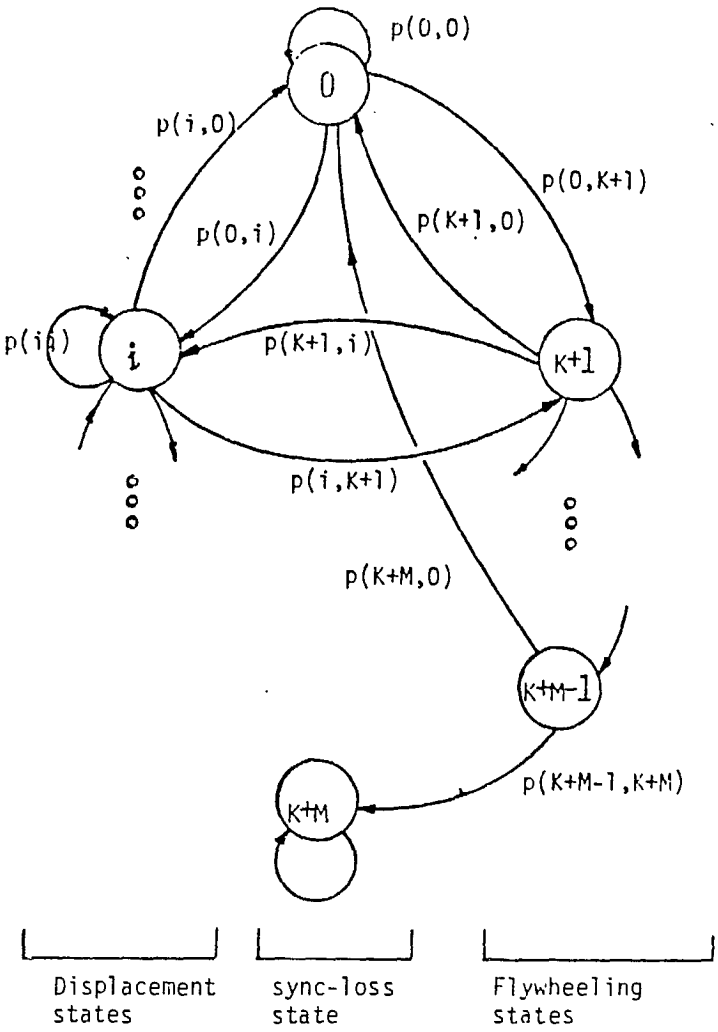

a) sample transitions in the chain.

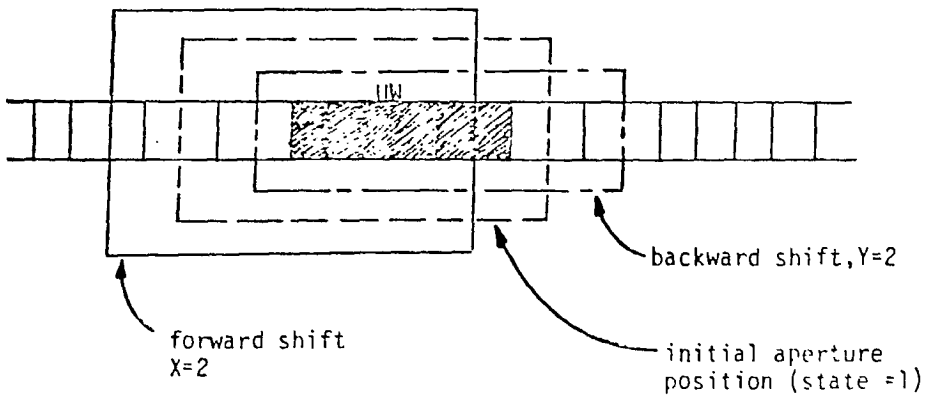

b) nomenclature for aperture shifts (A_{VN}=4).

Figure 4.7 General Retention Model.

where I is the identity matrix. The meantime before terminal's sync loss (MTBSL) is given by the sum of the elements in the first row of N. i.e.

$$MTBSL = \sum_{i=1}^{\frac{A_{VN}}{2} + M-1} \eta_{1i} \qquad (4.15)$$

From Figure 4.6 it is clear that a <u>conditional</u> probability of false detection can be defined by

$$P_{FDB}(j) \approx \sum_{i=1}^{\frac{A_{VN}}{2} + j} P_D(i); \quad 1 < j < A_{VN}/1 \qquad (4.16)$$

where $P_{FDB}(j)$ is the probability of a false detection occurring while the UW is displaced by j bits from its nominal position in the aperture. Denoting π_j as the steady state probability of being in state (j), the unconditional probability of a false detection occurring in the aperture A_{VN} is approximated by

$$P_{FDB} \approx \sum_{j=0}^{A_{VN}/2} P_{FDB}(j)\, \pi_j \qquad (4.17)$$

such that the probability of a no-detection (missed) P_{NDB} is given by

$$P_{NDB} \approx (1-P_{FDB}) \sum_{i=I+1}^{n} \binom{n}{i} p^i (1-p)^{n-i} \qquad (4.18)$$

and the probability of losing frame sync as

$$PSLOSS = \sum_{i=0}^{k+M-1} \left[\prod_{j=i}^{k+M-1} P(j,j+1) \right] \pi_i \qquad (4.19)$$

Sections 4.2 and 4.3 detail the main aspects of Markovian analysis used to model initial acquisition and retention of frame sync in [2]. Appendices A and B list the general expressions for the chains transition probabilities. An underlying assumption in these models is that the regenerated bit-stream at the input to the UW detector is only corrupted by channel noise. Notably absent is the effect of the modem's performance. This issue is briefly addressed in the following section.

4.4 Dependence of Sync Detection On Modem Performance

The detection probabilities derived as a function of the bit-error probability (in Appendix A) assume that the demodulator phase reference is noiseless. One significant result of this assumption is that the detection probabilities can be "improved" by increasing the sync word's length. Another assumption in the models of Section 4 is the negligible effect of cycle-slipping on the UW detector's performance. Measurements in [12] indicate that both disturbances have some effect on UW detection. Also shown is that detection is even affected by cycle-slipping in differentially-encoded coherent detection of QPSK. Regarding carrier phase noise, results in [12] suggest that since the sync word is typically in the range $10 \leq n \leq 30$ bits, it is reasonable to assume that "phase jitter" over this interval is negligible.

The inter-relationship of carrier phase noise and cycle slipping is also addressed in [12, 13]. Non-detections occurring as a result of phase jitter causing miscorrelation between the received UW and the expected pattern can be reduced by narrowing the CR circuit's bandwidth. However, in burst-mode transmission, rapid carrier acquisition limits reduction of the CR circuit's bandwidth. Consequently, non-detections arise, not only due to miscorrelation but also due to cycle-slipping of the recovered carrier. In [13] a new CR circuit is proposed that can sufficiently reduce the CR bandwidth and yet not impair acquisition or inter-burst interference.

Existing analytical models of frame sync detection do not address the detector's dependence on the modem's performance. However, measurement tests of the terminal's synchronization performance should evaluate the degradation in error-rate at the input to the UW detector, as a result of a noisy phase reference and/or cycle slipping.

5.0 SOFTWARE MODULES USED IN ANALYSIS

5.1 Introduction

The preceding sections of this report focus on the analytical modelling of the Slim TDMA terminal's behaviour during initial acquisition and retention of frame sync. Markovian chains were used as a versatile means of representing the acquisition and flywheeling strategies (algorithms), and facilitate the first-order estimates of the terminal's performance parameters. Four software modules are developed as a convenient means of evaluating the terminal's performance for a given set of operational parameters. The modules are structured such that: individually, each addresses a distinct aspect of frame sync detection that can be subjected to a parametric analysis; together, they constitute a flexible tool for quantifying the operational parameters of the Slim TDMA terminal. A brief description of each module's usage is presented in this section, but more detailed documentation is relegated to appropriate appendices.

5.2 Selection of Candidate Unique Words: SELECT

The software module SELECT embodies the procedure outlined in Section 3 and the algorithm depicted in Figure 3.3 for word lengths in the range $4 \leq n \leq 63$ bits. The output of this module is a set of n-bit patterns that are candidates for use as the FRUW and DBUW. Appendix C contains a detailed documentation of the SELECT module and a source listing of the program accompanies the report.

5.3 Performance Of The Digital Correlator: CORREL 8

Close scrutiny of the criteria used in SELECT underscores the fact that the candidate bit-patterns are generated

with the assumption that only one sync word is embedded in the data. However, unlike most PCM telemetry and radar applications, the periodic auto-correlation of the FRUW (or DBUW) is not the only relevant issue. During initial acquisiton the received bit stream is differentially decoded before being passed through the detector. In this mode the first detection of the FRUW likely occurs after the digital correlator has scanned several DBUWs! During steady state retention differential decoding is inhibited, and apertures restrict the correlaor's output.

From this sequence of operations it is evident that after a FRUW and DBUW are identified (using SELECT) their compatibility together (as a pair) must be assessed, as well as each's cross correlation with its non-random preamble. Specifically:

i) during acquisition the DBUW should not be mistaken for the FRUW; and

ii) during retention partial segments of the UW and its preceding preamble are in the digital correlator while the aperture (for FRUW or DBUW) is open.

CORREL8 is a software module that reproduces the digital correlator's output during initial acquisition and retention for a given pair of sync words (FRUW, DBUW) and a given BTR preamble. The output correlation profile CORR(K) is listed as a function of K, the distance (in bits) between the current contents of the shift register and the position of te sync word being sought (see Figure 5.1). The operator DIFF (.) is used to imply the differential decoding of the regenerated bit-stream prior to its passage through the detector's shift register.

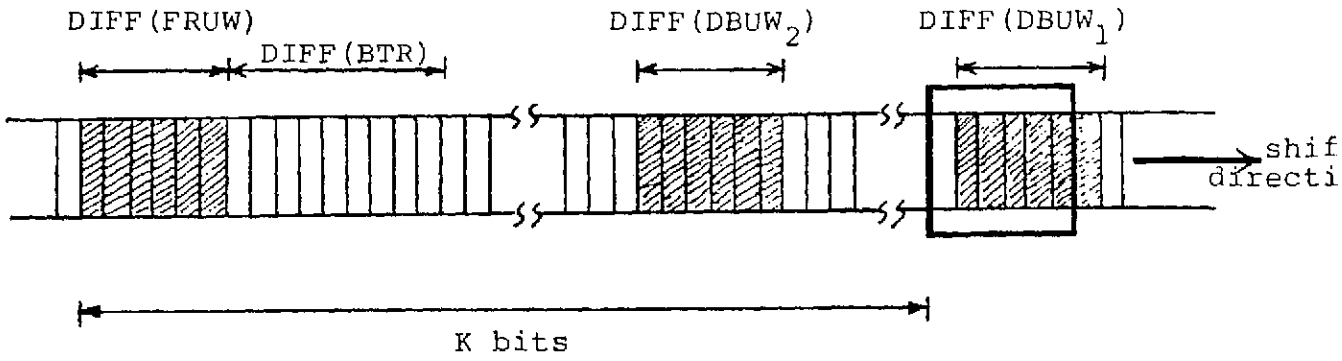

a) during initial acquisition
(apertures suppressed)
(& diff. decoding enabled)

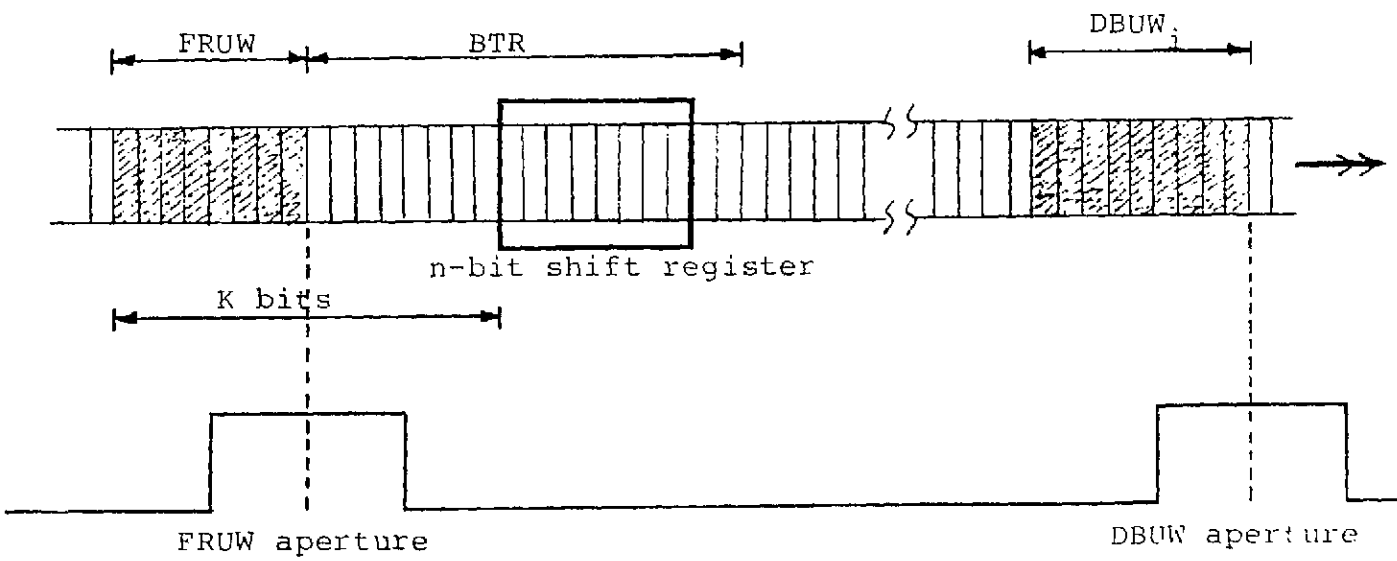

b) during retention
(no diff. decoding)

Figure 5.1 Digital Correlator Scanning Data Stream

The module's analysis of the resultant Markov chain(s) generates the following performance parameters:

a) the mean time (in frames) required to acquire frame sync, MTTA*, and its second moment;

b) the probability of false acquisition, P_{FA}, representing the likelihood of encountering an acceptable (but false) facsimile of the FRUW for consecutive frames - inducing false lock-up; and

c) the cumulative density funciton, PACQ(X), representing the probability of frame sync acquisition in X frames or less; $1 \leq X \leq IL+4$.

Secondary parameters, namely detection probabilities, are also listed in the module's print-out:

1) the probability of no-detection in a bit-by-bit scan of the frame, P_{ND};

2) the probability of a false detection in a bit-by-bit scan of the frame, P_{FDO};

3) the probability of false detection in <u>random data</u> within a wide aperture, P_{FDW}; and

4) The probability of false detection in the preamble preceding the FRUW within a wide aperture, P_{FDB}.

---

*A distinction is made between the terminal's lock-up on the true FRUW (denoted by $MTTA_c$) and lock-up on any n-bit pattern that resembles the FRUW (denoted by MTTA). For word lengths exceeding 16 bits, and the detector threshold set to zero (seeking a perfect match) $MTTA_c \approx MTTA$. See section 4.2.

These detection probabilites are used to derive the Markov chain's state transitions, and indicate the pattern of the detector's behaviour during acquisition.

An important point to note is the module's analysis of the Markov chain for configurations where the probability of a false detection is very large (P_{FDO}, $P_{FDB} \approx 1$) - see Figure 4.1a. In such cases the numerical resolution of the computer may not distinguish between a "near zero", or a "near one" and one. The resultant transformation in Figure 4.1a is shown in Figure 5.2 for the example of L=2. In this figure it is clear that state no. 2 has now become a non-recurrent state [14] and must be eliminated from the set S in equation 4.2. The resultant $MTTA_c \rightarrow \infty$. However, the program ACQUI only recognizes state no. L+2 as the only non-recurrent state representing "acquisition completed". This ambiguity plays havoc with the matrix inversion sub-routines: INVERT and SOLVD. As a result, a flag TEST is used to indicte satisfactory completion of the matrix inversion:

a) if TEST=0 then computer's truncation errors did not distort the matrix's inversion and the chain's analysis is valid; but

b) if TEST ≠ 0 then the chain's analysis is aborted, and $MTTA_c$ is estimated from equation 4.8 rather than from the chain.

Extreme cases where $MTTA_c$ is larger than the highest representable numerical value result in a diagnostic error message.

Appendix E presents further documentation of the module ACQUI, and a source listing for the program accompanys the report.

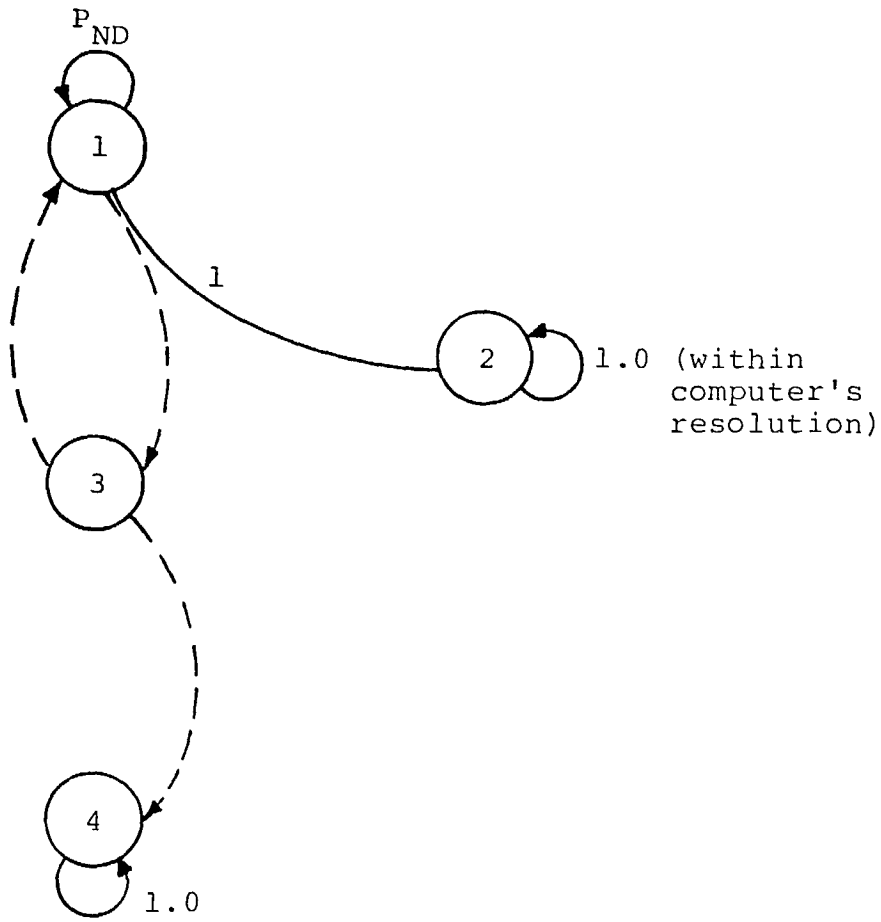

Figure 5.2 Fringe Performance At P_{FDB}, $P_{FDO} \approx 1$ (L=2)

5.5 Performance During Steady State: RETNTN

For a specified set of configuration parameters this module constructs and analyzes the Markov chain defined in section 4.3. As in ACQUI, arrays are used to store several configurations to facilitate parametric anlaysis. The configuration parameters that must be entered are:

i) the burst rate, RR (in Mbps);

ii) the nominal frame length T_F (in milliseconds);

iii) the range of BER values, specified by the array's size NBER and the array's elements BER(I), I=1,2,---NBER;

iv) an array of narrow aperture widths AAVN(I)*, I=1,2,---NAVN;

v) an array of flywheel-counts IM(I), I=1,2---NM;

vi) an array of detection threshold values THR(I), I=1,2---NTHRSH;

vii) an array of timing-error values SNS(I), I=1,2---NSNST.

The module's analysis of the resulting Markov chain(s) generates the following performance parameters (equations 4.15, 4.17 and 4.19):

a) the mean time lapsed (in frames)before the terminal relinquishes frame sync RMTBSL;

b) the probability of losing frame sync, PSLOSS' due to M consecutive non-detections of the FRUW within its aperture; and

---

*Note: APERTURE WIDTHS MUST BE EVEN!

c) the probability of a false detection occuring within the narrow aperture, PFDBC.

Similarly, secondary parameters (e.g. P_{NDB}) can be listed in the program's print-out.

A second set of performance parameters {MTBSL, PBSL, PFDB} is evaluated from equations 3.2, B.1 adn B.16 in [2]. These latter performance parameters neglect the effects of accumulated timing-error, and the position of the UW within its aperture, on detection. These performance parameters are listed for two reasons: 1) to indicate their approximation errors relative to the analysis of the chain; and 2) to serve as a reasonable estimate of steady state performance for fringe configurations. An example of fringe configurations is a scenario for which false detections preceding the true FRUW are very likely [PFDBC, PD(ℓ)→1] - refer to explanation in Section 5.4. In general, the estimate for P_{BSL} is valid if P_{FDB} does not appear as zero; and PSLOSS is valid if PFDBC does not appear as zero.

Several comments must now be made concerning the results from RETNTN, which must be carefully interpreted. The considerations stem from the fact that optimum performance, characterized by increasing intervals between sync-loss (MTBSL→∞) and decreasing misdetection probabilities (P_{NDB}, P_{FDB} →0), extends beyond the numerical resolution of the computer. Consequently availability, the up-time ratio (UTR) and other performance criteria are used to identify suitable operating parameters. The first comment concerns estimating the MTBSL. If the entries of the transition matrix Q (see equation 4.13) are sufficiently small as to

be indistinguishable from zero, inversion of the matrix [I-Q] (see equation 4.14) becomes difficult. In this event a flag TEST is set to a non-zero value, and MTBSL is approximated by the closed form equation 3.2 in [2].

The second comment pertains to the estimates of P_{FDB} and P_{BSL} using Markovian analysis —— refer to equations 4.17 and 4.19. In RETNTN these probabilities are denoted by {PFDBC,PSLOSS} and assume that π_j (the state occupation probability) is uniformly distributed in the interval $0 \leq j \leq k+M$. This assumption avoids the increased computational complexity of deriving the steady state probabilities $\{\pi_j\}$ and is a reasonable approximate for $\pi_j \ll 1$. Finally, detection probabilities P_{NDB} or P_{FDB} that are sufficiently small (as to be indistinguishable from zero) are recorded as being zero.

Appendix F presents further documentation of the module RETNTN, and a source listing accompanys this report.

5.6 Utilization Of The Software Modules

The partitioning of the aspects of TDMA frame sync detection into four software modules was executed in such a manner as to delegate a closed set of operations to each module. This allows each module to be used independently as an analytical tool to investigate a specific issue (e.g. an N,-tuple's correlation profile, acquisition performance etc.) or together as a design tool used to quantify the terminal's operating parameters (e.g. word length and format, aperture width etc). A possible configuration of the software modules as a design tool is depicted in Figure 5.3a. In the following

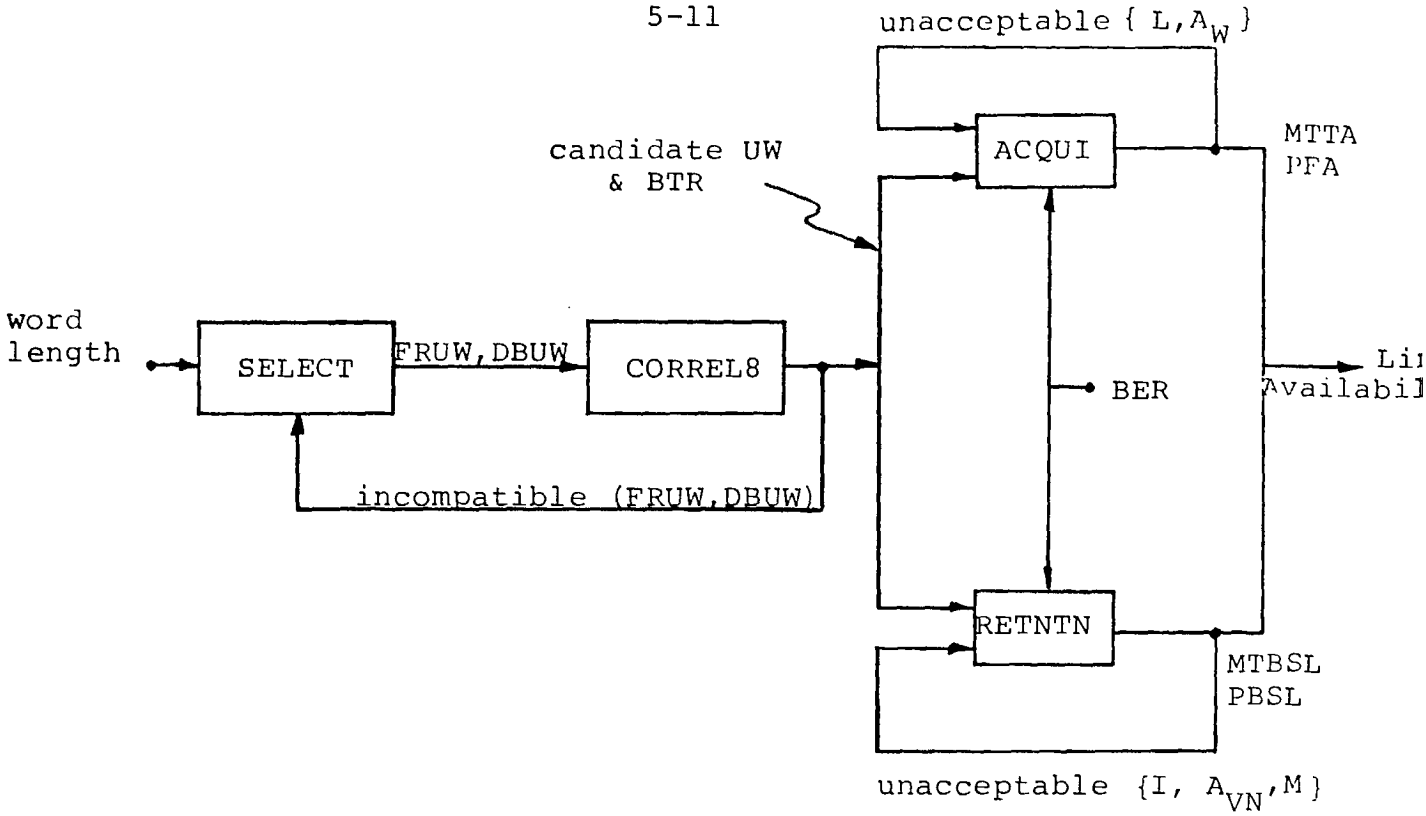

a) use of modules as a design tool

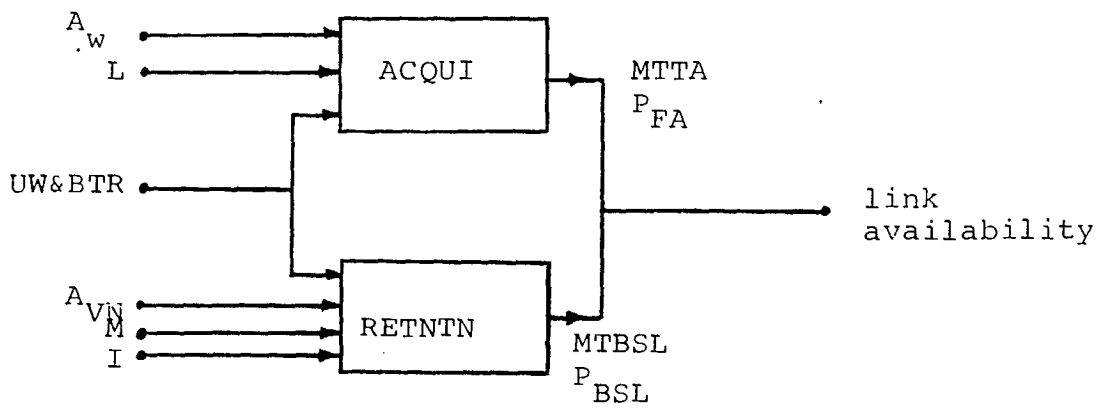

b) evaluation of system's current operational parameters

Figure 5.3 Utilization of Software Modules

section these modules are used to evaluate the performance of the current system parameters (see Figure 5.3b). Having established current performance, an iterative analysis will be used to identify possible improvements to the current system.

6.0 PERFORMANCE OF CURRENT SYSTEM*

In an effort to limit the proliferation of statistical data (an inevitable result of most parametric analyses), any recommendations anticipated in this report will be made with reference to the terminal's current performance. In this section the analytical models developed are used to quantify this performance. Table 6.1 summarizes the current parameters of the Slim TDMA terminal's unique word detector.

6.1 Correlation Profiles Of The Sync Patterns

The identification of the sync words in Table 6.1 pre-empts the use of the program SELECT. However, results from CORREL8 are used to assess the compatibility of the {FRUW, DBUW} pair during acquisition subject to the specified detector threshold. Figure 6.1 presents the ideal output (BER=0) of the digital correlator as it approaches the FRUW and DBUW during the initial bit-by-bit SCAN. Note that, in this mode, the detector seeks the differentially decoded version of the FRUW. With the detector's acquisiton threshold set to zero, this correlation profile indicates that 10 bit-errors or more must occur in the DBUW before its is mistaken for the FRUW. This likelihood is approximated by the probability

$$\sum_{i=10}^{32} \binom{32}{i} p^i (1-p)^{32-i} \qquad (6.1)$$

which is very small even at a nominal BER of 1×10^{-4}. This result merely confirms that simply random channel errors cannot easily cause the DBUW to be mistaken for the FRUW. Together with the multiple verification count

*The Slim TDMA terminal developed by MCS for CNCP [1] is used in this report as a representative case study.

	Parameter Values
Configuration Parameters	Burst Rate : 3.1584 Mbsp Frame Length : 20 msec. FRUW : B121C17E (HEX) DBUW : 3731D7ED (HEX) CR sequence : 1111.....111 (184 bits) BTR sequence : 1100.....1100 (40 bits)
Acquisition Parameters	Wide Aperture A_W : 100 bits Detection Threshold : 0 bits (perfect match) Verification count L: 5 frames
Retention Parameters	Narrow Aperture A_{VN} : 32 bits Detection Threshold : 3 bits Flywheel Count M : 50 frames RMS Timing Error Accrued per frame ε : 1×10^{-6} bits/bit

Table 6.1 Current System Configuration

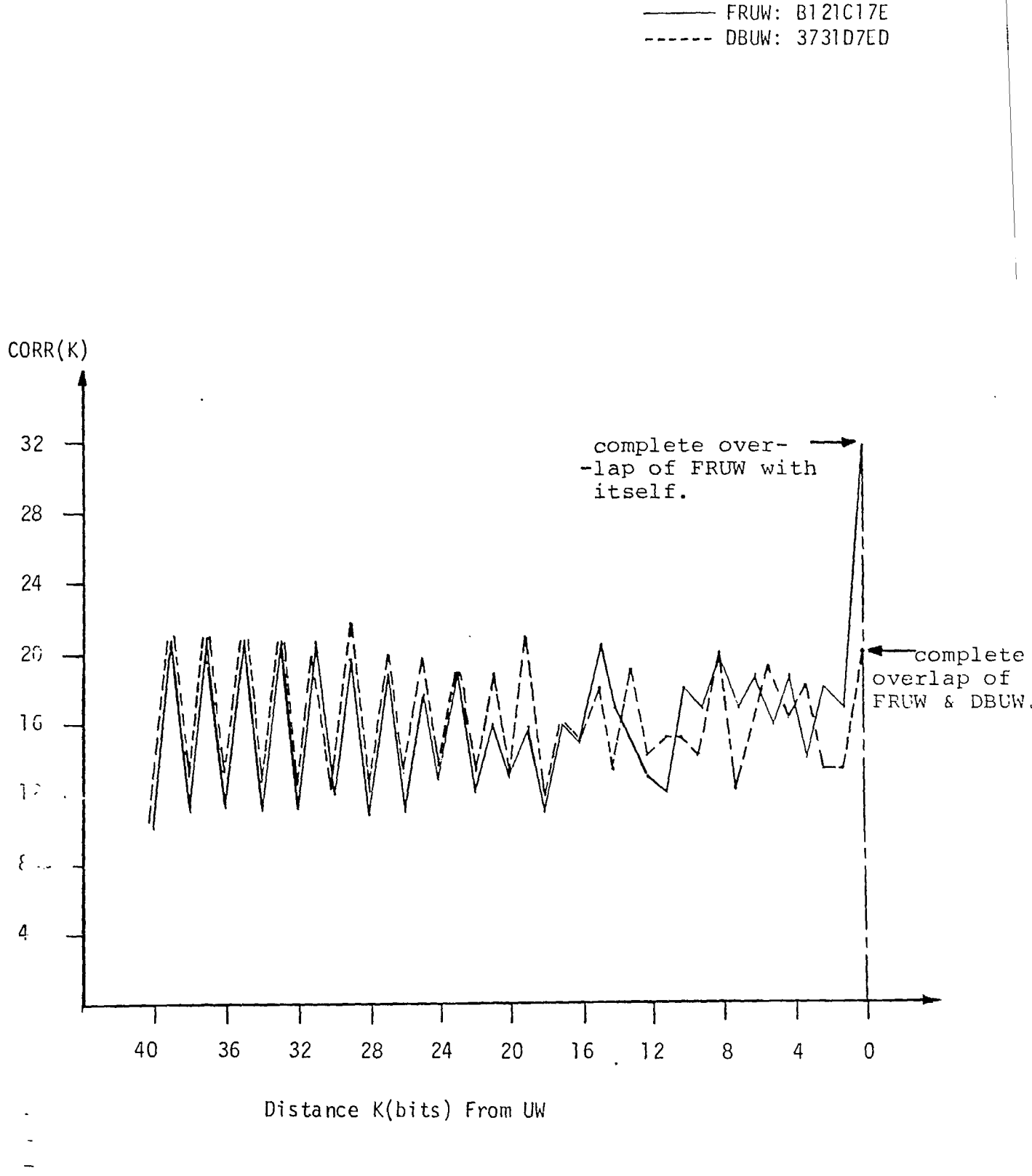

Figure 6.1 Correlation Profile for Acquisition (existing configuration).

of 5 frames, false acquisition is expected to be a very remote event. However the zero detection threshold will equally reject the true FRUW if a single bit is in error. Nevertheless, the disruptive consequences of a terminal that incorrectly acquires frame sync warrants the longer acquistion time. Figures 6.2a and 6.2b illustrate the correlator's ideal output after apertures have been positioned for periodic detection of the FRUW and DBUW. In this mode the received bit stream is not differentially decoded, the DBUW is not expected to appear within the FRUW's aperture (nor vice versa) and a detector threshold of 3 bits is in effect. Both profiles in Figure 6.2 imply that false detections are not very likely to occur within the narrow aperture of $A_{VN} = 32$ bits. Note that the correlation profile for the DBUW has several "peaks" that render it more vulnerable to false detections in a "relative" sense. It is only such a qualitative assessment of the performance of the sync words that can be made from the results of CORREL8: i) a comparative evaluation of the compatibility of {FRUW, DBUW}, and ii) a preliminary value for the detector threshold.

6.2 Acquisition Performance

The expected performance of the current system during attempts to acquire frame sync is derived using the program ACQUI. Figure 6.3 presents estimates of the MTTA as a function of the BER. Typically, BER values for links carrying data are below $1x10^{-5}$, and for voice links are below $5x10^{-2}$ (although this is a function of the voice codec). Figure 6.3 indicates that over this "operational" range of BER values the terminal acquires frame sync in an interval of 5 frame durations (≈ 100 msecs). For BER values greater than $1x10^{-2}$ the acquistion time increases sharply. However, it remains questionable whether or not the modem itself (preceding

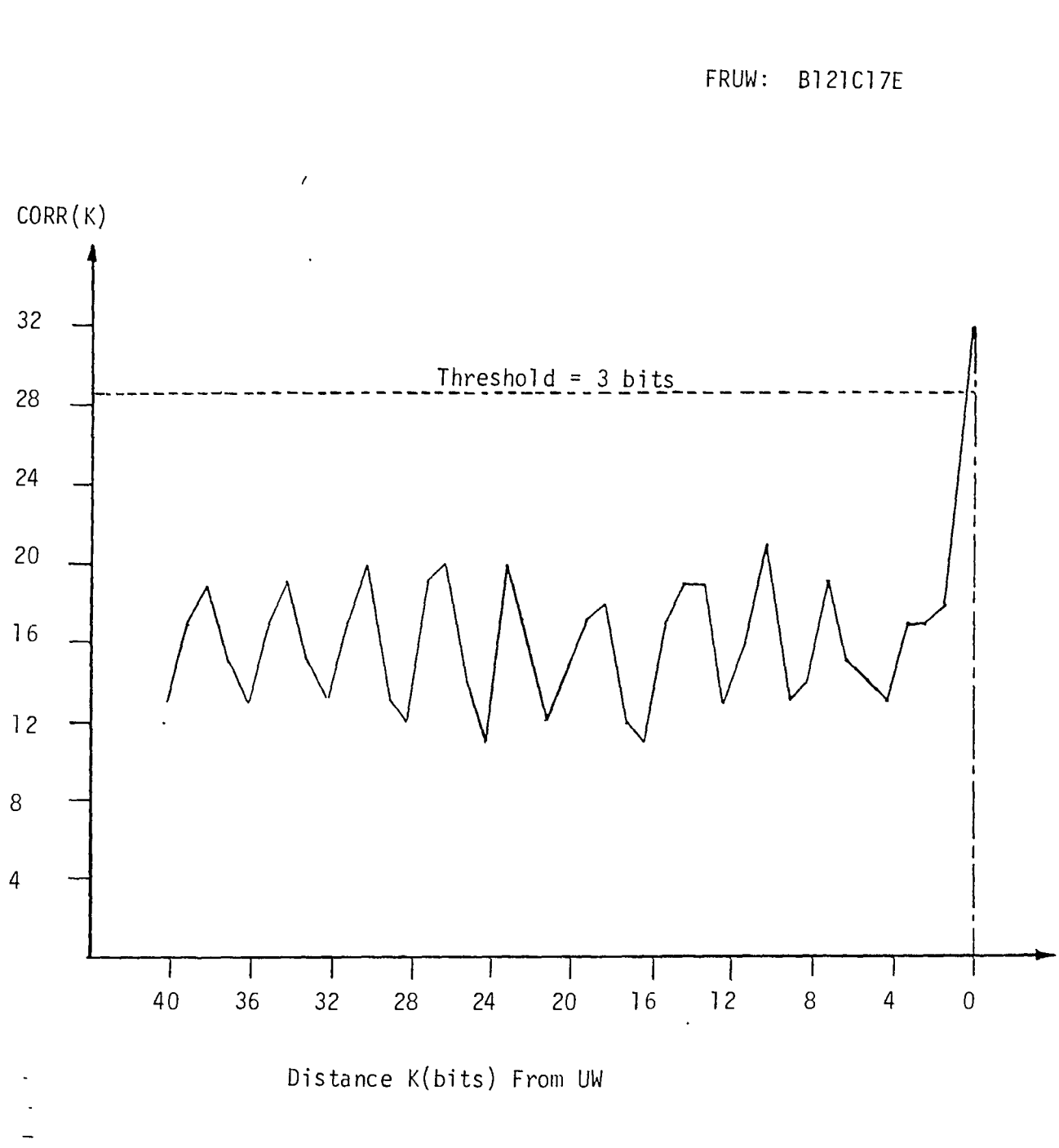

Figure 6.2(a) Correlation Profile For Retention: Scanning The FRUW

DBUW: 3731D7ED

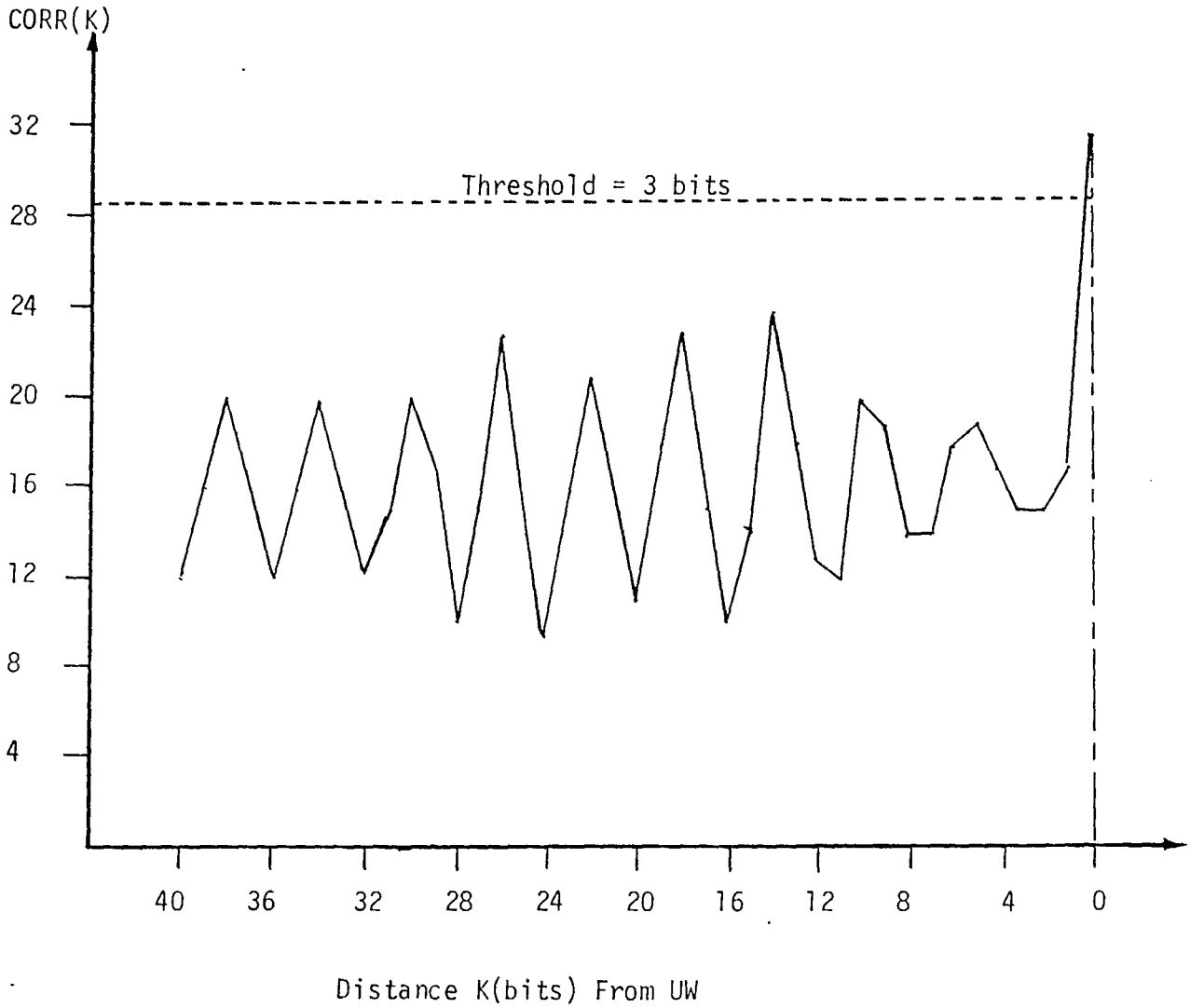

Figure 6.2(b) Correlation Profile For Retention: Scanning the DBUW

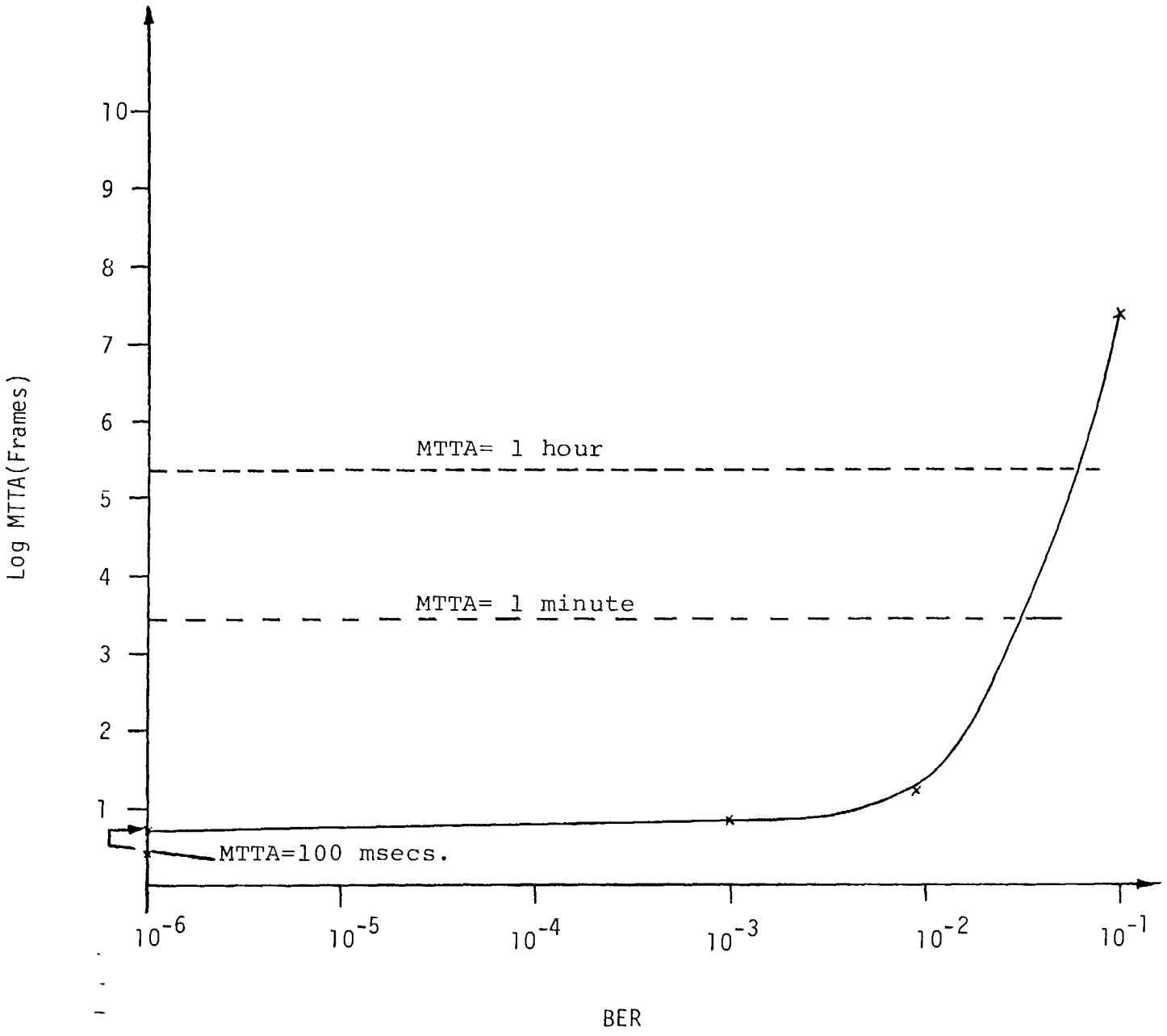

Figure 6.3 Acquisition Time Versus BER (Current Configuration)

the burst synchronizer) will adequately function under such conditions. Consequently, results for BER>$5x10^{-2}$ must be interpreted accordingly. The effects of modem performance on the UW detector were briefly addressed in Section 4.4.

Figure 6.4 estimates the cumulative distribution function; i.e. the likelihood of acquiring frame sync in X frames or less. Although the MTTA remains near 100 msecs over a wide range of BER values, the probability of acquiring frame sync within this interval is only 0.85 at a BER of $1x10^{-3}$. i.e. acquistion while the link is experiencing noticeable levels of fading is likely to prove difficult. Furthermore, if PACQ(x) is a criterion by which service is rated it may be necessary to improve this performnce (e.g. a 95th percentile may be required for acquisition within 5 frames over a specified BER range). The output listing from ACQUI also estimates the probability of <u>false</u> acquistion being less than $1x10^{-30}$ for BER values lower than $1x10^{-3}$; i.e. false detections within the 100 bit aperture are unlikely to cause accidental false terminal synchronization.

6.3 Retention Performance

Using the parameters in Table 6.1 the computer program RETNTN evaluates the terminal's performance once frame sync has been acquired. Again it is cautioned that results presented for BER> $5x10^{-2}$ must be interpreted within the context that this may exceed the nominal operating range of the link (modem). Figure 6.5 depicts the variation of MTBSL and P_{FDB} as functions of the bit-error rate. Note that a Log(MTBSL) = 10 corresponds to approximately six years! Also note that these results assume a flywheel count of M=20 frames whereas Table 6.1 lists a count M=50 frames. The discrepancy, as

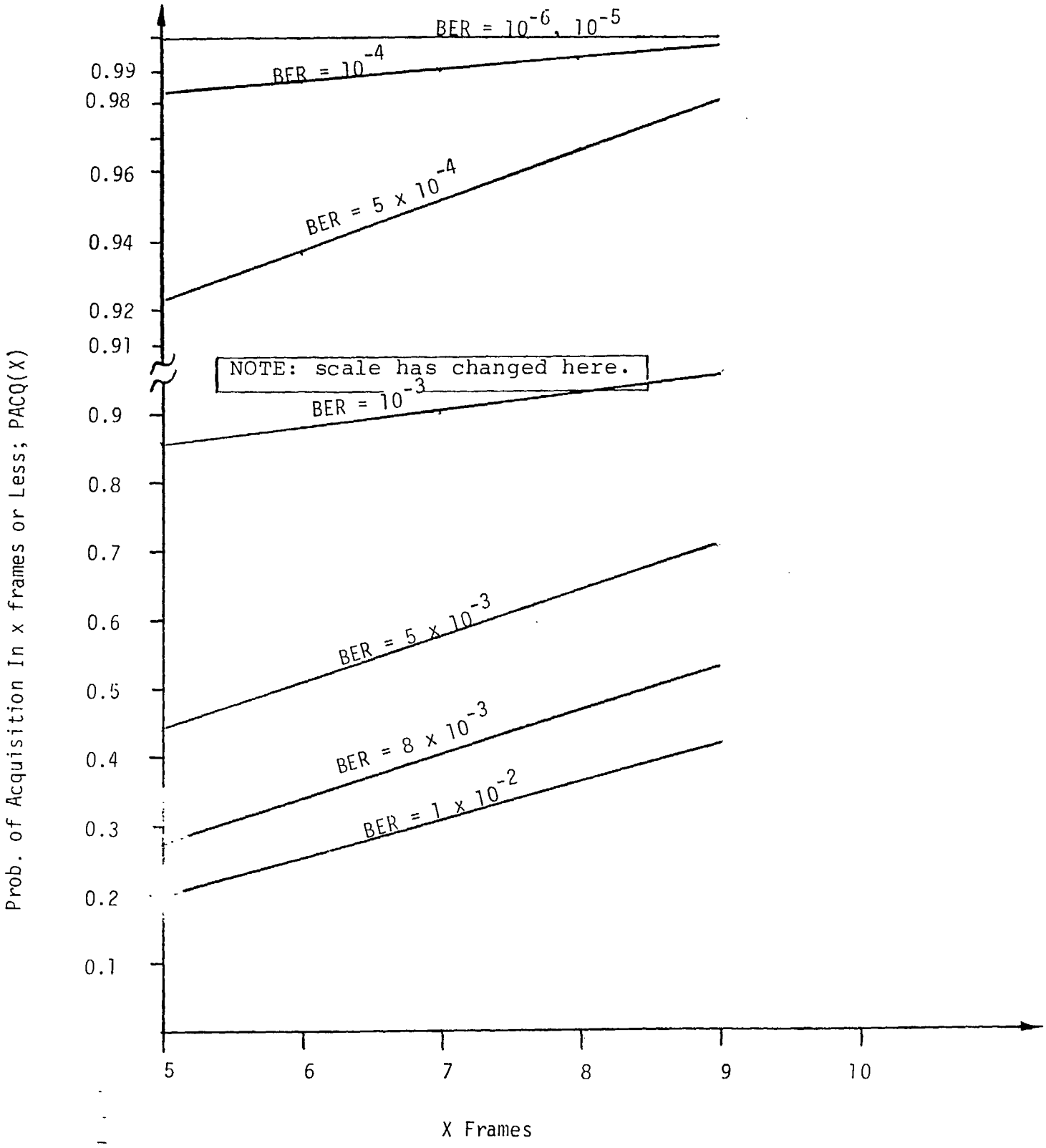

Figure 6.4 Cumulative Distribution Function For Acquisition

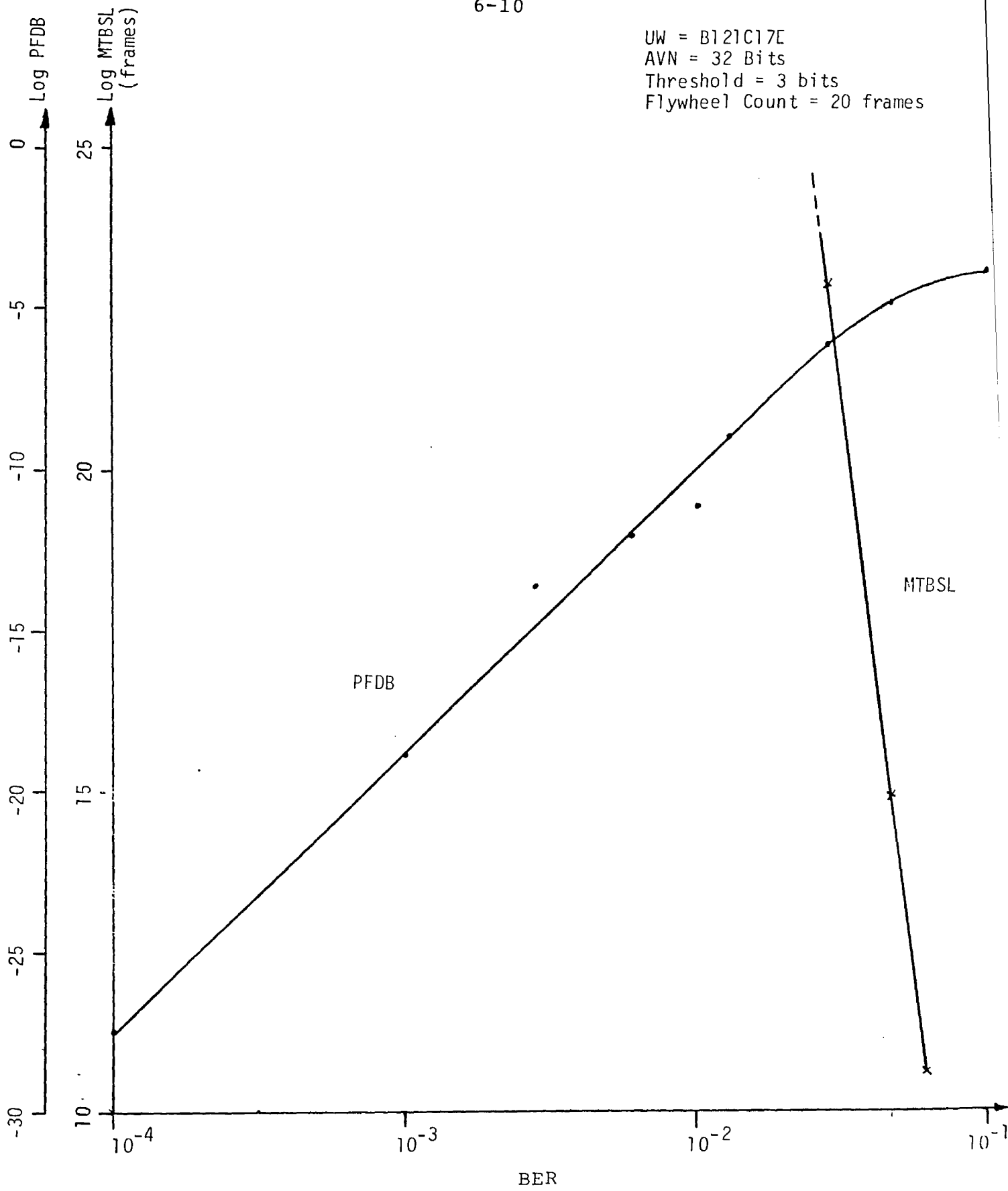

Figure 6.5 Retention and Prob. of False Detection
(current Configuration)

explained in item 3(c) in [20], lies in the fact that the arrays' sizes in RETNTN are a function of the flywheel count M. Consequently, computer memory limitations prevent the declaration of large array sizes.* This limitation may not prove to be an insurmountable obstacle: if performance objectives are satisfied with a flywheel count of M=20, then they are satisfied for M=50 provided the FRUW is not likely to drift beyond the aperture due to accrued timing errors.

In figure 6.5 the MTBSL exceeds $1x10^{25}$ frames for BER values below $1x10^{-2}$. However, the rate of decline is very steep. Using equation 2.1 and the acquistion/retention results, estimates of the terminal's availability (i.e. UTR of burst synchronizer) are listed in Table 6.2 as a function of BER. The performance objective specified in equation 2.2 is achieved at BER values less than $7x10^{-2}$. Again it is noted that this BER may also be the upperbound for acceptable modem performance. Furthermore, performance during retention assumes that the UW detector is never exposed to an "empty" segment of the frame once it activates its retention threshold to a non-zero value. (See section 8.2).

6.4 Comments On Current Performance

The analytical results in Section 6.0 represent the performance of the current system. From these results, guidelines for the investigation of detector sensitivity must be extracted.

---

*Use of computer systems that permit larger memory allocations, or the declaration of "virtual" arrays, may extend the limitations on the value of M.

BER	MTTO (Frames)	MTBSL (Frames)	UTR
10^{-6}	5	$> 10^{35}$	>99.99
10^{-4}	5.0493	$> 10^{35}$	>99.99
10^{-2}	14.519	$> 10^{35}$	>99.99
7×10^{-2}	1.2233×10^{5}	$\approx 5.72 \times 10^{14}$	>99.99
10^{-1}	2.17×10^{7}	$\approx 4 \times 10^{5}$	$\approx$ 0.018

Table 6.2 Estimate of Expected Availability
(Current Configuration)

An important first point to note is that the pair of sync words (FRUW, DBUW) curently in use were arbitrarily generated from one of the shift-register configurations listed in Table 3.1. The resulting performance of the detector in both acquisiiton and retention modes satisfied the specified availability (UTR) for BER$\leq 5\times10^{-2}$. All patterns generated by the configurations in Table 3.1 are potentially "good" sync words; but not all satisfy the Neuman-Hofman selection criteria defined in Section 3.3. These selection criteria were not "tailored" to the Slim TMDA terminal's acquisition/retention algorithms, but were single-event correlation criteria. Consequently, two initial questions that should be resolved are:

a) How compatible are the selection criteria and the acquistion/retention performances of the terminal?

b) Aside from obvious unacceptable sync patterns (refer to concluding paragraph of section 2.0) how relevant is the format of a 32-bit sync word to the terminal's performance ?

Answers to both these questions would ensure better use of the software program SELECT.

In [1] the following requirements were specified for the terminal's operation:

i) probability of acquiring in less than 100 msec should be ≥ 0.99 for $P_{FA}\leq 1\times10^{-12}$ at $E_b/N_o=10.4$ dB (BER$\approx 1.4\times10^{-4}$ for QPSK);

ii) in retention, the probability of missing a sync pattern shall not exceed $1x10^{-18}$ at BER=$1x10^{-4}$, and shall not exceed $1x10^{-6}$ at BER=$1x10^{-2}$;

iii) MTBSL > 1 week ($3x10^{7}$ frames) at BER=$1x10^{-4}$.

Results shown in Figure 6.4 indicate that the likelihood of acquiring in less than5 frames at a BER of 10^{-4} is slightly less them 0.99 (≈0.984). The probability of false acquisition assuming a random error channel is less than $1x10^{-30}$. In figure 6.5 the MTBSL exceeds $1x10^{25}$ frames at BER = $1x10^{-4}$. The probability of not detecting the sync word is estimated to be: a) $0.4x10^{-11}$ at BER = $1x10^{-4}$, and b) $0.4x10^{-7}$ at BER = $1x10^{-2}$. Only the second of these two probabilities satisfies the above requirements.

The current performance appears to satisfy most (but not all) requirements. As a result, the objective of the parametric analysis will be twofold: a) to determine the sensitivity of the terminal (or its ruggedness) to variations in its operating parameters, and b) to identify key parameters (if any) which may be altered to better satisfy the requirements.

7.0 DETECTOR SENSITIVITY TO OPERATING PARAMETERS

The assessment of the Slim TDMA terminal's sensitivity to its parameters of its operation is accomlished by iterative applications of the software modules. From the resulting performance trends guidelines are derived on how present parameters are to be modified.

7.1 Selection of Sync Word Formats

The program SELECT generates five (5) 32-bit patterns whihc satisfy criterion I, or II, or both (see section 3.1). These are (in Hexadecimal representation):

i) 7A392DD9
ii) 9ABF0431
iii) B7EB8CEC
iv) 2A7E8384
v) FAOE1236

From these, the Neuman-Hofman selection criterion for high BER applications is best met using FAOE1236. Since the motivating factor in using a long sync word is usually its detection performance in high bit-error rate conditions, this criterion may be more relevant here.

A significant point to note about the above set of n-tuples is that none of the sync words that have been used in the terminal's operation to date are members of this set. However, results of the system's current performance (detailed in Section 6) satisfies most of the guidelines specified in [1]. In Section 6.4 a question was posed as to the relevance of the sync word's format - specifically for long n-tuples. Each of the n-tuples generated by SELECT was subjected to a fixed iterative algorithm using the acquistion and retention modules (ACQU, RETNTN). Over the nominal BER range [$1x10^{-6}$ - $1x10^{-1}$] the single event detection probabilities (P_{NDO}, P_{FDO}, P_{FDW}, P_{FDB} etc.) differed, in some cases, by

several orders of magnitude. However, the probabilites of false detection within the apertures were sufficiently small that these differences did not translate into significant variations in the performance parameters $\{MTTA, P_{FA}, MTBSL, P_{BSL}\}$. For the parameter values used in these iterations the following conclusions can be made*:

> The Slim TDMA terminal's performance in acquiring, and retaining, frame sync will not be affected by the FORMAT of the 32-bit sync word used as the FRUW.

For the range of detection thresholds and apertures examined in this report the above conclusion also applies to n-tuples that are longer than 32-bits. For significantly shorter sync words this may no longer be true as the probability of false detection within the apertures increases. Note, however, that altering the length of sync word requires hardware modifications to the terminal's burst synchronizer. The remainder of this report discusses the terminal's performance with the sync word set to: FAOE1236.

7.2 Correlation Profile Of The Selected Sync Word

Figure 7.1(a) shows the output of the digital correlator as it scans the frame (bit-by-bit) during initial acquisition. Comparing this profile to that shown in Figure 6.1 note that: a) the correlator output never exceeds a value of 20 (once at K=25); and b) that the weighting factor in equations 3.1 and 3.5 ensures that sync words selected by the algorithm are not likely to

*Refer to Section 2.2 for the few exceptions to this conclusion.

UW = FA0E1236(HEX)

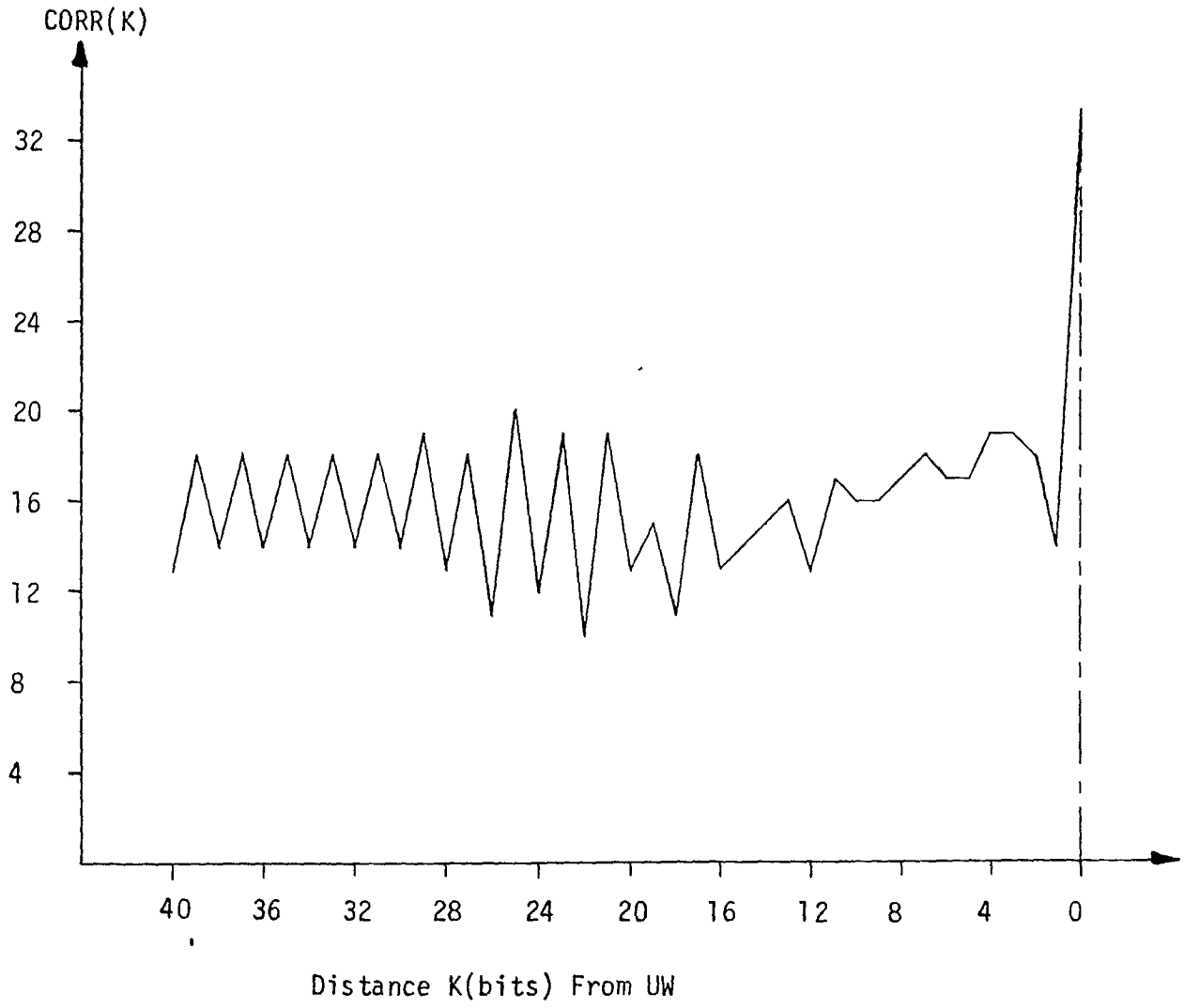

Figure 7.1(a) Correlation Profile During Acquisition (threshold = 0) (differential decoder enabled).

have large correlation values ("peaks") near the true position (K=0) of the UW. However, with the detection threshold set to I=0 (perfect match) the distinction between the performances of these n-tuples is diminished.

Figure 7.1(b) depicts the correlator's output after the apertures are set and differential decoding is inhibited. In comparing this profile with Figures 6.2 (pages 6-5 & 6-6) two items stand out: a) both sync patterns FAOE1236 and B121C17E show lower correlation peaks than 3731D7ED for k≠0, which renders them less vulnerable to false detections; particularly since the detection threshold is no longer set to zero; and b) the sync pattern FAOE1236 in Figure 7.1(b) exhibits lower correlation peaks in the vicinity of the true UW, as compared to B121C17E (Figure 6.2a). This latter attribute is useful if the detection threshold must be increased to prolong the terminal's retention of sync. The detector's enhanced vulnerability to false detections can be reduced by narrowing the aperture.

In short, the above distinctions between the correlations profiles generally translate into marginal differences in the terminal's performance parameters. This fact enforces the credibility of the selection criteria used, and identifies SELECT as an analytical tool for generating sets of "good" sync words for a given word length.

Note that cross-correlations between the FRUW and the DBUW are only relevant during initial acquisition (when the UW detector is loaded with the FRUW and encounters the DBUW in its initial scan). However, it is during initial acquisition that we seek a "perfect match" (threshold I=0). Figure 7.1c shows the cross-correlation

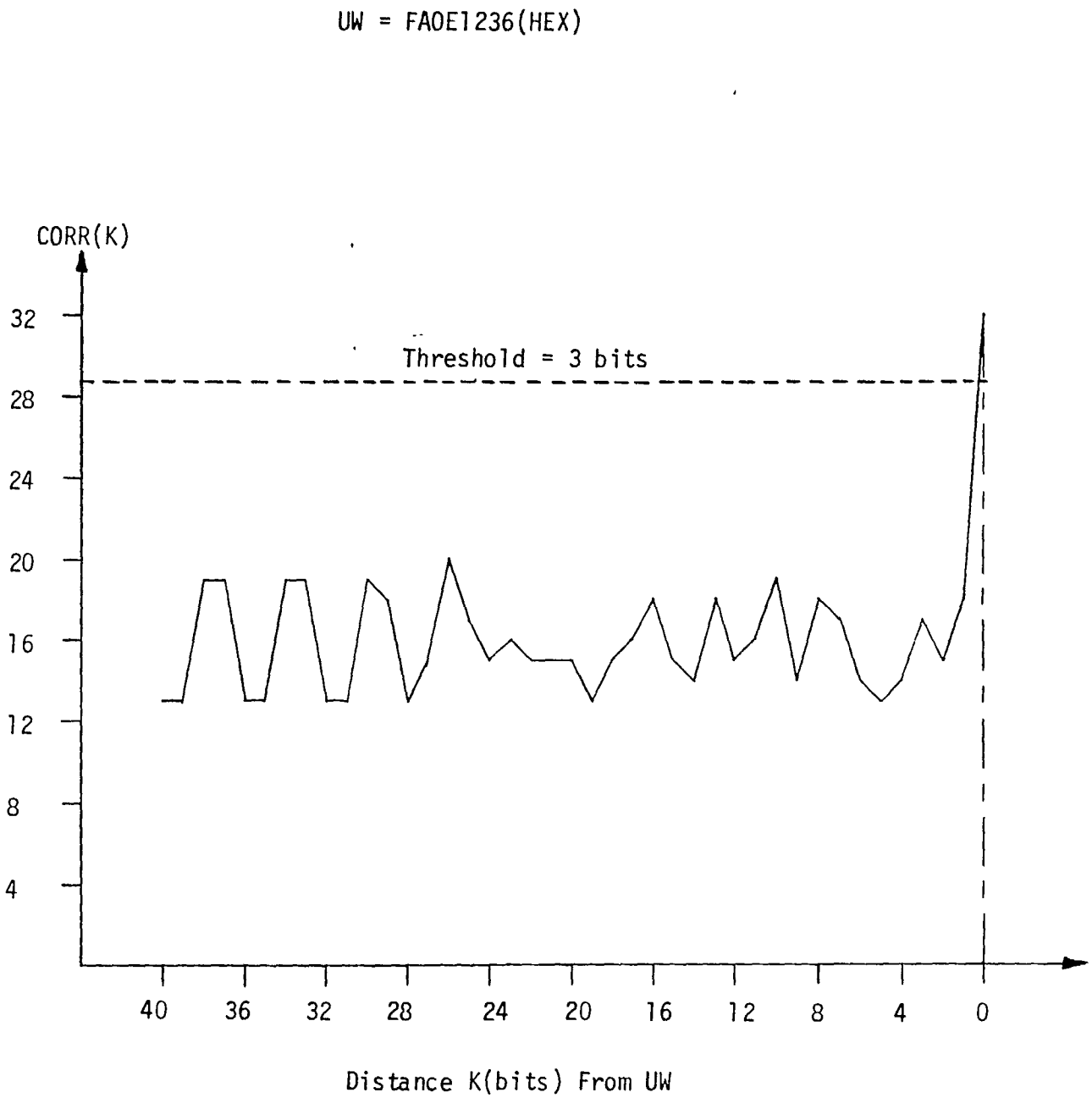

Figure 7.1(b) Correlation Profile After Apertures Are Set (differential decoder dis-abled)

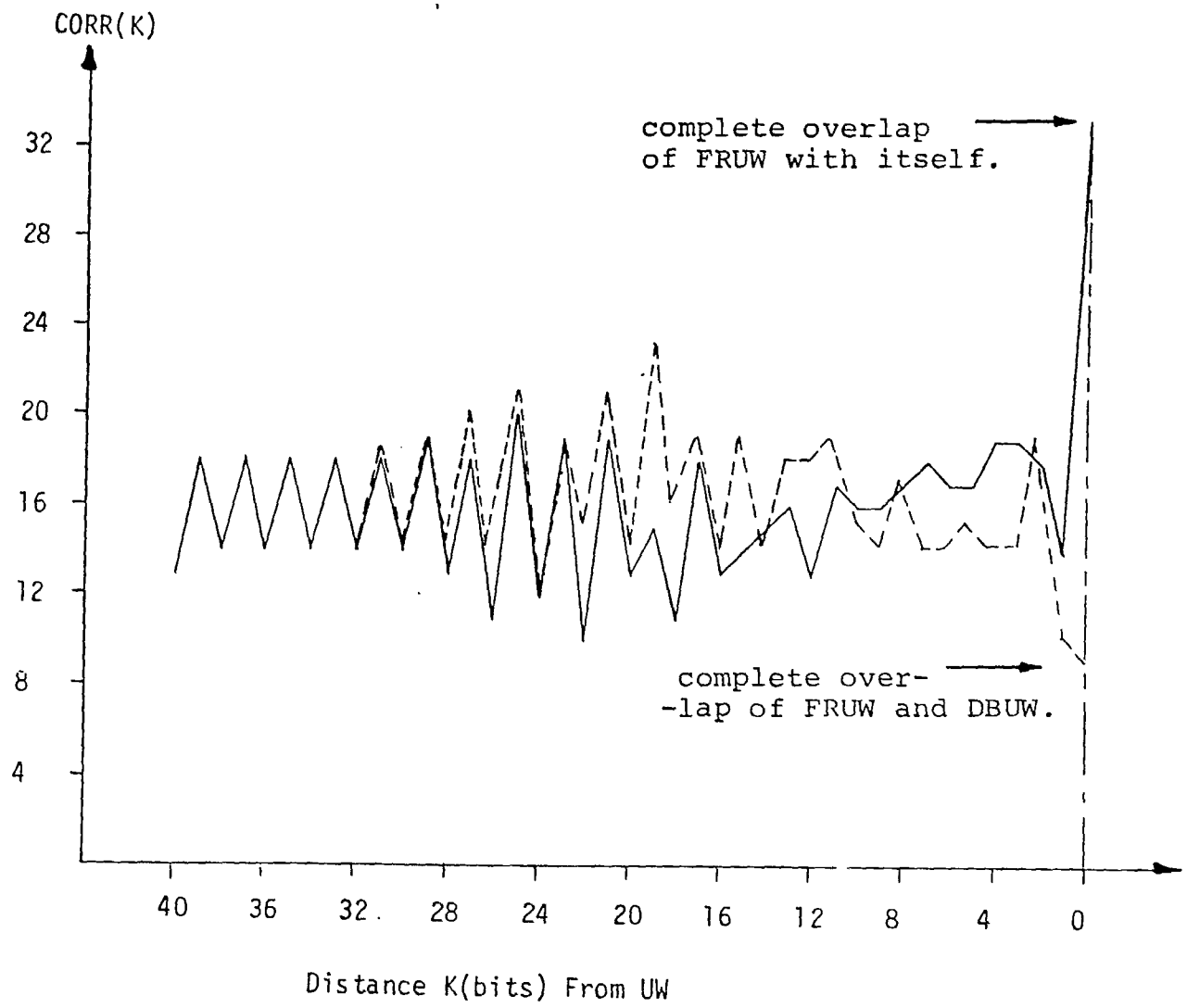

Figure 7.1(c) Correlation Profile For Acquisition (proposed configuration).

of FAOE1236 and B121C17E during acquisition (and with differential decoding).

7.3 Sensitivity Of The Terminal's Acquisition Performance

The acquisition algorithm shown in Figure 2.1 is executed by terminals that are entering the network for the first time, or have undergone lengthy outages. Ideally, the termnal should lock onto the correct FRUW in the shortest possible time. However, the meantime to acquire MTTA, and the probability of false acquisition P_{FA} are reciprocal functions of the verification count M. Two operational parameters are variable in the acquisition algorithm*: the aperture A_w and the verification count before lock-up L. Table 2.1 lists the tradeoffs in varying these parameters. Figure 7.2 shows the dependance of the terminal's MTTA on the count L. The wide aperture was set to values of 6, 20, 100 and 120 bits. However, the zero detection threshold rendered the likelihood of a false detection within any of these apertures sufficiently small as to be negligible. Consequently, the predominant event in acquisition becomes the non-detection of the FRUW, which does not depend on the aperture width. As a result, the curves in Figure 7.2 do not vary measurably with A_w. Furthermore, the results of this figure indicate that for BER $< 1 \times 10^{-2}$ the terminal acquires frame sync within the count of L frames. Although no measurements of modem performance are available, it is not expected to operate reliably at BER $> 10^{-2}$.

---

*The detection threshold for acquistion is fixed at I=0 to offset the double errors resulting from differential decoding.

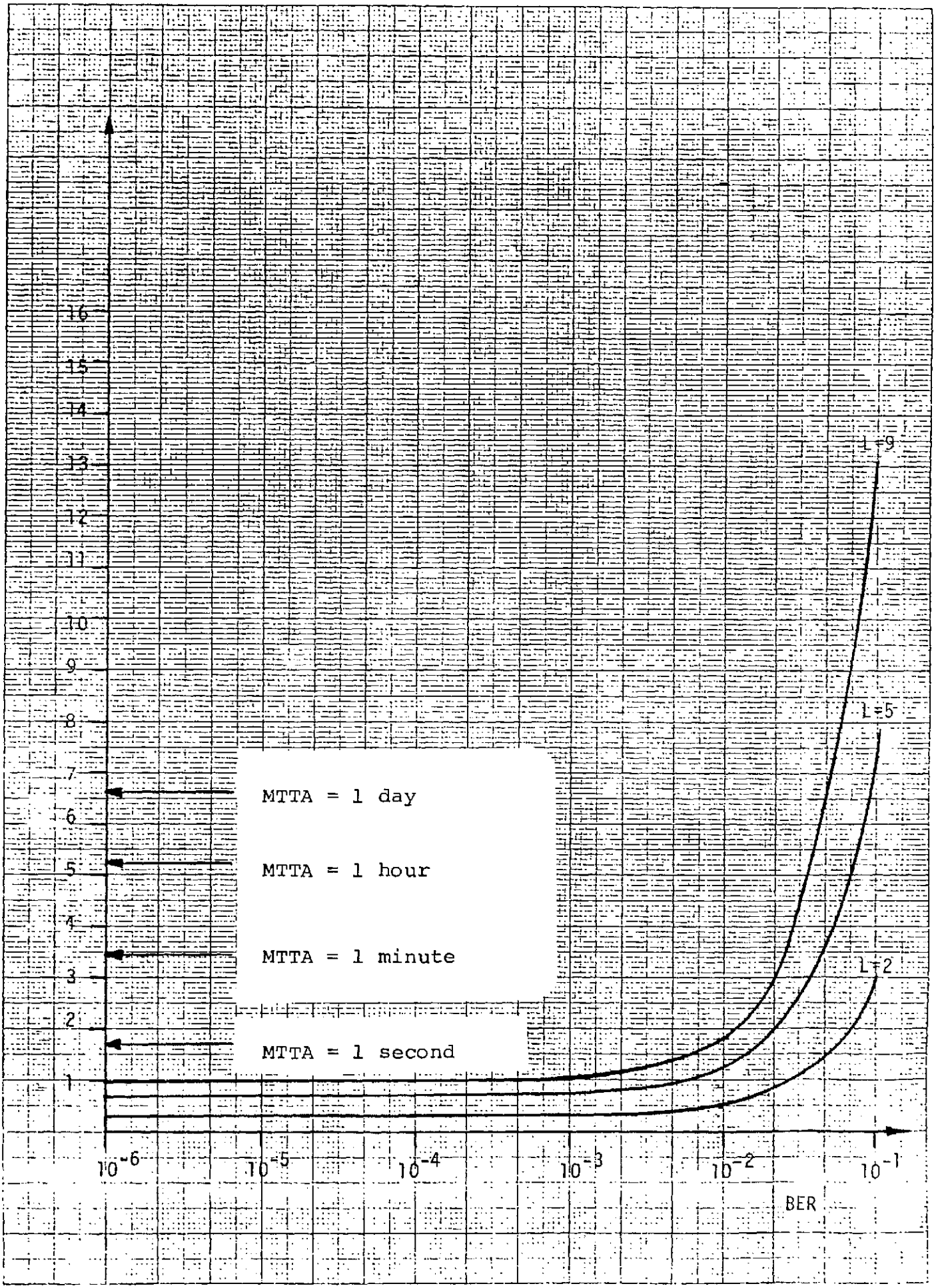

Figure 7.2 Variation In MTTA w.r.t. Verification Count, L [A_w =6,20,100,120 bits)

Figure 7.3 shows the probability of false acquisition as a functon of the aperture width A_w and the verification count L for a BER=$1x10^{-5}$. Note that for $A_w \geq 6$ bits the $P_{FA} < 1x10^{-12}$ (specified in Section 6.4) for L≥2 consecutive frames. Not shown in the figure is the P_{FA} for L=9 which lies beyond the scale of the graph and is less than $1x10^{-40}$ for $6<A_w<120$ bits and BER = $1x10^{-5}$. Figure 7.2 indicates that with L=2 and aperture widths much narrower than the current A_w=100 bits, the MTTA is approximately 40 msecs. Figure 7.3 assumes a worst case scenario by using a random-error channel (p=0.5) to show that $P_{FA}<10^{-12}$ for L=2. Thus for BER$<10^{-2}$ the P_{FA} will be significantly lower.

A final measure used to assess the terminal's acquisition performance is the cumulative distribution PACQ(X), or the probability that the terminal acquires in X frames or

less. The performance curves in Figure 7.4(a) show how this parameter varies as a function of the verification count L for BER = 10^{-6}, 10^{-5}, and 10^{-4}. Figure 7.4(b) depicts the parameter's values for BER=10^{-3}, $5x10^{-3}$ and 10^{-2}. It is interesting to note that PACQ(X) was not found to vary significantly with the aperture width. This fact seems to reinforce the conclusion that the zero detection threshold, and long sync word (32 bits) have minmized the effects of single-event false detections on the terminal acquistion.

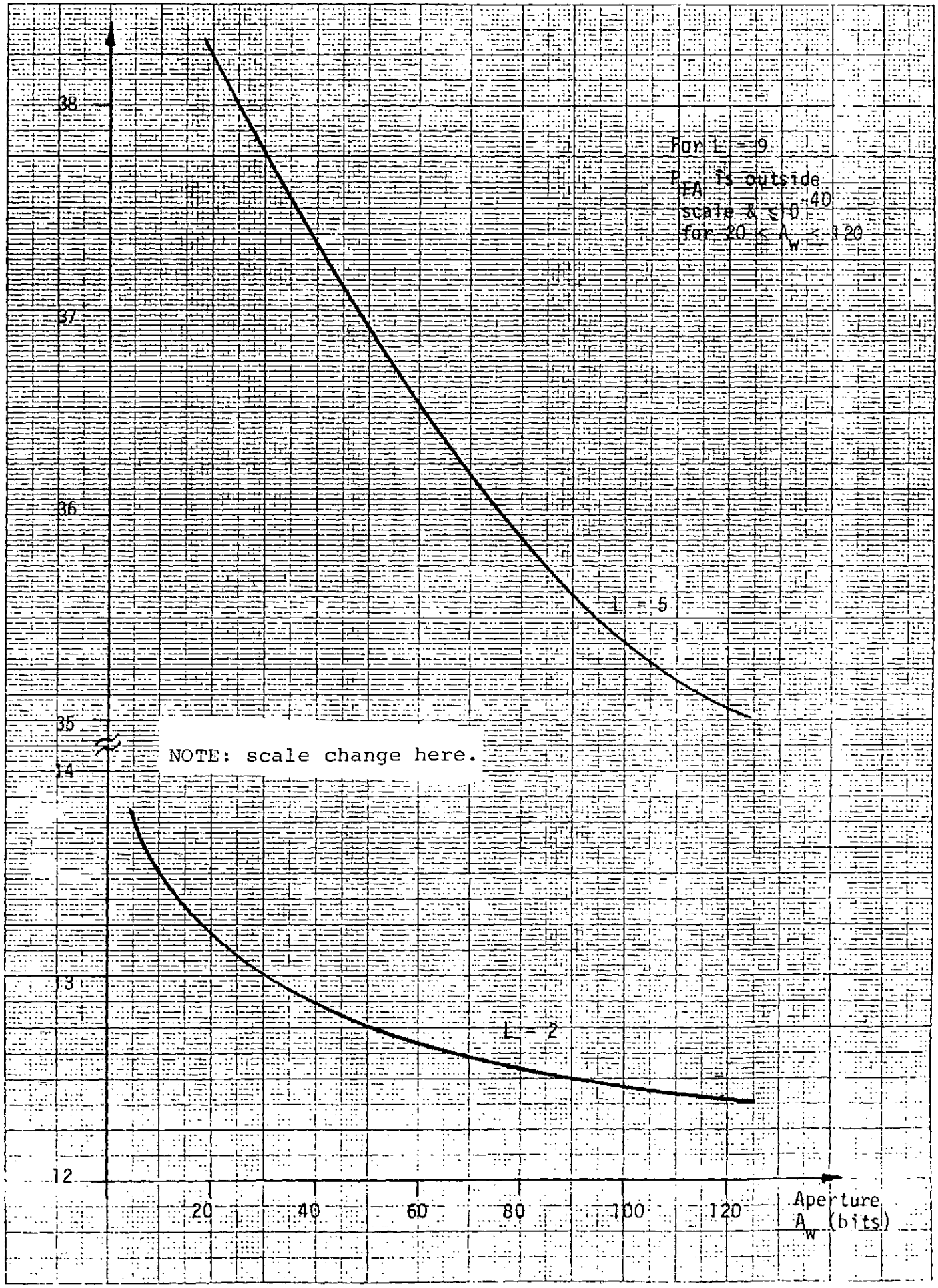

Figure 7.3 Prob. of False Acquisition vs Aperture Width (BER = 1 x 10^{-5})

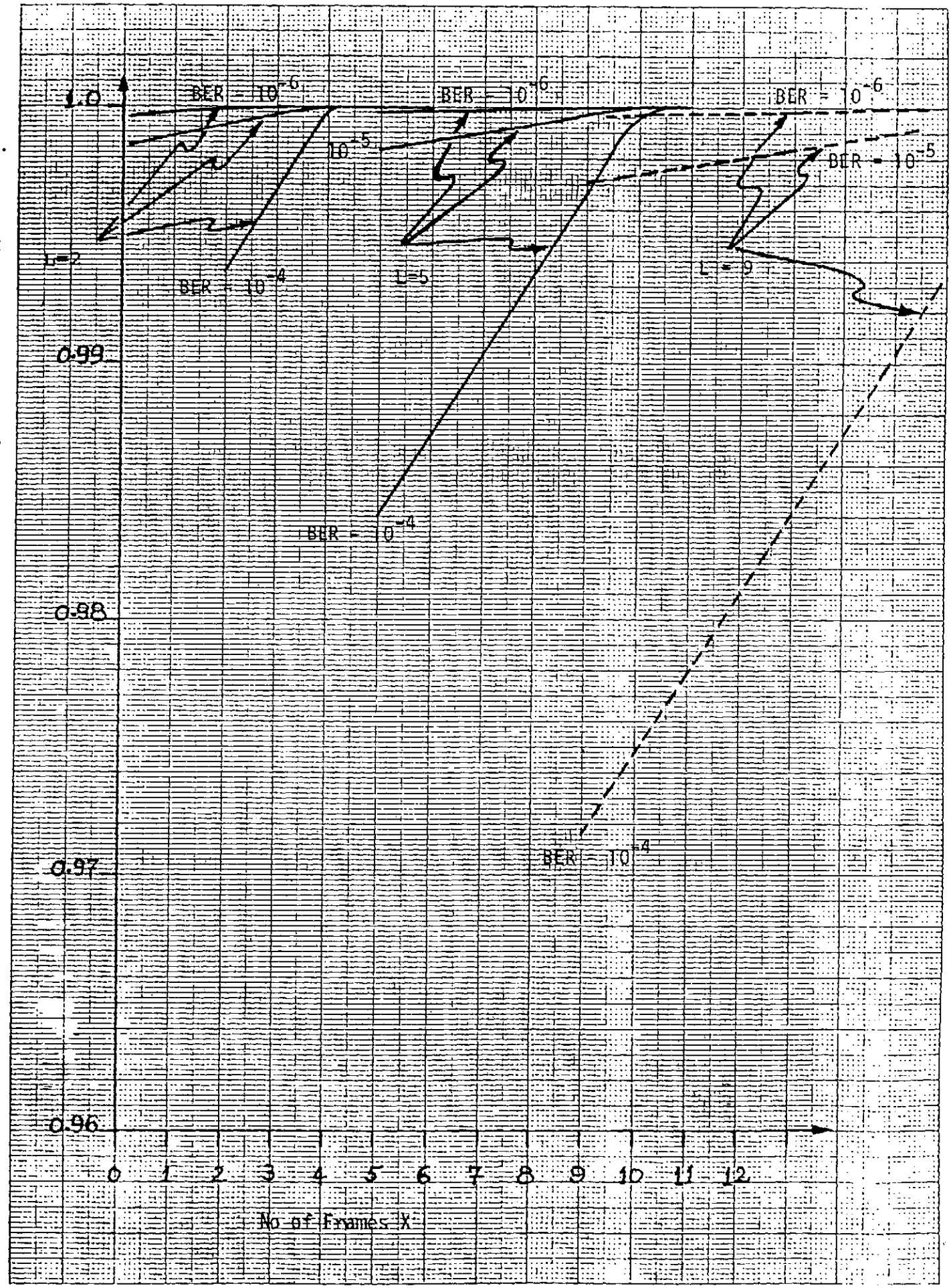

Figure 7.4(a) PACQ(x) As Function of BER and Verification Count L Frames ($BER \leq 10^{-4}$)

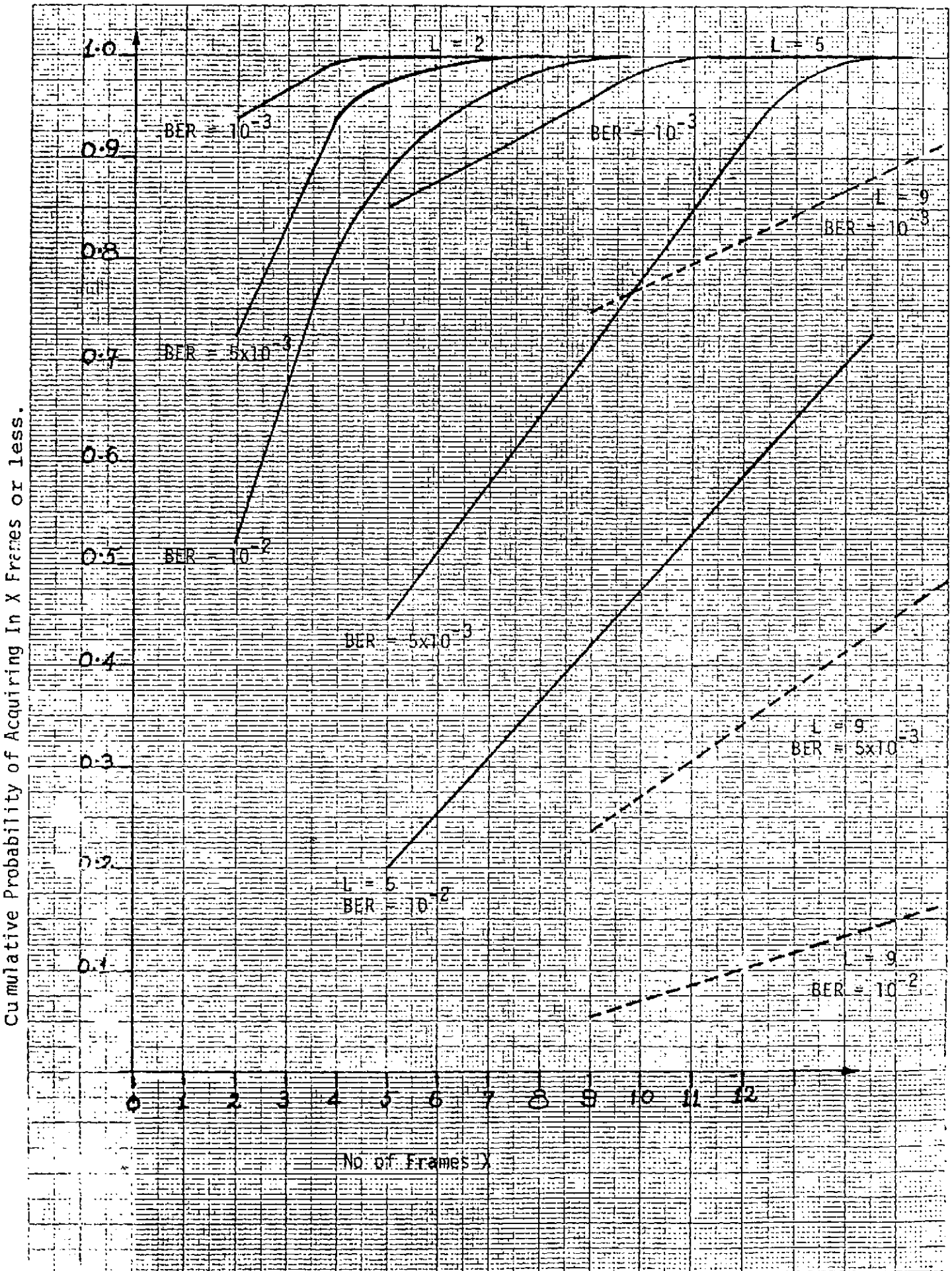

Figure 7.4(b) PACQ(X) As A Function of BER and Verification Count L frames (BER $\geq$ 10-3)

In reviewing the results discussed in this section and their interpretation, several conclusions can be drawn (given that the detector's threshold remains at zero, and the sync word used is 32-bits in length and chosen from the subset of n-tuples generated by SELECT):

a) For typical north-south and east-west satellite station keeping to within ±0.05° it can be shown that the accrued timing-error per 20 msec frame is less than one nanosecond [21]. Without station-keeping, and assuming a maximum inclination angle of 3° the accrued timing error per frame is less than 4 nanoseconds. For the 3.1584 Mbps burst rate used by the terminal, these errors correspond to less than a single bit-duration. This fact tends to favour a narrow aperture to minimize the probability of false acquisition. However, Figure 7.3 has shown that P_{FA} is an unlikely event with a 32-bit UW and threshold set to I=0 (even with L=2 and A_w=100 bits). Consequently, since timing failures or spurious pulses can cause sudden deterioration of local timing the tendency is to propose a wide aperture of up to 100 bits. This would withstand a temporarily erratic timing error of 50 times the rms error-value.

b) If the specification of acquiring within 100 msecs, noted in Section 6.4 is acceptable, the verification count of L=5 does ensure that $P_{FA} < 1 \times 10^{-12}$ at BER = 1.4×10^{-4}. However, Figures 7.4 show that the probability of acquiring in less than 100 msecs will not exceed 0.99 for BER higher

than 10^{-5} i.e. at BER=1.4×10^{-4}, P_{FA} is satisfied but not PACQ. If the count is reduced L=2 the P_{FA} remains below 1×10^{-12} for BER$<1.4\times10^{-4}$ and PACQ(x) remains above 0.99 for BER $< 10^{-3}$ (i.e. for a wider range of BER values than for L=5). Furthermore, the MTTA is reduced from 100 msecs to 40msecs. The fact that such a reduction in the MTTA is not a tangible improvment to the user is not the point. The point is that this reduction can be achieved without violating the specified requirements for the P_{FA}, and satisfies the requirement that PACQ (x=100 msecs) > 0.99 over a wider range of BER values.

At the risk of tedious repetition, it must be emphasized that the above modifications to the current operating parameters are proposed within the restriction that: i) the detector threshold remains at zero, and ii) the 32-bit sync word is chosen from the n-tuples generated by the program SELECT.

7.4 Sensitivity Of The Terminal's Steady-State Performance

The retention algorithm detailed in Figure 2.2 represents the terminal's steady-state behaviour until events promote the loss of frame sync. Ideally the terminal, having acquired frame sync and set its detection apertures, should continue receiving the FRUW indefinitely. However, Section 2.1 addressed several factors that disturb the terminal's long-term operation: i) false detections preceding the true UW that lure the aperture from its correct position; ii) drift of the locally generated aperture due to accrued timing errors between the reference terminal and the local terminal; and iii) noisy channel conditions that can result in a high probability of missing the UW in its aperture. It is noteworthy to recall that these factors are not

independent, with one element, precipitating or exacerbating the effects of the others.

In retention four operating parameters are at play: i) the detector threshold I (not necesssarily set to zero), ii) the narrow aperture width A_{VN}, iii) the flywheel count M and iv) the normalized rms timng error ε bits/bit. Figure 7.5 depicts the variation of the MTBSL with the BER as a functon of the threshold I and the flywheel count M for a rms timing error $\varepsilon=1x10^{-9}$. In section 5 the storage (memory) allocations available on the PDP-11/23 were shown to present limitations to the value of M that can be used in the program RETNTN. This primarily stems from the dependence of several transition matrices (RETAIN, QMTRX) in the program RETNTN on the value of M. As a result, the values shown in Figure 7.5 (M=5,10,15) are used to extrapolate "trends" for the terminal's behaviour. Two aspects to note regarding the results shown in this figure are: 1) that the MTBSL varies immeasurably with the variation of aperture width in the range $6<AVN<50$ bits; and 2): if $BER=10^{-2}$ is nearly an upperbound to the operational condition of the link, then the requirement that MTBSL>1week (specified in Section 6.4) is satisfied by all the configurations shown in Figure 7.5for anon-zero threshold. The first observation is primarily due to the fact that: a) the probability of false detections within the aperture (that can cause aperture shifts) is very small, and b) the rms timing error $\varepsilon = 1x10^{-9}$ translates to an accumulated time-shift of $6.3x10^{-5}$ bits per frame (i.e. the terminal would need to flywheel for an interval exceeding $15x10^{3}$ bits - nearly 5 minutes - before the accumulated shift of the FRUW within its aperture would equal 1 bit). However, an rms timing error of $1x10^{-9}$ can only be

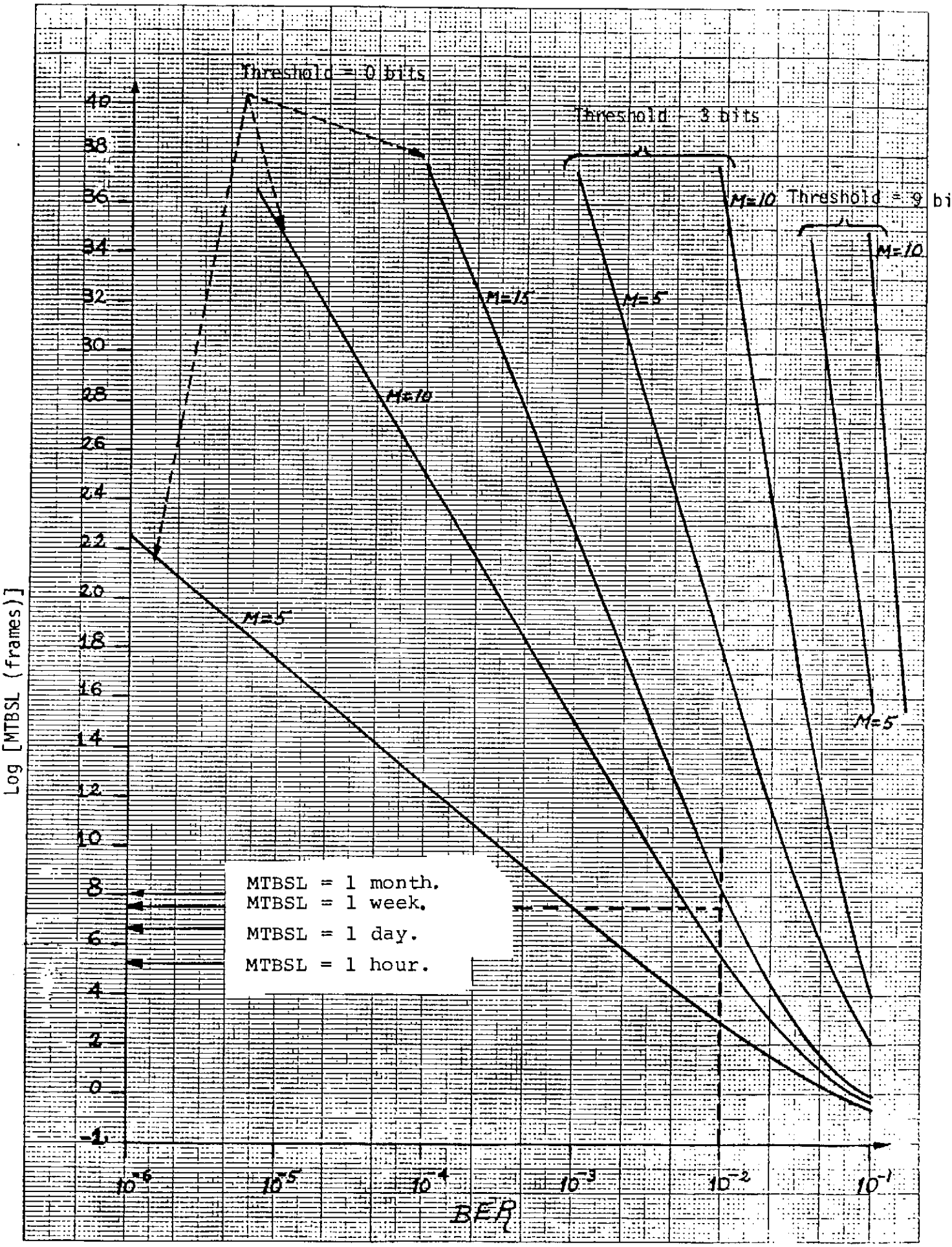

Figure 7.5 Variation of MTBSL with BER (All Apertures); $\varepsilon = 1 \times 10^{-9}$

achieved by "tighter-than-usual" station-keeping and the use of highly stable local timing references (atomic clocks or periodic timing corrections using a synchronization network (see refs. 40-46 in [2]) such as the LORAN-C or OMEGA networks.

In [1] a clock stability of $1x10^{-9}$ was specified only for the reference station. All other terminals were required to maintain a maximum timing error of $1x10^{-6}$ bits/bit. Figure 7.6 repeats the results of Figure 7.5 for an rms timing error of $\varepsilon = 1x10^{-6}$. Although this now represents an accrued time-shift (between the FRUW and its aperture) of 0.06 bits per frame this would still be accumulated over a count of M=50 if A_{VN} = 6 bits, and M=266 for A_{VN}= 32 bits. Comparison of the results for both values of ε shows very little degradation in the MTBSL. Consequently, the conclusion that for the aperture range $6 \leq A_{VN} \leq 50$ bits, and the detector threshold $3 \leq I \leq 9$ bits, the MTBSL exceeds 1 week ($\approx 3x10^7$ frames) at BER remains valid. This performance seems to be maintained for $\varepsilon \leq 1x10^{-6}$.

However, another specification recorded in Section 6.4 is that the probability of missing the FRUW within its aperture shall not exceed the $1x10^{-18}$ at BER=$1x10^{-4}$ and $1x10^{-6}$ at BER=$1x10^{-2}$. Figure 7.7 clearly shows that this requirement can only be satisfied by a threshold level set at $I > 3$ bits. The curve for I=9 obviously satisfies ths operational constraint. Further iterations of the program RETNTN show that it is satisfied for $I > 7$ bits ——— but <u>not</u> for the current threshold setting of I=3 bits. Note that increasing the threshold decreases the

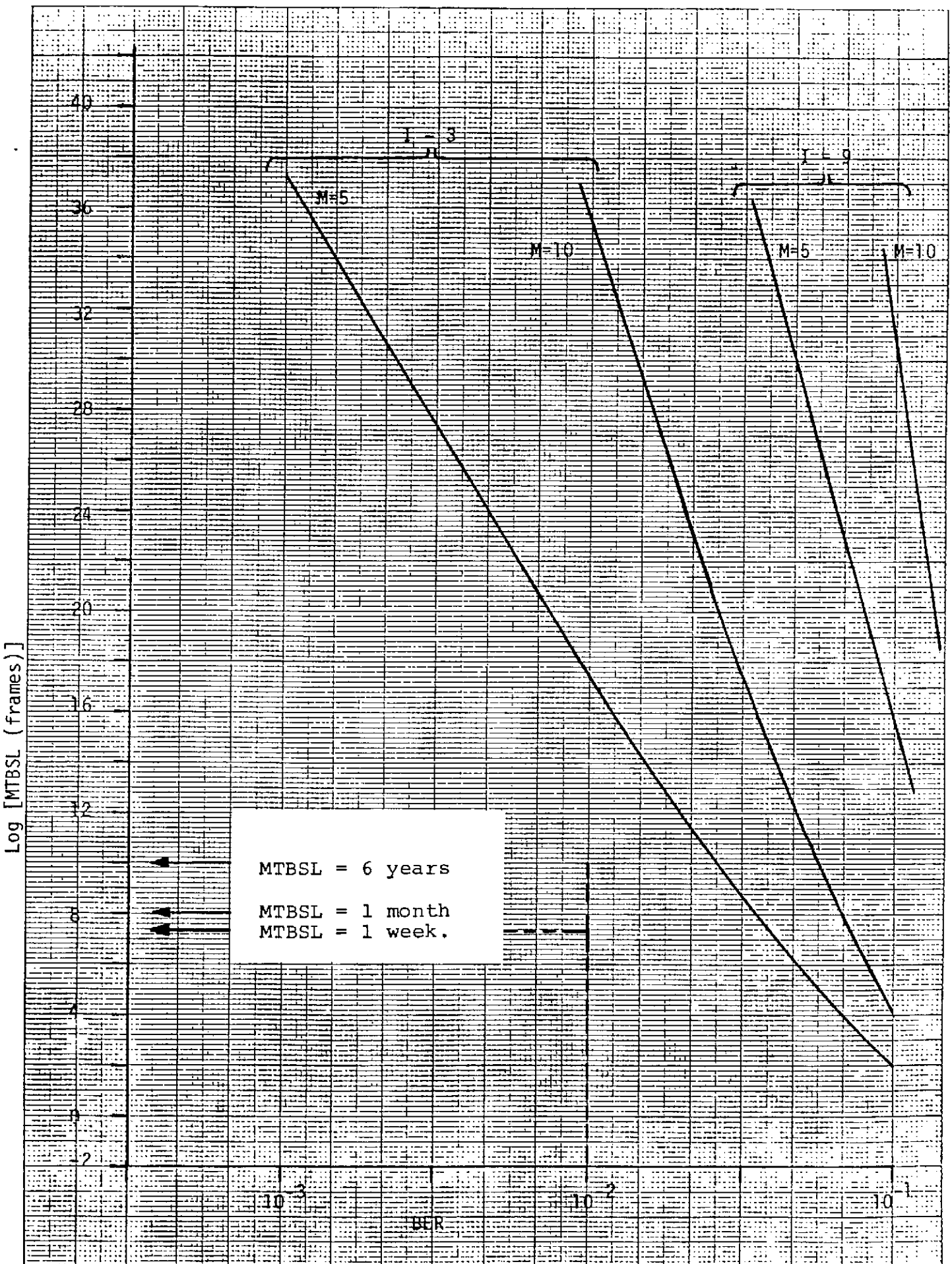

Figure 7.6 Variation of MTBSL with BER (All apertures); $\varepsilon = 1 \times 10^{-6}$

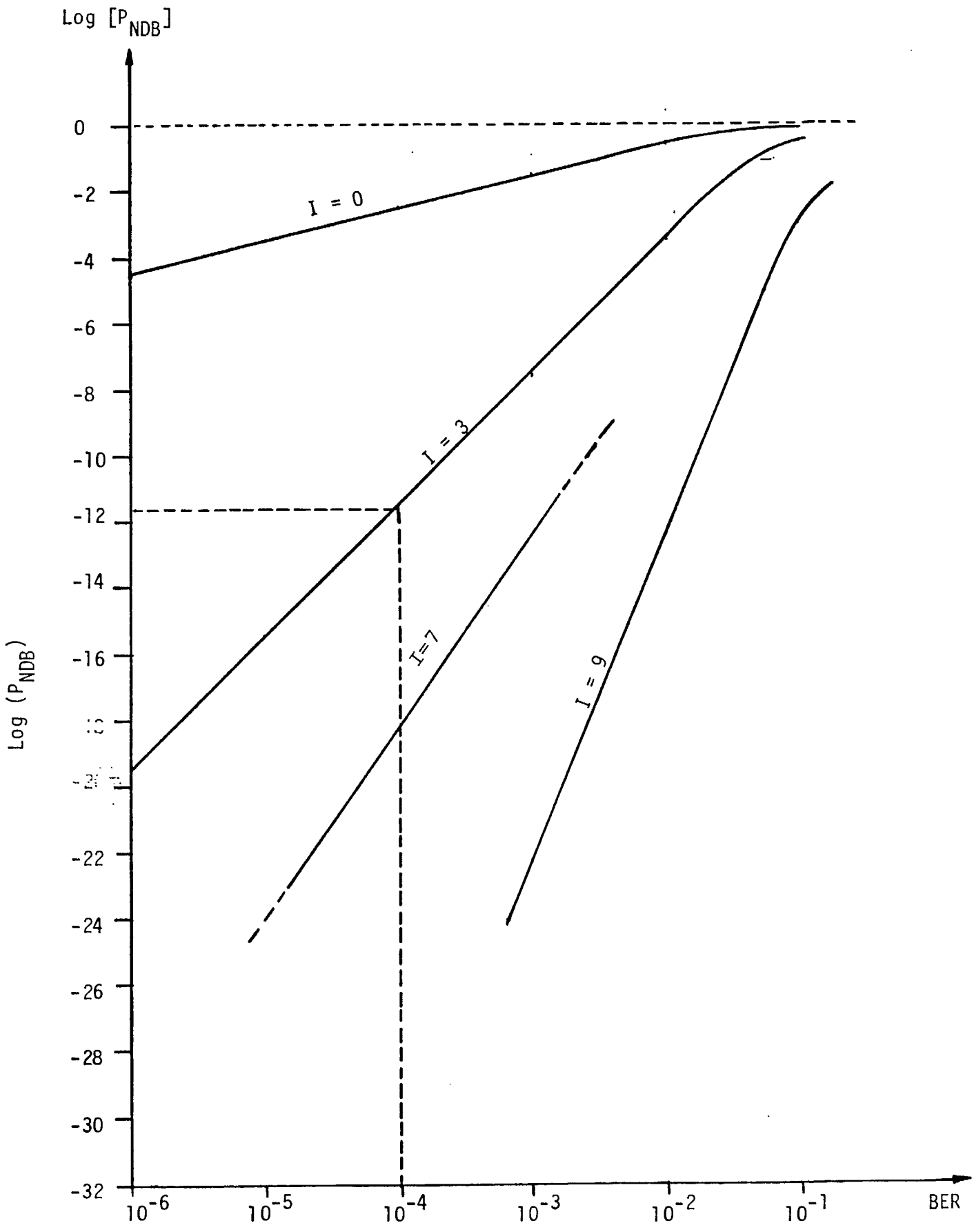

Figure 7.7 Probability of No-Detection Within Aperture (A_{VN} = 6,32,50)

likelihood of not detecting the FRUW and increases the probability of a false detection within the aperture. Here, the n-tuples generated by the program SELECT seem to have correlation profiles that can withstand the increase of I to 7 bits without significantly increasing P_{FDB}. However, Section 8.2 details the vulnerability of the detector at I=7bits if it is suddenly faced with scanning an empty frame (as in a data burst suddenly disappearing due to failure of its terminal).
The discussion in Section 8.2 argues that although a threshold of I=7bits achieves the miss-probability criterion, equipment failures that may result in the detector scanning an empty frame with a high threshold favour the use of a much lower value of I=3 or 4.

Figure 7.8 depicts the variation in the probability of burst sync loss P_{BSL} as a function of BER for A_{V_N} = 32 bits and $\xi = 1x10^{-9}$*. These results reinforce the above argument that a zero threshold is an unwarranted and harsh setting for the detector, and that an increase of I above 3 bits will prolong steady-state operations without measurably increasing the likelihood of false detections within the aperture. Increasing the rms timing error to $\xi = 1x10^{-6}$ produces a set of curves which lie approximately one order of magnitude higher than those shown since the contribution of time shifts (between FRUW and aperture) to sync loss increases P_{BSL}.

*Values for I = 7 maintain the trend and fall to the right and beyond the scale of the axes shown.

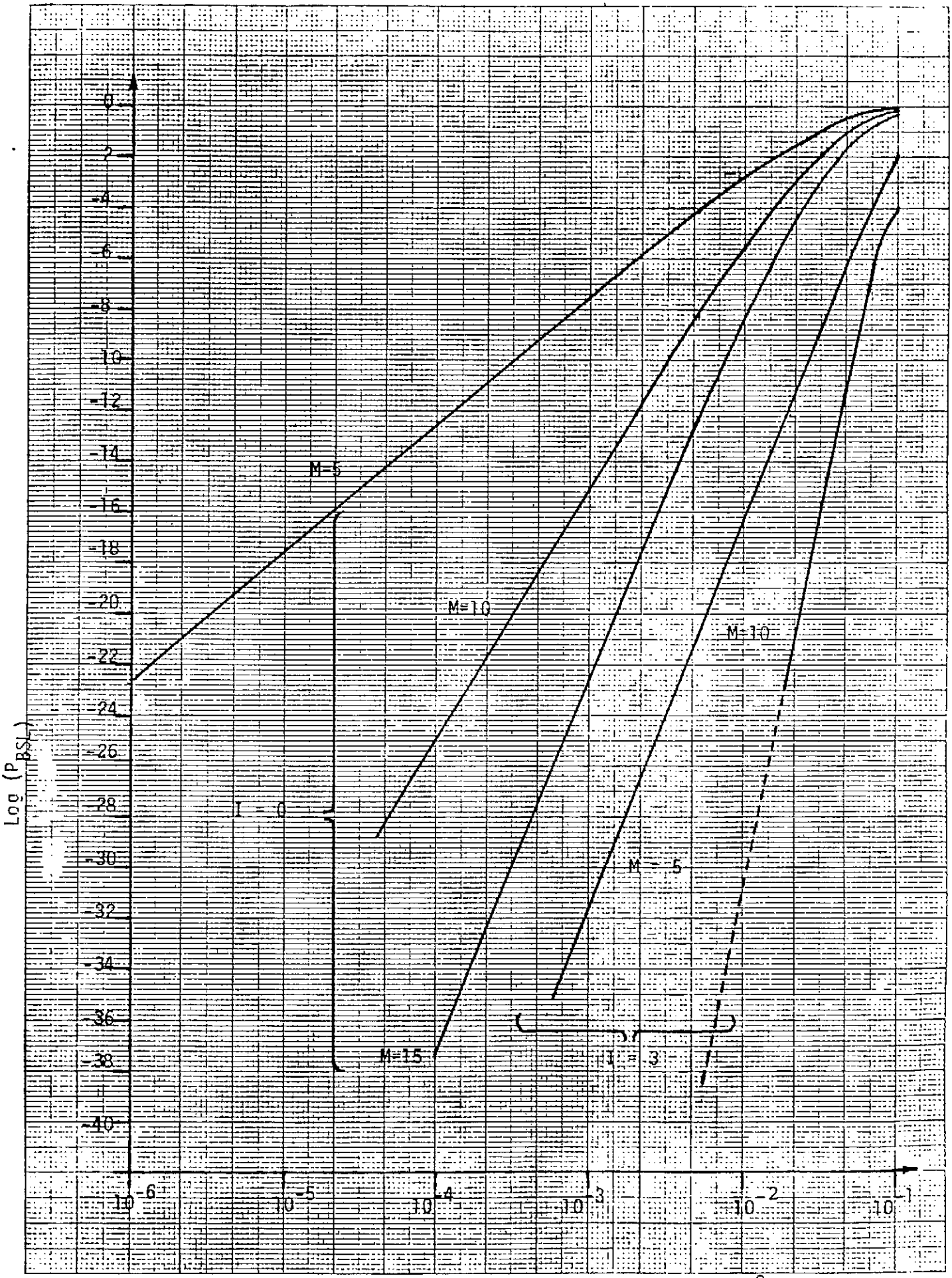

Figure 7.8 Variation of P_{BSL} with BER (A_{VN} = 32 bits; $\varepsilon = 1 \times 10^{-9}$)

The results presented in Sections 6 and 7 focused on the terminal's sensitivity to variations in parameters that can be modified from the operator's console or without major software modifications. These do not include the UW length n or the acquisition threshold. The software programs documented in Section 5 and appendices C-F can be used, however, to evaluate a wider range of configurations. The following section interprets the results of this report enroute to determining the terminal's sensitivity to its operational parameters. This interpretation is then used to identify those modifications to the current system which offer potential improvements to its performance.

8.0 CONCLUSIONS AND RECOMMENDATIONS

8.1 Synthesis of Results

The first major result in the analysis concerns the format of the sync word. All n-tuples in the set generated by SELECT were used to generate results similar to those presented in Section 7. Although the set of detection probabilities $\{P_{FDO}, P_{FDW}, P_{FDB}$ etc.$\}$ attributed to these syunc words were not the same, their differences were not sufficiently large to cause measurable variations in the performance parameters. This result is primarily due to:

(a) the length of the n-tuples, and

(b) the fact that the set of candidate n-tuples are PN sequences which are generally considered "good" sync words.

Conclusion: n-tuples generated by SELECT will generate similar sync performances*.
The second autcome of the parametric analysis concerns the probability of a false detection occurring within the aperture (A_W or A_{VN}).

Typically false detections can be minimized by narrowing the aperture and/or lowering the threshold of tolerable errors. In acquisition the threshold is already set to its lowest level (I = 0). Typical timing errors of

*Note however that the n-tuples that satisfy the Neuman-Hofman criteria exhibit better correlation profiles -- see Section 7.2.

and $\xi = 1x10^{-9}$ specified in [1] are not dominant factors in acquisition, a procedure that is expected to be completed within 100 msecs (5 frames). This fact permits the acquisition aperture A_w to be narrowed below its current 100 bits. This further reduces P_{FDB} and the probability of false acquisition P_{FA}. An aperture width of $A_W \approx 6$ bits provided further protection from spurious false detections and did not render the detector vulnerable to timing errors. Note that for BURST sync where the terminal's aperture does not track the DBUW (e.g. apertures set to receive bursts from remote terminals operating in open loop) slightly larger apertures are warranted.

The current verification count of L=5 consecutive frames did not meet all operational requirements discussed in Section 6.4. Specifically, for L=5, PACQ(X<100 msecs) $\neq$ 0.99 at BER $\approx 1.4x10^{-4}$. However, for L=2 frames this condition is satisfied for BER$< 1x10^{-2}$ and the P_{FA} is still maintained below $1x10^{-12}$. This reduction in verification count reduces the MTTA by a mere 60 msecs, but satisfies the acquisition requirements listed in Section 6.4 and in [1].

As in acquisition, the timing errors characterized by $\xi=1x10^{-9}$ or $\xi=1x10^{-6}$ do not measurably affect the MTBSL for aperture widths $6<A_{V_N}<50$ bits and detector thresholds $0<I<9$ bits. Again here the P_{FDB} increases with A_{VN} but

not to an extent where it plays a major role in the estimate of MTBSL. This may be due to the high degree of non-correlation between the FRUW and its deterministic preamble (CR & BTR sequences).

A detection event that does play a major role is the probability of not detecting the sync pattern P_{NDB}. For a threshold of I=0, or the current value of I=3 the requirement that $P_{NDB} < 1x10s^{-18}$ at BER = $1x10^{-4}$ is not satisfied. However, for I=7 P_{NDB} is below this bound over a wider range of BER values. The resulting increase in P_{FDB} (or decrease in MTBSL) is negligible. However, equipment failure and other factors discussed in the following Section induce the return to a lower threshold of I=3 where the miss-probability P_{NDB} is merely increased to $4x10^{-12}$.

8.2 Focus On False Detections And Lock-up:

Two characteristics of this system have contributed to the minimization of effects of false detections:

(i) the 32-bit sync word relegates P_{FDW} and P_{FDB} to minor roles in the evaluation of the performance parameters; and

(ii) the low burst rate of 3.1584 Mbps results in a wide bit duration ($\approx 0.3\mu$secs) and apertures can be reduced without increasing the likelihood of the UW drifting beyond them. Given that an rms timing error of $\xi = 1x10^{-6}$ represents a drift of 0.06 bits per frame, a retention algorithm in which I=7 bits and A_{VN}=32 bits can sustain a flywheel interval of M≈ 260 frames as opposed to the current value

of M=50 frames. Note however that a closed-loop guard time of 16 bits (≈5μsec) is narrower than the aperture A_{VN}=32 bits. This would-allow terminals to remain in sync after their bursts have overlapped. Consequently, it is recommended that the FRUW aperture be constrained to 16 bits.

A tenuous assumption that reduces the model's estimates of false detections to a rare event is that the UW detector is never exposed to a random bit stream with a non-zero threshold:

(i) during acquisition the open aperture approximates the scanning of random data but the threshold is set to a perfect match (I=0) and

$P_{FDO} \approx 1-(1-1/2^{32})^{T_b-1}$ [see appendix A] which is near-zero;

(ii) during retention the narrow aperture sees a portion of a deterministic BTR sequence appended to the UW [see Figure 4.7] such that the cross-correlation operations of the detector (with threshold set to 7 bits) reduce the P_{FDB} below 10^{-10} for BER=10^{-4}.

The following potential event during retention demands that a third scenario be considered. Failures in the transmit or receive terminals can cause the latter to suddenly have its burst receive aperture (s) enabled at a vacant portion of the frame (see Figure 8.1). The UW detector is now exposed to empty seqments of the frame with its threshold set to I=7 bits. If the noise level at the input to the modem is sufficiently high the output of the demodulator (input to the UW

detector) will be a random binary stream. From equation A.6 the single-event probability of a false detection in random data is approximately 10^{-3}.

The resulting probability of a false detection in random data (with a 16-bit aperture) is approximately $1-(1-10^{-3})^{16} \approx 0.02$, and the most likely number of false detections in any empty frame is $[10^{-3} \times T_b] \approx 63$ occurrences (where $[x]$ denotes the largest integer value less than X).

This high frequency of false alarms is due to random data being correlated with a high detector threshold of I=7 bits. Two solutions are proposed for this problem: (a) a software solution, and (b) a hardware solution.

The details of both are discussed below.

(a) The Software Solution:

If the event of examining random data after acquisition is incorporated into the model, two operational parameters must be changed:

(i) If the verification count L is increased from L=2 to L=5 frames, the probability of acquiring within 100 msecs cannot be maintained for BER $> 10^{-5}$ (see Figure 7.4). This probability will drop below 0.85 for BER $> 10^{-3}$.

(ii) If the retention threshold I is reduced from 7 bits to 3 bits, the requirement that

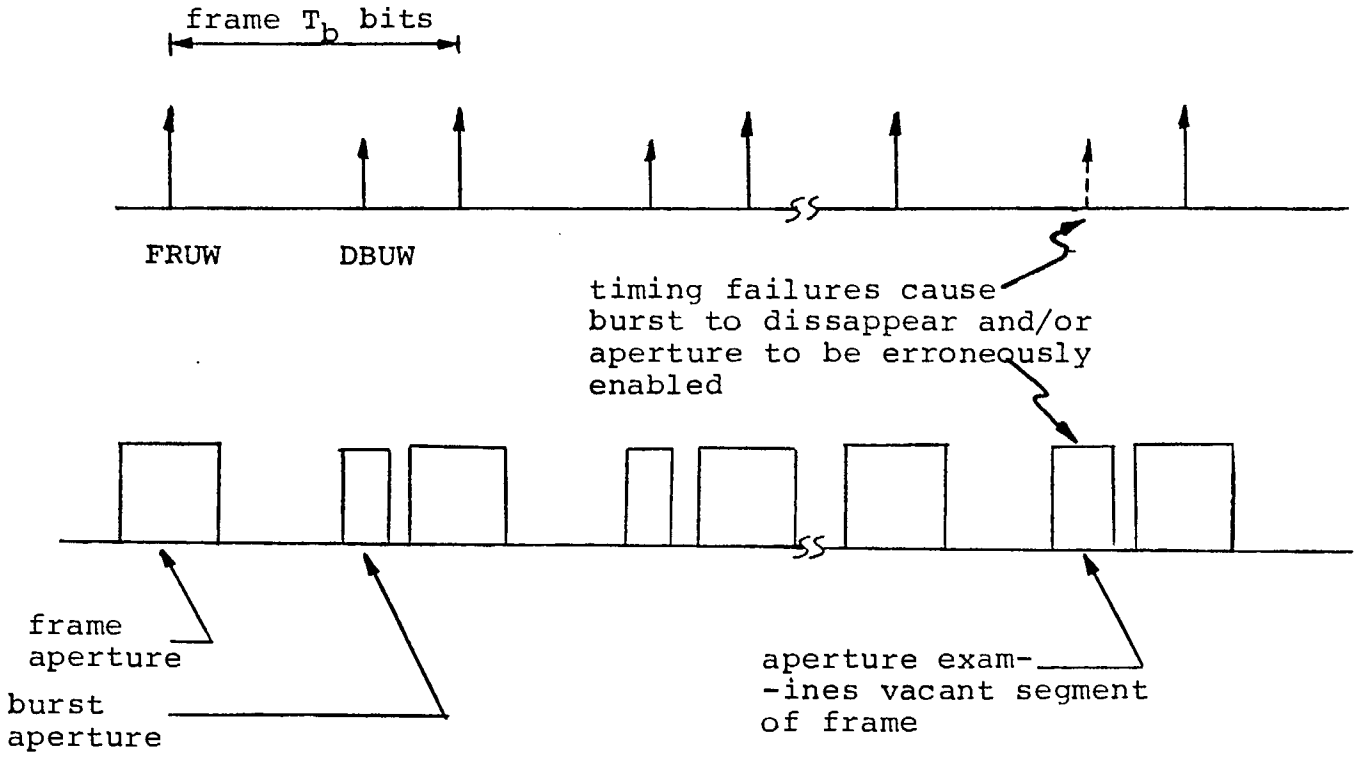

Figure 8.1 UW Detector Scanning Vacant Frame Segment.

$P_{NDB} < 10^{-18}$ at BER = 10^{-4} is not satisfied. Figure 7.7 shows that at this BER the $P_{NDB} \approx 10^{-12}$ which is acceptable-considering the hazards of using high threshold values (discussed earlier in this section).

Realizing that false detections within the aperture also cause loss of data, the reduction of the detection threshold increases P_{NDB} but decreases P_{FDB}.

(b) The Hardware Solution:

From Figure 8.1 and the ensuing discussion it is evident that the compelling factor is the occurrence of random data at the output to the demodulator when no data burst is present. A circuit may be designed in the modem to detect the absence of the burst. The threshold for this circuit must be set such that the "worst" thermal noise level at the input to the demodulator cannot trigger an output. Figure 8.2 proposes a block diagram detailing how this circuit can be used to "gate" the output from the demodulator. The absence of a data burst causes the UW detector to see a DC level which cannot trigger a SYNC DETECT pulse. The proposed circuit can be enabled <u>after</u> initial acquisition of frame sync and be triggered by the phase deviation $\Delta\emptyset$ in the CR loop exceeding a pre-estimated threshold. This solution allows us to define the operational parameters that satisfy the requirements specified in Section 6.4. However, its incorporation into the existing TDMA terminals would involve additions to the existing hardware.

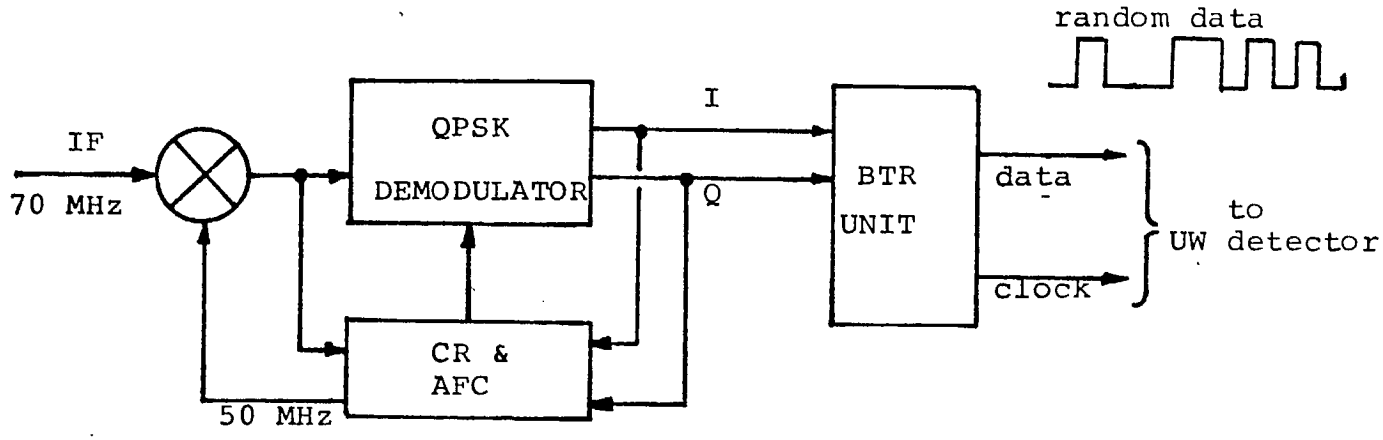

a) existing demodulator circuit

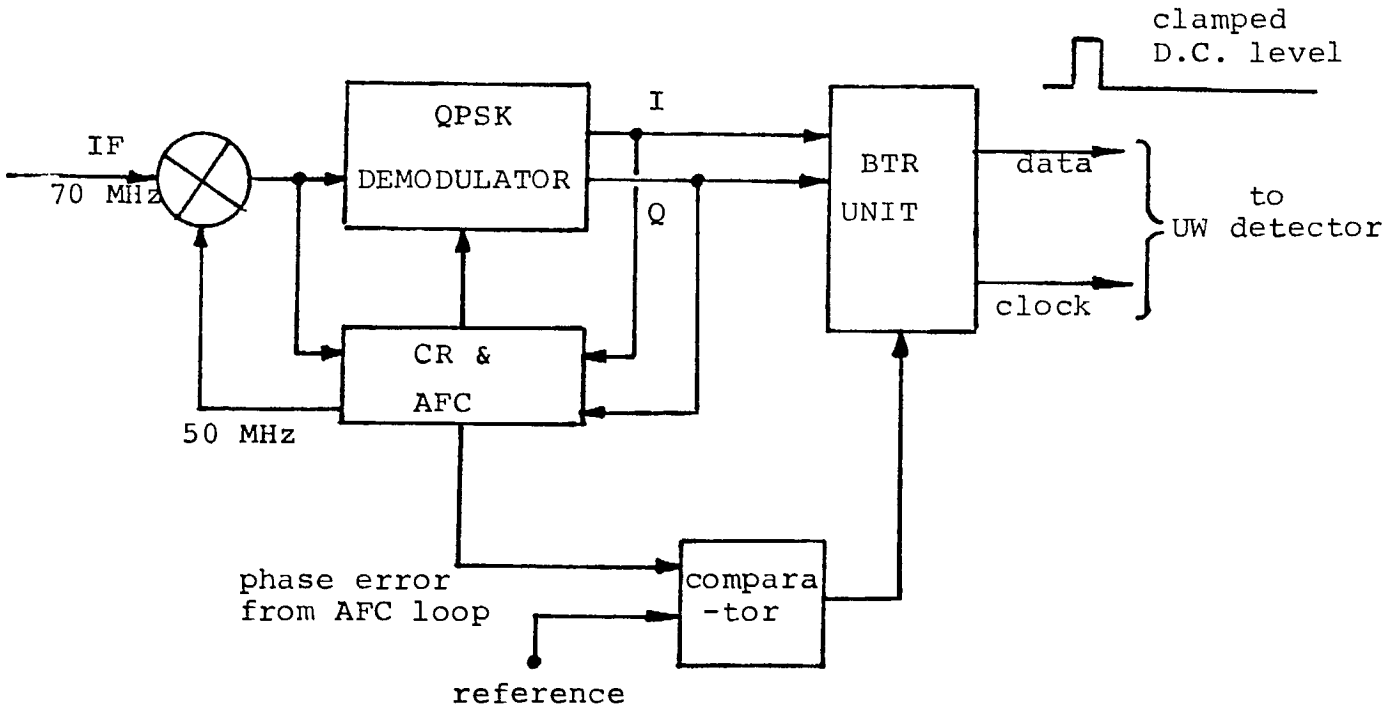

b) proposed hardware solution

Figure 8.2 Gating output of the demodulator.

8.3 Proposed Modifications

The concluding section of this report must re-emphasize the importance of correctly interpreting the results detailed herein. The burst rate, frame interval, preamble lengths are all factors which, if altered, may alter the terminal's sensitivity to its operational parameters. Table 8.1 lists the proposed changes to the current parameters, and the expected improvements in the terminal's performance. Using equation 2.1 and the proposed configuration Table 8.2 lists the terminal's availability versus BER.

Note that nowhere in the report are the effects of hardware/software failure included in the availability estimates. Availability here refers to the terminal being in the steady-state retention mode. However, an estimate of the "overall" availability can be derived as follows for a given BER.

(i) define A_{TDMA} to represent the availability of the terminal's burst synchronizer unit (in steady-state) as listed in Table 8.2; and

(ii) derive the hardware/software equipment redundancy necessary to achieve an equipment availability A_{EQP} [22].

Assuming that both types of "failures" are independent (which is not strictly true as shown by the effects of equipment failure on the UW detector in Section 8.2), the overall availability A_{TOT} is given by

	Parameter	Current System	Proposed Modification	Improvement
ACQUISITION	Detection Threshold	0 bits	0 bits	Not applicable
	Wide Aperture Aw	100 bits	50 - 100 bits	Although timing errors allow an aperture of 10 bits, hardware failure can affect local timing. Wider aperture has little effect on false acquisition (Figure 7.3).
	Verification Count L	5 frames	(i) 2 frames if PACQ requirement is to be satisfied (ii) 5 frames if PACQ$>$0.85 is acceptable.	L=2 satisfies the requirement that PACQ (X$<$100msecs) be greater than 0.99 at BER= 1.4×10^{-4}
RETENTION	Detector Threshold I	3 bits	(i) 7 bits if demod. detects absence of data burst; (ii) 3 bits if no hardware provisions taken.	I = 7 satisfies P_{NDB} $<1\times10^{-18}$ at BER=1×10^{-4} without causing P_{FDB} to reduce the MTBSL. However, implications of hardware failure favour I=3 (see Section 8.2).
	Narrow Aperture	32 bits	16 bits	Not applicable
	Flywheel Count M	50 frames	126 frames if $\xi=1\times10^{-6}$ 3×10^{3}/frames if $\xi=1\times10^{-9}$	Prolongs the MTBSL & reduces P_{BSL}

Table 8.1 Proposed Modifications to the Current Detection Parameters

BER	MTTO	MTBSL (frame)	UTR
10^{-6}	2 frames	$>10^{40}$	>99.99
10^{-5}	2 frames	$>10^{40}$	>99.99
10^{-4}	2 frames	$>10^{40}$	>99.99
10^{-3}	2 frames	$>10^{40}$	>99.99
10^{-2}	3.16 frames	$>10^{40}$	>99.99

Table 8.2 Estimate of Expected Availability
(Proposed Configuration)

$$A_{TOT}(BER=P) = A_{TDMA} * A_{EQP}. \qquad (8.1)$$

It is evident from Table 8.2 however, that the overall availability of the terminal is not measurably affected by the time it spends acquiring synchronism. The proposed list of parameters shown in Table 8.1 therefore characterizes a terminal whose TDMA synchronization procedures do not contribute to its aggregate down-time (outage) ------- which is an important conclusion to reach in itself. Furthermore, the analytical tools provided throughout this study facilitate the generation of other TDMA detection parameters that must meet various other users' objectives.

REFERENCES

[1] ."Slim TDMA System Operational Requirements". MCS document to the Department of Communications. DSS File No. 12SV.36001-8-4892. October 1979. Revised January 1980.

[2] Kamal, S.S. "Synchronization Aspects of TDMA Satellite Communication Systems". Doctoral Dissertation. Carleton University, Canada, August 1981.

[3] Ekstrom, B. "Optimized UW Detection For TDMA Communications". Proc. of The Third ICDSC, Kyoto, Japan. 1975. (pp. 265-272).

[4] Davidovici, S. and Schilling, D.L. "Minimum Acquisition Time of a PN-Sequence". Proc. of National Telecomm. Conf. Alabama, U.S.A. 1978.

[5] Ziemer, R. E. And Tranter, W. H. "Principles of Communications Systems, Modulation and Noise". Houghton Mifflin Publishing Company. Boston, Ma. U.S.A. 1976.

[6] Goode, G. E. and Phillips, J. L. "Optimum PCM Frame Synchronization Codes And Correlation Detection". Proc. of Nat'l Telemetry Conf. 1961. (pp. 11-15 to 11-50).

[7] Massey, J. L. "Optimum Frame Synchronization". IEEE Transac. on Comm. Vol. COM-20, No. 2, April, 1972. (pp. 115 - 119).

[8] Levitt, B. K. "Long Frame Sync Words For Binary PSK Telemetry", IEEE Transac. On Comm. November, 1975. (pp. 1365-1367).

[9] _____, "Optimum Frame Synchronization For Biorthogonally Coded Data". IEEE Transac. On Comm. Vol. COM-22, August 1979 (pp. 1130 - 1133).

[10] Newman, F. and Hofman, L. "New Pulse Sequences With Desirable Correlation Properties". Proc. of Nat'l Telem. Conf. Wash. D.C., April, 1971. (pp. 277 - 282).

[11] Peterson, W.W. "Error-Correcting Codes". Cambridge, Mass. MIT Press, 1961.

[12] Fujino, T. and Umeda, Y. "Effects of Jitter and Cycle Slipping of Phase Reference Upon Unique Word Missed Detection In QPSK Systems". Proc. of Ninth AIAA Communications Satellite Systems Conference. San Diego, Calif. U.S.A., March, 1982. (pp. 92-99).

[13] Kurihara, H. et.al. "Carrier Recovrey Circuit With Low Cycle Skipping Rate For CPSK/TDMA Systems". Proc. of Fifth ICDSC, Genoa, Italy, March, 1981. (pp. 319-324).

14 Parzen, E. "Stochastic Processes". Holden Day Publishers, San Francisco, 1962.

15 Rau, John G. "Optimization And Probability In Systems Engineering". Van Nostrand Reinhold Publishing Company. New York, 1970. Chapter 7.

16 Minutes of progress meeting convened on March 31, 1982.

17 Xerox Extended FORTRAN IV: User's Manual. Publication no. 900956E.

18 Riddle, D.F. "Calculus And Analytic Geomatry". Second edition. Wadsworth Publishing Co., Inc. Belmont, California, 1974. Section 21.10 (pp.711).

19 Spiegel, M.R. "Schaum's Outline Series: Theory And Problems Of Advanced Calculus". McGraw-Hill Book Company, New York. 1963 (pp. 164, 172-174).

20 Technical notes accompanying the Agenda for March 31st interim-report meeting. Ottawa. 31st March, 1982.

21 Spilker, J. "Digital Communications By Satellite". Prentice Hall Publishing Co. 1977.

22 Kamal, S. S. and Lyons, R. G. "Effect of Reliability On Network Responisiveness". To be submitted to IEEE Transac. On Reliability for publication.

APPENDIX A

DERIVATION OF ACQUISITION MODEL's DETECTION PROBABILITIES

The detection probabilities defined in Section 4.2 are used to develop the acquisition model's transition probabilities. Here these expressions are developed as functions of the UW length, the BER, and the detector's aperture A_W and thresholds I. To do so, it is necessary to develop an understanding of the detection mechanism.

A useful means of representing detection events is by a by a geometric model. The model used here consists of mapping n-bit sequences of 1's and 0's onto the vertices of an n-dimensional signal space. In this space of 2^n points a metric, or measure of distance, is based on the recognition that a single change in an n-tuple produces a single change in its coordinates. Consequently, using this metric the distance between two points in this space is represented by the number of bit positions in which they differ. This measure of distance is defined by the Hamming Metric. Thus, a vector $\vec{U}$ surrounded by a sphere of radius I represents a geometrical boundary of all vectors that are I bits or less away from the vector $\vec{U}$. With this representation, shown in Figure A-1a, an error vector $\vec{\Delta}$ is defined such that the received vector (n-tuple) $\vec{R}$ is the vector-sum of the transmitted vector plus $\vec{\Delta}$. Figures A-1b and A-1c represent the events of no-detection and false detection respectively. In the SCAN mode, any n-bit word in the frame can be sufficiently corrupted to trigger one or the other of these events shown. In the VERIFY and lock-up modes, these words must fall within the restricted aperture A_W.

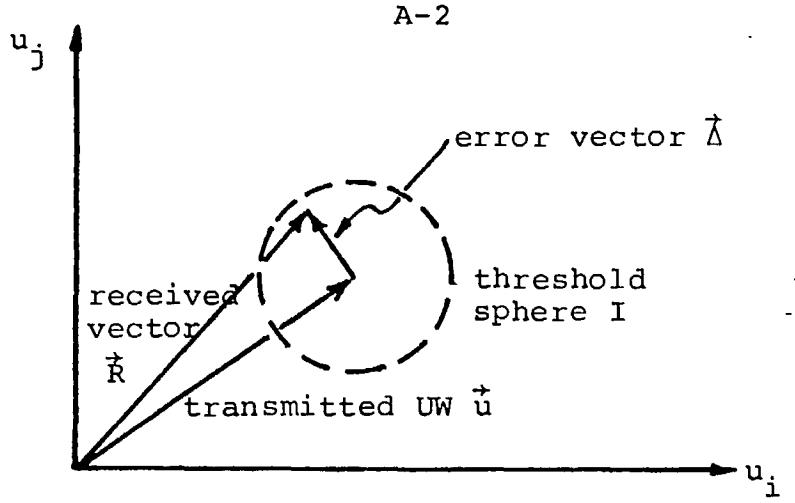

a) transmitted & received patterns.

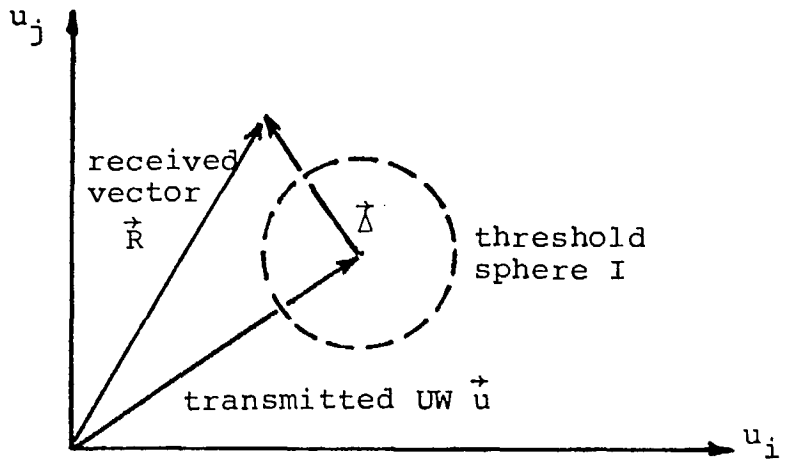

b) non-detection event

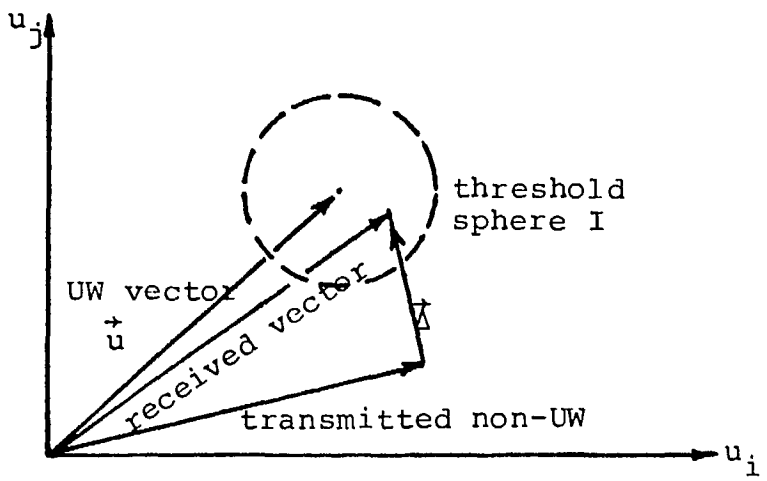

c) false detection event

Figure A-1 Vector Representation Of UW Detection.

During the initial scan, we denote the channel's BER by p, the threshold by I and the aperture is suppressed. Within such a wide setting, it is assumed that the entire bit stream through the correlator can be viewed as random data. For random, uncorrelated errors the probability of i errors in n bits is given by

$$\binom{n}{i} p^i (1-p)^{n-i} \tag{A.1}$$

and the probability of I + 1 or more errors in n bits is therefore given by

$$\sum_{i=I+1}^{n} \binom{n}{i} p^i (1-p)^{n-i} \tag{A.2}$$

Since the FRUW must be encountered once a frame (in a scan of T_b bits) then the above equation represents the probability of not detecting the FRUW when encountered, providing no false detections occur earlier. Thus, the unconditional probability of no detection P_{ND} is expressed by

$$P_{ND} = (1-P_{FDO}) \sum_{i=1}^{n} \binom{n}{i} p^i (1-p)^{n-i} \tag{A.3}$$

The probability of misdetection P_{MD} is defined as the probability of not detecting the FRUW. This is an event which can occur in one of two ways: either a false detection procedes the FRUW or the FRUW is missed, so

$$P_{MD} = [P_{FDO} + P_f(pre)] + P_{ND} \tag{A.4}$$

where

$P_f(pre)$= probability of premature sync pulse with only part of FRUW in the shift register;

P_{FDO}= probability of a false detection in the random data of the frame preceding this FRUW.

By choosig the FRUW such that its cross-correlation with the preceding BTR sequence is minimal, $P_f(pre)$ is rendered negligible*. Thus, equation A.4 reduces to

$$P_{MD} = P_{FDO} + (1-P_{FDO}) \sum_{i=1}^{n} \binom{n}{i} p^i (1-p)^{n-i} \quad (A.5)$$

The probability that a specific n-bit sequence appears in random data is given by $1/2^n$. The likelihood of a false detection to occur at any point in the frame is given by

$$P_{ff} = \frac{1}{2^n} \sum_{i=0}^{I} \binom{n}{i} \quad (A.6)$$

An upper bound to the likelihood of a false detection during the initial scan can be derived if it is assumed that the detector starts scanning the beginning of a frame. In doing so it must scan (T_b-1) n-bit patterns before reaching the true FRUW. Using equation A.6 the probability of detecting a specific sequence after K attempts (shifts) is given by

*Probability of error during most of the BTR sequence will be sufficiently low to render this assumption valid for practical values of channel BER and reasonable threshold levels.

$$(1-P_{ff})^{K-1}P_{ff} = \left[1-\frac{1}{2^n}\sum_{i=0}^{I}\binom{n}{i}\right]^{K-1}\cdot\frac{1}{2^n}\sum_{i=0}^{I}\binom{n}{i} \quad (A.7)$$

Consequently, an upper bound for P_{FDO} in random data is estimated as

$$P_{FDO} < \sum_{K=1}^{T_b-1}(1-P_{ff})^{K-1}P_{ff} = 1-(1-P_{ff})^{T_b-1} \quad (A.8)$$

A similar approach is used to estimate the probability of a false detection P_{FDW} once the aperture A_W is applied. However, the bit error probability p is used as the data stream scanned within the aperture is not of random data. i.e.

$$P_{FDW} < 1-\left[1-\sum_{i=0}^{I}\binom{n}{i}p^i(1-p)^{n-i}\right]^{A_W-1} \quad (A.9)$$

The estimates of detection probabilities in equation A.1 to A-9 now describe the detector's behaviour within a single frame. The general acquisition algorithm may require several frames before lock-up. However, a preliminary estimate of the probability of false acquisition P_{FA} can be developed by expressing

$$P_{FA} = \prod_{i=1}^{L}(\text{Probability of i-th detection being false}). \quad (A.10)$$

or

$$P_{FA} < (P_{FDW})^{L-1} P_{FDO} \qquad (A.11)$$

Using an expression for P_{FDW} given by equation (A.9) the probabilities of no detection and misdetection within the aperture A_W are given by

$$P_{NDW} = (1-P_{FDW}) \sum_{i=1}^{n} \binom{n}{i} p^i (1-p)^{n-i} \qquad (A.12)$$

and

$$P_{MDW} = P_{FDW} + P_{NDW} \qquad (A.13)$$

respectively. These derivations complete the set of detection probabilities required to describe the Markovian representation of initial acquisition.

APPENDIX B

State Assignment of Generalized Retention Model

The state variables defined for the aperture tracking model are maintained i.e. the transition probability p(i,j) represents the probability sum of all possible events that result in net displacements of (j-i) bits; if the displacement sufficiently ejects the UW outside the aperture it is undetectable and the flywheel unit is activated. Assuming that ($K=A_{VN}/2$) is, at least, equal to a single bit duration (i.e. some aperture exists). In general, p(i,j) is given by*

$$\text{(a)}\quad P(i,i) = \sum_{X=0}^{K-i+2} P_{t_E(0)}(X) \prod_{j=i+1}^{K+i+X} [1-P_D(j)]P_D(i) +$$

$$\sum_{Y=1}^{K+i} P_{t_E(0)}(-Y) \prod_{j=i+1}^{K+i-Y} [1-P_D(j)]P_D(i);\ 0<i<K \qquad \text{(B.1)}$$

$$\text{(b)}\quad P(i,j= \sum_{X=0}^{k-i+2} P_{t_E(0)}(X) \prod_{s=j+1}^{K+i+X} [1-P_D(S)]P_D(j) +$$

$$\sum_{Y=1}^{k+i-j} P_{t_E(0)}(-Y) \prod_{S=j+1}^{K+i-Y} [1-P_D(S)]P_D(j);\ 0<i<K-1 \text{ and } i+1<j<K \qquad \text{(B.2)}$$

*In all these transition probabilities summation terms for which lower limit exceeds upper limit are set to zero, and product terms for which lower limit exceeds upper limit are set to one.

(c) $$P(i,j)=\sum_{X=0}^{K-i+2} P_{t_E(0)}(X) \prod_{T=j+1}^{K+i+X} [1-P_D(T)]P_D(j) +$$

$$\sum_{Y=1}^{K+i-j} P_{t_E(0)}(-Y) \sum_{T=j+1}^{K+i-Y} [1-P_D(T)]P_D(j); 1 \leq i \leq K \text{ and } 0 \leq j \leq i-1 \qquad (B.3)$$

(d) $$P(i,K+1)=\sum_{X=0}^{K-i+2} P_{t_E(0)}(X) \sum_{j=0}^{i+K+X} [1-P_D(j)] +$$

$$\sum_{Y=1}^{K+i} P_{t_E(0)}(-Y) \prod_{j=0}^{K+i-Y} [1-P_D(j)] + \sum_{Y=K+i+1}^{K+i+2} P_{t_E(0)}(-Y) +$$

$$\sum_{X=0}^{K-i+2} P_{t_E(0)}(X) \left[\sum_{W=K+1}^{K+i+X} P_D(W) \prod_{j=W+1}^{K+i+X} [1-P_D(j)] \right] +$$

$$\sum_{Y=1}^{K+i} P_{t_E(0)}(-Y) \left[\sum_{W=K+1}^{K+i-Y} P_D(W) \prod_{j=W+1}^{K+i-Y} [1-P_D(j)] \right] ; \quad 0 \leq i \leq K \qquad (B.4)$$

(e) $P(i,K+M)$ = identical to the transition probability $P(0,K+1)$ except that the drift density function is given by $P_{t_E(i-K)}(X)$;

$K+1 \leq i \leq K+M-1$ (B.5)

(f) $P(k,j)$ = identical to the transition probability $P(0,j)$ except that drift density fucntion is given by $P_{t_E(i-K)}(X)$;

$(K=1 \leq i \leq K+M-1)$ and $(0 \leq j \leq K)$ (B.6)

(g) $P(i,i+1)$= identical to the transition probability $P(0,K+1)$ except that the drift density function is given by

$P_{t_{E(i-K)}}(X)$; $(K+1 \leq i \leq K+M-1)$ (B.7)

(h) $P(K+M,K+M) = 1.0$ (B.8)

Note that in equation (B.6) our assumption that $P(i,j)$ is identical (in form) to $P(0,j)$ implies that our last detection before flywheeling has centered the aperture about the true UW. This assumption avoids the complexity of defining (M-1) flywheel states for each state $(0 \leq i \leq K)$.

APPENDIX C

DOCUMENTATION FOR SOFTWARE MODULE: SELECT

This program was designed to select the best n-tuples for use as TDMA frame (and burst) sync words using the selection criteria detailed in Section 3. The program is efficient in search time and storage requirements by avoiding the testing of all 2^n possible bit sequences. The program was written in XEROX Extended FORTRAN IV, and the reference manual [17] should be consulted if other FORTRAN compilers are used. The program was designed and tested in a structured manner, the segments of which will be discussed below.

Input of Parameters: Only three variables must be input from some logical unit (console):

(a) the initial word length (KMIN),

(b) the final word length (KMAX), and

(c) the iterative step-size (STEP).

All three variables are defined as an integer number of bits. The PN sequences generated are for a range of KMIN$\geq$16 bits and KMAX$\leq$63 bits. However, truncated n-bit PN sequences can be generated for n$\geq$4 bits.

Initialization of Variables: Only two variables must be initialized. The first is the word length denoted by K which must be initialized to KMIN. The second is to initialize the variable L to a value of 5 or 6 subject to the inequality

$$2^{L-1} < K+1 < 2^{L} \qquad (5.1)$$

If L=5 all six formulae listed in Table 3.1 are used to generate the set of candidate K-bit words for $4<K<31$. If L=6 only the latter three formulae generate the set of sync words for $32<K<63$. For a given value of L, the subroutine GENERATE is designed to implement the recursion formulae.

Calculation of C_{max} and D_{min}: This segment of code evaluates C_{max} and D_{min} for each memeber of the set of n-tuples (equations 3.1 to 3.5). It also identifies the sync word(s) having the smalles C_{max}, and the largest D_{min} respectively.

The Application Of The Selection Criteria: The array CSMLL is used to store the identifiers of all the sync words whose C_{max} is equal to the min $\{C_{max}\}$. Similarly, the array DLRG is used to store the identifiers of all the sync words whose D_{min} is equal to the max $\{D_{min}\}$. The subset of words in CSMLL for which D_{min} is a maximum satify criterion I (Section 3.3), and the subset of words in DLRG for which C_{max} is a minimum satisfy criterion II. An array CRTRN is used to store the EBCDIC values "I", "II" or "I and II" depending on whether the corresponding words in CSMLL and DLRG satisfy criterion I, or criterion II, or both*.

Error Diagnostics: Parameter tests are performed on all the input variables and within execution of the subroutine GENERATE. Appropriate diagnostic messages are printed as illustrated in the sample run shown in Figure C.1.

*The module SELECT was tested to reproduce the results presented in [8].

```
!SELECT.
 WORD LENGTHS: (INITIAL,FINAL)?
?51,24
*** ERROR: KMIN>KMAX ***
RE-INSERT
?64,64
*WARNING* KMAX TO LARGE.
RESETTING EQUAL TO 63
 STEP SIZE (BITS)?
?-1
*** ERROR STEP SIZE INVALID ***
MUST BE GREATER THAN  ZERO
REINSERT
?4
 *** ERROR DETECTED IN SUBROUTINE GENERATE ***
     VALUE OF 'L' INCORRECT    ( 7 )
 *STOP* 0

!
```

Figure C.1 Diagnostic Messages In SELECT

Formatting The Output: Comprehensible formatting of the results from this module occupies the largest of the code-segments. Figure C.2 depicts the resultant output of an "error-free" run for n=32 bits. For a given word length, the subset of wrods in arrays CSMLL and DLRG which satisfy either (or both) of the selection criteria are printed in the Hexadecimal radix, using the subroutine HEXCONV. For each sync word its values for C_{max} and D_{min} are printed, as well as the criterion it satisfies, the recursion formula (shift register configuration [8]) used to generate the sync word, and the seed $\{S_i, i=0, 1,...L-1\}$ used with the recursion formula. Also listed in the output are those words best suited for high and low BER applications respectively (see the Neuman-Hofman selection algorithm in [8, 10]).

Recursion-Formulae Implementation: The subroutine GENERATE is used to generate the candidate sync words. An aspect to note in the development of this subroutine is the procedure used to facilitate the deviation of the recursion formula in Table 3.1. The Exclusive-Or logical operation is simplified by using "-1" to represent the binary "0". This results in the reduction of $S_a \oplus S_b$ (a logical operation) to $-S_a x\ S_b$ (a mathematical operation). Similarly, $(S_a \oplus S_b \oplus S_c)$ is reduced to $-S_a \times S_b \times S_c$. However, before calling the subroutine HEXCONV the k-tuple is reverted to its binary form of ones and zeros.

Hexadecimal Conversion: The subroutine HEXCONV is used to perform the conversion of sync word representation from the binary radix to the hexadecimal. Two aspects of this subroutine's operation are noted here. First, the distinct word patterns whose length is <u>not</u> an integer multiple of 4 bits may be assigned the same HEX representation e.g. the following bit patterns all map into the HEX representation 2B1:

```
!SELECT.
 WORD LENGTHS; (INITIAL,FINAL)?
?32,32
 STEP SIZE (BITS)?
?1


 FOR WORD LENGTH 32;

 INDEX      WORD FORMAT        C-MAX    D-MIN    CRITERION    CONFIGURATION    SEED
 =====      ===========        =====    =====    =========    =============    ====

    1       7A392DD9             6      22.42        II            6H         011110
    2       9ABF0431             5      22.20         I            6A         100110
    3       B7EB8CEC             6      22.90       I&II           6B         101101
    4       2A7E8384             6      22.84        II            6C         001010
    5       FA0E1236             5      22.64         I            6C         111110

      FOR HIGH BER APPLICATIONS THE BEST WORD(S)
        TO USE ARE;
                WORD FORMAT          CONFIGURATION    SEED
                FA0E1236                   6C         111110

      FOR LOW BER APPLICATIONS THE BEST WORD(S)
        TO USE ARE;
                WORD FORMAT          CONFIGURATION    SEED
                B7EB8CEC                   6B         101101

      WORD LENGTH     TOTAL NO. OF WORDS GENERATED
           32                  189



TOTAL NUMBER OF WORD-LENGTHS =       1
TOTAL NUMBER OF WORDS =            189
 *STOP* 0

!
```

Figure C.2 Sample Results For 32-bit Pattern

(a) 0010/1011/1 (9 bits);

(b) 0010/1011/01 (10 bits);

(c) 0010/1011/001 (11 bits);

the only distinction being their word length. Secondly, to translate the HEX representation to the EBCDIC code governing the printer, simply add 240 to values less than A (decimal 10) and 183 to values greater than or equal to A.

Assignment Of Logical Units: Three logical unit assignments must be made before the module SELECT is compiled and executed. To maintain compatibility with the assignment in the source program, the following mapping must be made:

(a) logical unit 7 is used for the output (WRITE);

(b) logical unit 10 is used for input (READ or INPUT);

(c) and logical unit 12 is used to receive the input prompts and error messages.

Alterations to these assignments must be accompanied by corresponding changes to the source file SELECT, and be compatible with I/O operations defined in [17].

APPENDIX D

DOCUMENTATION FOR SOFTWARE MODULE: CORREL8

This module was developed to reproduce the output of the detector's digital correlator as it scans a received stream of regenerated data bits. In its simplest mode the program allows the user to define the length and format of a sync pattern (NUW bits) and its preceding preamble (NBTR bits). Starting from the first NUW bits of the preamble the program evaluates the correlator's output and stores it in the array CORR(K), K= NBTR, NBTR-1, ... 3, 2, 0. The index K represents the current distance (in bits) of the detector from the true position of the sync word (see Figure D.1a). A sample output of the correlator is shown in Figure D.1b. Such correlation profiles can be used to set preliminary detector thresholds.

In a more complex mode, the program accepts the definition of <u>two</u> sync words and their preambles. These can represent candidate bit-sequences for the FRUW and DBUW. To emulate the terminal's behaviour during initial acquisition the program differentially decodes both UWs and their preambles before performing the correlation. This is executed by the subroutine DECODE. Correlation profiles are then generated for the cases when: (a) the decoded FRUW and its preamble pass through the detector, and (b) the decoded DBUW and its preamble pass through the detector. This is to ensure that the decoded DBUW is not mistaken for the FRUW during initial acquisition.

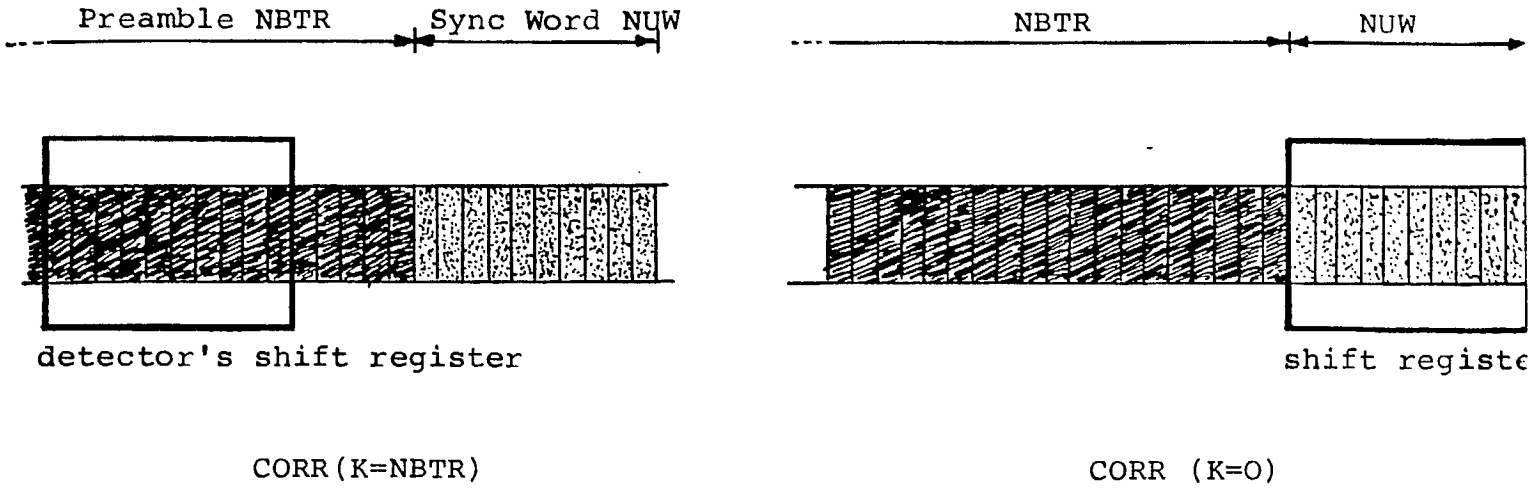

a) displacement K of the detector from the UW

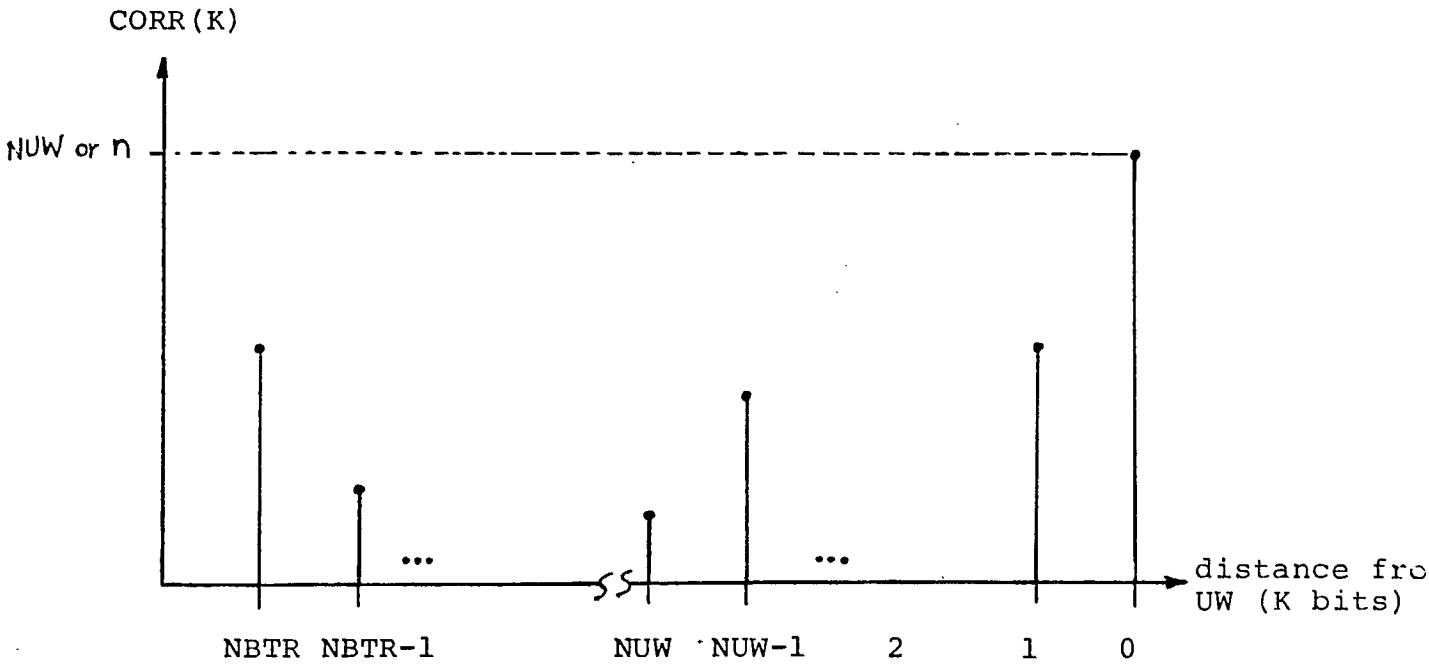

b) sample output of the digital correlator

Figure D.1 Emulation Of the Digital Correlator
(Correlation Profile)

The execution of the DECODE subroutine is invoked by entering "1" when prompted by the program. An entry of "0" bypasses the differential decoder. The decoding of a bit stream occurs by determining the phase change between each pair of bits. e.g. the phase change between the pair 11 and 10 is equal to $\pi/2$. The output of the decoder, as it consecutively moves from 11 to 10, is set to a pre-determined pair of bits representing a relative phase change of $\pi/2$ - say 01. The decoding scheme used in the Slim TDMA terminal is given by the following table:

Output of Diff. Decoder	Relative Phase Change
00	0
01	$\pi/2$
10	π
11	$3\pi/2$

and is independent of the reference phase. To implement this decoding operation the subroutine DECODE begins at the start of the premable preceding the sync word. BIT1 and BIT2 are logical variables that are assigned the first two bits of the preamble, respectively. BIT3 and BIT4 are assigned the third and fourth preamble bits, respectively. The decoder's FSM (shown in Figure D.2a) is implemented by using the matrix shown in Figure D2b. DECODE calls a nested subroutine MAP which translates (BIT1, BIT2) into a SOURCE state, and (BIT3, BIT4) into a DSTINation state. The matrix is used to determine the resultant output of the decoder for a transition between the source and destination states.

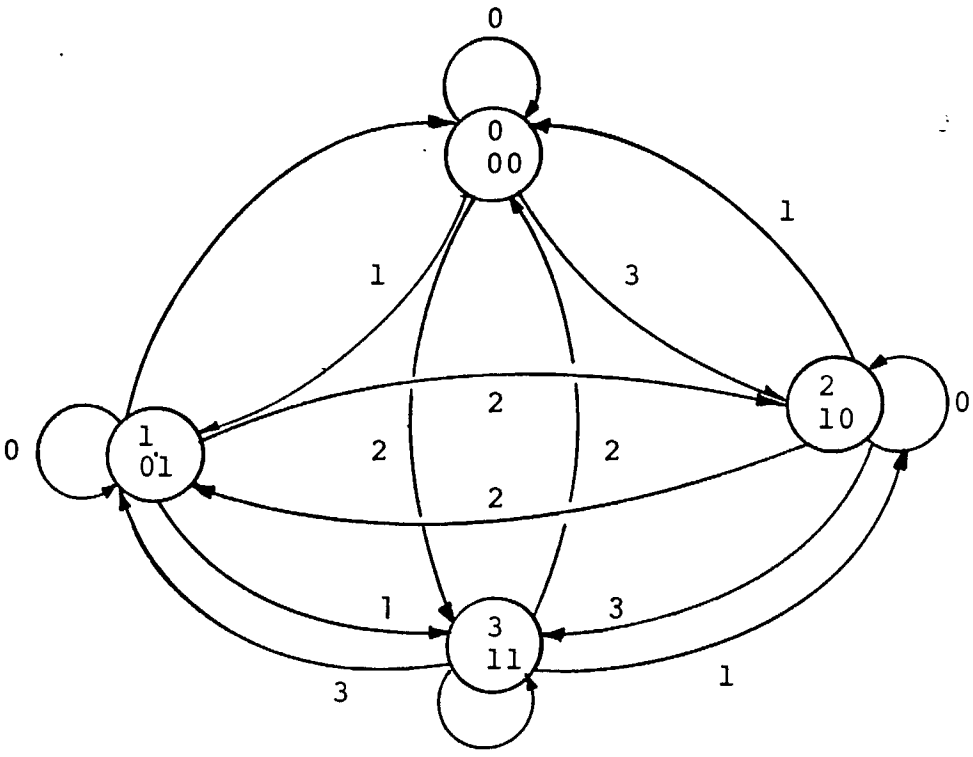

a) Differential decoding FSM

DESTIN

SOURCE	0	1	2	3
0	0	1	3	3
1	3	0	2	1
2	1	2	0	3
3	2	3	1	0

b) Decoding map [matrix CODE (i,j)]

Figure D.2 Emulation Of Differential Decoder

The subroutine DECODE then updates (BIT1,...BIT4) as the decoder scans the entire preamble and sync word.

Example: consider the four consecutive bits 0111.

Bit1 = 0 Bit3 = 1
Bit2 = 1 Bit4 = 1

From Figure D.2a 01 represents the SOURCE state 1, and 11 represents the DESTINation state 3. The transition from state 1 → state 3 is 1. The decoding map stored in array CODE indicates that the resultant decoder output is 01.

A sample of the module's output is depicted in Figure D.3.

```
 RUN CORRLL8.TSK


IF DIFF. DECODING REQUIRED TYPE:1,ELSE TYPE:0
5
ERROR! DIFF = 1 IF DECODING REQUIRED, AND DIFF = 0 IF NOT. TRY AGAIN!
1
NUMBER OF WORDS TO BE ENTERED(1 OR 2):
-3
ERROR! NO. OF WORDS MUST BE 1 OR 2. TRY AGAIN!
1
ENTER LENGTH OF WORD NO.1:
600
ERROR! WORD LENGTH MUST BE POSITIVE AND AT MOST 40 BITS. TRY AGAIN!
16
ENTER WORD NO.1 AS A STRING (E.G. 10110...):
0010110101110111
ENTER LENGTH OF BTR SEQUENCE:
49
ERROR! BTR SEQUENCE LENGTH MUST BE POSITIVE AND AT MOST 40 BITS. TRY AGAIN!
40
ENTER BTR SEQUENCE AS A STRING (E.G. 10110...):
1100110011001100110011001100110011001100

PASSING DECODED WORD #1 FAST ITSELF
RECEIVED BY THE DECODED BTR YIELDS THIS PROFILE:
CORR(40)= 7     CORR(39)=10     CORR(38)= 6     CORR(37)=10     CORR(36)=
CORR(35)=     CORR(34)= 6     CORR(33)=10     CORR(32)= 6     CORR(31)=
CORR(30)= 6     CORR(29)=10     CORR(28)= 6     CORR(27)=10     CORR(26)= 6
CORR(25)=10     CORR(24)= 6     CORR(23)=10     CORR(22)= 6     CORR(21)=10
CORR(20)= 6     CORR(19)=10     CORR(18)= 6     CORR(17)=10     CORR(16)= 6
CORR(15)= 9     CORR(14)= 7     CORR(13)= 9     CORR(12)= 6     CORR(11)= 8
CORR(10)= 9     CORR( 9)=11     CORR( 8)=10     CORR( 7)= 7     CORR( 6)= 7
CORR( 5)= 6     CORR( 4)= 7     CORR( 3)= 5     CORR( 2)= 8     CORR( 1)=
CORR( 0)=16     CORR(

PASSING UNCODED WORD #1 FAST ITSELF YIELDS:
CORR(40)= 6     CORR(39)= 6     CORR(38)=10     CORR(37)=10     CORR(36)= 6
CORR(35)= 6     CORR(34)=10     CORR(33)=10     CORR(32)= 6     CORR(31)= 6
CORR(30)=10     CORR(29)=10     CORR(28)= 6     CORR(27)= 6     CORR(26)=10
CORR(25)=10     CORR(24)= 6     CORR(23)= 6     CORR(22)=10     CORR(21)= 6
CORR(20)= 6     CORR(19)= 6     CORR(18)=10     CORR(17)=10     CORR(16)= 6
CORR(15)= 5     CORR(14)= 8     CORR(13)= 9     CORR(12)= 7     CORR(11)= 7
CORR(10)= 7     CORR( 9)= 9     CORR( 8)= 8     CORR( 7)= 7     CORR( 6)= 9
CORR( 5)=10     CORR( 4)= 7     CORR( 3)= 7     CORR( 2)=10     CORR( 1)=
CORR( 0)=16     CORR(
TTZ --  e!oP
```

Figure D.3 Sample Run for CORREL8

APPENDIX E

DOCUMENTATION FOR SOFTWARE MODULE: ACQUI

The module ACQUI constructs the Markovian model outlined in Section 4.2 and Appendix A. It is used to estimate the terminal's acquisition performance for a given set of operational parameters (e.g. the detector's threshold, aperture width, UW length etc...). The performance indices defined for acquisition are:

(i) mean time required to acquire (to complete the acquisition algorithm) MTTA;

(ii) probability of false acquisition (lock-up on a false sync word) P_{FA}; and

(iii) mean time required to acquire <u>correctly</u> (terminal lock-up on the true sync word) $MTTA_c$, and its second moment.

To define the detector's intermediate states from start-up (and before lock-up) the following detection probabilities are also included in the output:

(a) probability of no detection in the initial bit-by-bit scan of a frame interval, P_{ND};

(b) probability of false detection in the initial bit-by-bit scan of a frame interval, P_{FDO};

(c) probability of false detection in the wide aperture (during verification) assuming random data surrounds the sync word P_{FDW}, and assuming a deterministic premable P_{FDB};

(d) cumulative distribution of the probability that the terminal acquiring in X frames or less, PACQ(X).

The specification of two false detection probabilities P_{FDW} and P_{FDB} is used to identify the bounds of our assumption that the detector "sees" random data if A_W is sufficiently wide. P_{FDB} is estimated for a specified BTR preamble using equation 4.9 in a manner similar to that employed in CORREL8 (Appendix D).

Each set of input variables entered by the user (operational parameters) defines a specific detection configuration for which the set of performance indices are estimated. The input variables are:

(1) burst rate RR (in Mbps);

(2) nominal frame length TF (in milliseconds);

(3) a set of BER values BER(I), I=1, 2,...NBER such that NBER is an integer;

(4) a set of WIDE aperture values AW(I), I=1, 2,...NAW such that AW(I) is an even integer number of bits and NAVN is an integer;

(5) a set of verification-count values IL(I), I=1, 2,...NL such that NL is an integer;

(6) a set of detector threshold values THR(I), I=1, 2, ...NTHRSH such that NTHRSH is an integer;

(7) the lengths of the candidate sync word NUW and the preceding preamble NBTR, as integers;

(8) the format of the sync word UW(I) as a string of 1's and 0's;

(9) the foramt of the preamble BTR(I) as a string of 1's and 0's; and

(10) a flag NCDF whose value is set to "1" if the cumulative distribution PACQ(X) is required, and to "0" if not.

Table E.1 lists the input variables, their data types and their valid numerical bounds.

A flag TEST is used in the matrix-inversion subroutine SOLVD. If the inversion operations are not complete successfully the flag TEST is assigned a non-zero value. This signals the main program segment to abort the analysis of the Markov chain and estimate the $MTTA_C$ from equation 4.8. This occurs when the processor's numerical representation cannot distinguish between a transition probability that is nearly equal to 1.0 but not 1.0. The result is that the sub-matrix QMTRX contains one or more recurrent states which violate its definition (see Section 4.2.3) as a transition matrix of non-recurrent states.

The module ACQUI verifies that validity of each input parameter entered. Figure E.1 illustrates a sample of the diagnostic messages that are displayed when erroneous values are entered. Figure E.2 lists the output results of a correct entry procedure.

Variable/Array	Symbol	Variable Type	Variable Bounds	Format Example
Burst rate (Mbps)	RR	Real	0<RR<100	03.088
Frame interval (msec)	TF	Integer	0<TF<1000	020
No. of BER values	NBER	Integer	1<NBER<100	08
Array of BER values (bits/bits)	BER(I)	Real	0<BER<1	3E-4
No. of aperture widths	NAW	Integer	0<NAW<10	5
Array of aperture width (bits)	AW(I)	Integer (even)	2<AW(I)< NTBR	040
Length of BTR preamble (bits)	NBTR	Integer	0<NBTR<45	40
Length of sync word (bits)	NUW	Integer	0<NUW<45	32
No. of verification counts	NL	Integer	0<NL<10	5
Array of verification counts (frames)	IL(I)	Integer	1<IL(I)<10	7
No. of detector thresholds	NTHRSH	Integer	1<NTHRSH<9	2
Array of thresholds (bits)	THR(I)	Integer	0<THR(I) <7	6
Sync Word	UW(I)	Integer string	UW(I)=0,1	011001... (NUW bits)
Preamble	BTR(I)	Integer string	UW(I)=0,1	00110011.. (NBTR bits

Table E.1 List of Input Variables: ACQUI

```
 RUN ACQUI.TSK


      CONFIGURATION  PARAMETERS:
      **************************
ENTER TRANSMISSION RATE,R,IN MBPS :
-60
ERROR! BURST RATE MUST BE POSITIVE. TRY AGAIN!
03.1584
ENTER FRAME LENGTH,TF,IN MILLISECS.(UP TO 3 DIGITS):
-60
ERROR! FRAMELENGTH MUST BE A POSITIVE INTEGER, LESS THAN 1 SECOND. TRY AGAIN!
020
      ************************

      INPUT  PARAMETERS :
      *******************
NO.OF BER VALUES(2 DIGITS, E.G. 04)
-60
ERROR! NUMBER OF BER VALUES MUST BE POSITIVE AND LESS THAN 100. TRY AGAIN!
01
BER VALUES(E-FORMAT, E.G. 3E-6,1E-5):
5E+5
ERROR! BER VALUE MUST BE POSITIVE AND LESS THAN ONE. TRY AGAIN!
5E-5
ENTER NUMBER OF WIDE APERTURE VALUES(<10,1 DIGIT):
-60
ERROR! NUMBER OF APERTURE WIDTHS MUST BE POSITIVE AND LESS THAN 10.
TRY AGAIN!
1
ENTER THESE APERTURE VALUES(3 DIGITS, E.G. 032,068) ONE PER LINE:
-60
ERROR! APERTURE WIDTH MUST BE A POSITIVE INTEGER. TRY AGAIN!
010
ENTER LENGTH OF BTR SEQ.,NBTR,IN BITS (LESS THAN 45 BITS; 2 DIGITS):
-60
ERROR! BTR SEQUENCE LENGTH MUST BE POSITIVE AND LESS THAN OR EQUAL TO 45 BITS
TRY AGAIN!
40
ENTER LENGTH OF UW,NUW,IN BITS (LESS THAN 45 BITS; 2 DIGITS):
-60
ERROR! UW LENGTH MUST BE POSITIVE AND LESS THAN OR EQUAL TO 45 BITS.
TRY AGAIN!
16
NO.OF L-VALUES(<10,1 DIGIT):
-60
ERROR! NUMBER OF L-VALUES MUST BE POSITIVE AND LESS THAN 10. TRY AGAIN!
1
L-VALUES(1 DIGIT, E.G. 5,6) LESS THAN 10:
-60
ERROR! L-VALUE MUST BE POSITIVE AND LESS THAN 10. TRY AGAIN!
2
NO.OF THRESHOLD VALUES(<10,1 DIGIT):
-60
ERROR! NUMBER OF THRESHOLD VALUES MUST BE POSITIVE AND LESS THAN 10.
TRY AGAIN!
```

Figure E.1 Incorrect Entry of Data (ACQUI)

```
 RUN ACQUI.TSK


      CONFIGURATION  PARAMETERS:
      **************************
ENTER TRANSMISSION RATE,R,IN MBPS :
03.1584
ENTER FRAME LENGTH,TF,IN MILLISECS.(UP TO 3 DIGITS):
020
      ************************

      INPUT  PARAMETERS :
      *******************
NO.OF BER VALUES(2 DIGITS, E.G. 04)
01
BER VALUES(E-FORMAT, E.G. 3E-6,1E-5):
1E-5
ENTER NUMBER OF WIDE APERTURE VALUES(<10,1 DIGIT):
1
ENTER THESE APERTURE VALUES(3 DIGITS, E.G. 032,068) ONE PER LINE:
100
ENTER LENGTH OF BTR SEQ.,NBTR,IN BITS (LESS THAN 45 BITS; 2 DIGITS):
40
ENTER LENGTH OF UW,NUW,IN BITS (LESS THAN 45 BITS; 2 DIGITS):
16
NO.OF L-VALUES(<10,1 DIGIT):
1
L-VALUES(1 DIGIT, E.G. 5,6) LESS THAN 10:
2
NO.OF THRESHOLD VALUES(<10,1 DIGIT):
1
THRESHOLD VALUES(1 DIGIT, E.G. 5,6) ONE PER LINE:
0
ENTER CANDIDATE UW,UW(I),AS VECTOR:
1111001101110011
ENTER BTR SEQUENCE,BTR(I),AS VECTOR:
11001 1100110011001100110011001100
IF CUMULATIVE PROBABILITY OF ACQUIRING IN 'X' FRAMES OR LESS IS REQUIRED,
TYPE:1; ELSE TYPE:0
1
```

Figure E.2(a) Correct Data Entry (ACQUI)

```
PROB. OF FALSE DETEC. IN PREAMBLE (WITHIN WIDE APERTURE)=  0.24496815E-14
MATRIX INVERSION HAS BEEN SUCCESSFULLY COMPLETED IF 'TEST'
IS ZERO AND 'DET' IS POSITIVE AND LESS THAN ONE:
    TEST= 0.00000     DET= 0.38228



     RESULTS  OF THIS ANALYSIS :
     **************************
THE CHANNEL BER IS :  .000010000000000
WIDTH OF WIDE APERTURE:  100BITS.
LNGTHS.OF UW AND BTR SEQS.RESPEC.:16  BITS.AND   40BITS.
NO.OF SUCCESS.DETECS.BEFORE ACQ.:   2
DETECTOR THRESH.:    0BITS.

INITIAL ACQUISITION RESULTS :
*****************************
PROB.OF INITIAL NO-DETEC. IN SCAN:    0.61039759E-04
PR.OF FALSE DET.,IN A BIT-BY-BIT SCAN,PFDO.:    0.61853540E+00
PR.OF FALSE DETEC.,WIDE APERTURE(IN RANDOM DATA) PFDW:    0.15094912E-02
PR.OF FALSE ACQUIS.:    0.93293461E-03
M:'A(CORRECT ACQUIS.)=.36249E+01     2ND MOMENT=  .17304E+02
M:'A(ANY ACQUIS.)=.36161E+01

PROP. OF ACQUIRING IN  1 FRAMES OR LESS IS:   0.00000000E+00

PRO   OF ACQUIRING IN  2 FRAMES OR LESS IS:   0.38134256E+00

PRO   OF ACQUIRING IN  3 FRAMES OR LESS IS:   0.61688365E+00

PRO   OF ACQUIRING IN  4 FRAMES OR LESS IS:   0.76239188E+00

PROB. OF ACQUIRING IN  5 FRAMES OR LESS IS:   0.85228126E+00

PROB. OF ACQUIRING IN  6 FRAMES OR LESS IS:   0.90781146E+00
TT2  --  STOP

>
```

Figure E.2b Result of Correct Run (ACQUI)

It should be noted that, although the module ACQUI implements the acquisition algorithm shown in Figure 2.1, it may be reconfigured to represent any algorithm. This is accomplished by redefining the detector's states and updating the transition matrix TPMTRX.

APPENDIX F

DOCUMENTATION FOR SOFTWARE MODULE: RETNTN

The software module RETNTN implements the retention algorithm detailed in Figure 2.2 by constructing the Markov chain shown in Figure 4.7. The module is used to predict the Slim TDMA terminal's performance in steady-state (after acquistion), and the conditions under which it may lose frame sync. The performance indices defined for retention are:

i) mean time between consecutive losses of sync;

ii) probability of successive events causing sync loss; and

iii) the single-event probability of a false detection occuring within the narrow aperture A_{VN}.

The output for RETNTN lists two distinct sets of values for the above three performance indices: {RMTBSL, PSLOSS, PFDBC} derived from the Markov chain, and {MTBSL' PBSL, PFDB} derived from equations (3.2), (B.1-B.2) adn (B.15-B.16) in [2]. This latter set of performance parameters neglects the effects of accumulated timing-errors and false detections that may shift the aperture from its nominal position.

The listing of <u>two</u> sets of performance indices serves a dual purpose: a) presents a relative indication of the merits of including the effects of timing-errors and false detections in the Markovian model, and b) presents reasonable estimates of the performance indices when analysis of the Markov chain proves to be difficult.

As in the acquisition module ACQUI, cases for which the numerical resolution of the computer cannot distinguish between a probability of "nearly 1" and the certain event present an obstacle to the inversion of the matrix QMTRX (see equation 4.14). A flag TEST is used to abort the chain's analysis for such cases and estimates of the performance indices are derived from closed-form (worst-case) formulae. For such cases the relevant parameters appear in the program's output as being set to zero.

Each set of input variables entered by the user (operational parameters) defines a specific detection configuraton for which the set of performance indices are derived. The input variables are:

1) burst rate RR(in Mbps);

2) nominal frame interval TF (in msecs.);

3) a set of BER values BER(I), I=1,2,---NBER such that NBER is an integer;

4) a set of narrow aperture values AAVN(I), I=1,2,---NAVN such that NAVN is an integer and AAVN(I) is even;

5) a set of flywheel counts IM(J), J=1,2,---NM such that NM is an integer;

6) a set of detector threhold values THR(I), I=1,2,---NTHRSH such that NTHRSH is an integer;

7) the length of th candidate sync word NUW, and the preceeding preamble NBTR, as integers;

8) the format of the sync word UW(I) as a string of 1's and 0's;

9) the format of the preamble BTR(I) as a string of 1's and 0's; and

10) the set of rms timing-error values SNS(I), I=1,2,...NSNST such that NSNST is an integer.

Table F.1 lists these input variables, their data types and valid bounds.

The module RETNTN verifies the validity of each input variable entered. Figure F.1 presents a sample listing of an incorrect entry procedure. Figure F.2 lists the output results of a correct entry procedure.

As in ACQUI, the current structure of this module implements the retention algorithm of Figure 2.2. However, redefinition of the states transition TPMTRX permits the use of alternative retention procedures.

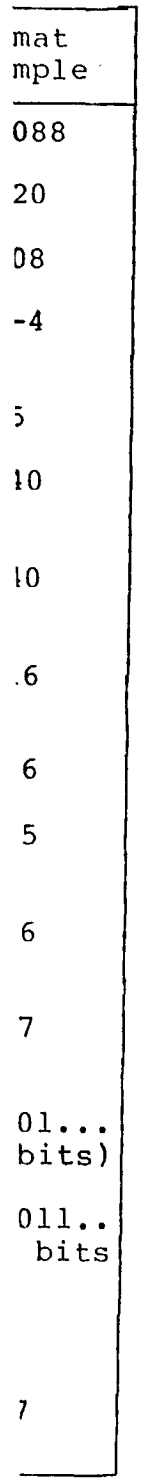

```
 RUN DL:RETNTN.TSK


     CONFIGURATION  PARAMETERS:
     **************************
ENTER TRANSMISSION RATE,R,IN MBPS :
-60.3
ERROR! BURST RATE MUST BE POSITIVE. TRY AGAIN!
03.1584
ENTER FRAME LENGTH,TF,IN MILLISECS.(UP TO 3 DIGITS):
-60
ERROR! FRAME LENGTH MUST BE POSITIVE AND LESS THAN ONE SECOND. TRY AGAIN!
020
     ************************

     INPUT  PARAMETERS :
     *******************
ENTER NO.OF BER VALUES(2 DIGITS,E.G. 04):
-60
ERROR! NO. OF BER VALUES MUST BE POSITIVE AND LESS THAN 100.
TRY AGAIN!
01
ENTER BER VALUES(E-FORMAT,E.G. 3E-6) ONE PER LINE:
1E+6
ERROR! BER VALUE MUST BE POSITIVE AND LESS THAN ONE. TRY AGAIN!
1E-6
ENTER NO.OF VERY-NARROW APERTURE VALUES(<10,1 DIGIT):
-60
ERROR! NO. OF APERTURE WIDTHS MUST BE POSITIVE AND LESS THAN 10. TRY AGAIN!
1
ENTER THESE APERTURE VALUES(3 DIGITS) ONE PER LINE:
-60
ERROR! APERTURE WIDTH MUST BE A POSITIVE INTEGER. TRY AGAIN!
002
ENTER LENGTH OF BTR SEQ.,NBTR,IN BITS
(LESS THAN 45 BITS; 2 DIGITS, E.G. 32):
-60
ERROR! LENGTH OF BTR MUST BE POSITIVE AND LESS THAN OR EQUAL TO 45.
TRY AGAIN!
40
ENTER LENGTH OF UW,NUW,IN BITS
(LESS THAN 45 BITS; 2 DIGITS, E.G. 16):
-60
ERROR! LENGTH OF UW MUST BE POSITIVE AND LESS THAN 45 BITS. TRY AGAIN!
16
NO.OF M-VALUES(<10,1 DIGIT):
-60
ERROR! NO. OF M-VALUES MUST BE POSITIVE AND LESS THAN 10. TRY AGAIN!
1
ENTER THESE M-VALUES (2 DIGITS; LESS THAN 40) ONE PER LINE:
05
NO.OF THRESHOLD VALUES(<10,1 DIGIT):
-60
ERROR! NO. OF THRESHOLD VALUES MUST BE POSITIVE AND LESS THAN 10.
TRY AGAIN!
1
```

Figure F.1 Incorrect Data Entry (RETNTN)

```
 RUN DL:RETNTN.TSK


      CONFIGURATION  PARAMETERS:
      **************************
ENTER TRANSMISSION RATE,R,IN MBPS :
03.1584
ENTER FRAME LENGTH,TF,IN MILLISECS.(UP TO 3 DIGITS):
020
      **************************

      INPUT  PARAMETERS :
      *******************
ENTER NO.OF BER VALUES(2 DIGITS,E.G. 04):
01
ENTER BER VALUES(E-FORMAT,E.G. 3E-6) ONE PER LINE:
1E-6
ENTER NO.OF VERY-NARROW APERTURE VALUES(<10,1 DIGIT):
1
ENTER THESE APERTURE VALUES(3 DIGITS) ONE PER LINE:
002
ENTER LENGTH OF BTR SEQ.,NBTR,IN BITS
(LESS THAN 45 BITS; 2 DIGITS, E.G. 32):
40
ENTER LENGTH OF UW,NUW,IN BITS
(LESS THAN 45 BITS; 2 DIGITS, E.G. 16):
32
NO.OF M-VALUES(<10,1 DIGIT):
1
ENTER THESE M-VALUES (2 DIGITS; LESS THAN 40) ONE PER LINE:
05
NO.OF THRESHOLD VALUES(<10,1 DIGIT):
1
ENTER THRESHOLD VALUES (1 DIGIT) ONE PER LINE:
0
ENTER THE CANDIDATE UNIQUE WORD,UW(I),AS A VECTOR :
1111001011101100
ENTER THE BTR PRE-SEQUENCE,BTR(I),AS A VECTOR :
1100110011001100110011001100110011001100
ENTER NO. OF TERMINAL TIMING STABILITY VALUES(<10,1 DIGIT):
1
ENTER THE STABILITY VALUES(E-FORMAT) ONE PER LINE E.G. 2E-4:
1E-9
```

Figure F.2a Correct Data Entry (RETNTN)

```
     ******************


PNDB=0.3199949060E-04  M=  5
MATRIX INVERSION HAS BEEN SUCCESSFULLY COMPLETED IF 'TEST' IS ZERO,
AND DET IS POSITIVE AND LESS THAN ONE:
    TEST= 0.00000     DET=-0.00003
     RESULTS  OF THIS ANALYSIS :
     ************************
THE CHANNEL BER IS :    0.10000000E-05
WIDTH OF VERY NARR.APERT.:    2BITS.
LNGTHS.OF UW AND BTR SEQS.RESPEC.:32  BITS.AND   40BITS.
NO.OF SUCC.NO-DETEC.BEFORE SYNC-LOSS:   5
DETECTOR THRESH.:    0BITS.
BTR SEQ.IS :  1100110011001100110011001100110011001100
THE UW BEING TESTED IS :  1111001011101100000000000000000000
THE RMS TIMING ERROR IS SET AT:  0.99999997E-09 BITS PER BIT!

BURST DETECTION RESULTS :
*************************
PR.OF NO-DETEC.WITHIN THE APERTURE PNDB:    0.31999491E-04
PROB. OF FALSE DETECTION WITHIN APERTURE,PFDB:    0.00000000E+00
PROB.OF BSL(FLYWH.):  0.33551756E-22
MTBSL(FLYWH,I.E. M>1)DERIVED FROM THE CLOSED-FORm EXPRESION:  0.29804693E+23
USING THE GENERAL MARKOV CHAIN, THE FOLLOWING ESTIMATES ARE MADE:
     MTBSL CALCULATED FROM MARKOV CHAIN IS:  0.29804698E+23
     THE PROB. OF FALSE DETECTION,PFDBC:  0.00000000E+00
     PROB. OF SYNC-LOSS,PSLOSS:  0.54043294E-05

**********************END  OF DATA**********
TT2  --  STOP

>
```

Figure F.2b Sample Results (RETNTN)